2020

Cellular Localization Of Inflammatory Signaling As A Determinant Of Tumor-Immune Biology

Lexus Johnson
University of Pennsylvania

Cellular Localization Of Inflammatory Signaling As A Determinant Of Tumor-Immune Biology

Abstract

Immune therapies have significantly improved outcomes for cancer patients with poor prognosis, but mechanisms that underlie response or resistance to therapy remain elusive. Inflammatory cytokines such as interferon-gamma (IFNG) augment immune function yet also promote T cell exhaustion through inhibitory ligands such as PDL1. How these opposing effects are integrated in the tumor microenvironment is unclear. We show that while inhibiting tumor IFNG signaling decreases interferon-stimulated genes (ISGs) in cancer cells, it increases ISGs in immune cells by enhancing IFNG produced by exhausted T cells (TEX). In tumors with favorable antigenicity, these TEX mediate rejection. In tumors with neoantigen or MHC-I loss, TEX instead utilize IFNG to drive maturation of innate immune cells, promoting tumor clearance. Thus, interferon signaling in cancer cells and immune cells oppose each other to establish a regulatory relationship that limits both adaptive and innate immune killing. In melanoma and lung cancer patients, perturbation of this relationship is associated with response to immune checkpoint blockade independent of tumor mutational burden.

In addition to these suppressive mechanisms, tumor infiltration and antigen loss are common mechanisms that limit effectiveness of T cell responses in solid tumors, in particular chimeric antigen (CAR) T cells. Delivery of pattern recognition receptor agonists is one strategy to improve immune infiltration and prime adaptive immunity; however, targeting these agonists to immune cells is challenging, and off-target signaling in cancer cells can be detrimental as described above. Here, we engineer murine CAR-T cells to deliver RN7SL1, an endogenous RNA that activates RIG-I/MDA5-dependent interferon signaling. RN7SL1 is deployed in extracellular vesicles and preferentially transferred to intratumoral immune cells. Unlike other RNA agonists, RN7SL1 restricts development of myeloid-derived suppressor cells and decreases TGFB expression. In dendritic cells, it fosters DC subsets with anti-viral and costimulatory features. Consequently, endogenous effector-memory CD8 T cells expand, while exhausted T cells contract. Armed with the

ability to activate endogenous immune responses, these CAR-T cells effectively reject solid tumors and tumors with CAR antigen loss by drawing on our insights into tumor resistance mechanisms.

Degree Type
Dissertation

Degree Name
Doctor of Philosophy (PhD)

Graduate Group
Immunology

First Advisor
Andy J. Minn

Second Advisor
Carl H. June

Subject Categories
Allergy and Immunology | Immunology and Infectious Disease | Medical Immunology

CELLULAR LOCALIZATION OF INFLAMMATORY SIGNALING AS A DETERMINANT OF TUMOR-IMMUNE BIOLOGY

Lexus R. Johnson

A DISSERTATION

in

Immunology

Presented to the Faculties of the University of Pennsylvania

in

Partial Fulfillment of the Requirements for the

Degree of Doctor of Philosophy

2020

Supervisor of Dissertation

Andy J Minn, MD, PhD

Associate Professor of Radiation Oncology

Co-Supervisor of Dissertation

Carl H. June, MD

Professor of Pathology and Laboratory Medicine

Graduate Group Chairperson

David M. Allman, PhD

Professor of Pathology and Laboratory Medicine

Dissertation Committee

Malay Haldar, MD, PhD; Assistant Professor of Pathology and Laboratory Medicine

Sara Cherry, PhD; Professor of Microbiology

Gerald Linette, MD, PhD; Professor of Medicine

Christopher Hunter, PhD; Professor of Pathobiology

Dedicated to those that supported me along the way.

Kelly, Libby, Jean, and Chris.

ACKNOWLEDGMENT

This thesis would not have been possible without the mentorship and support of my two advisors Carl June and Andy Minn. With their guidance over the past 5 years, I have grown tremendously as a scientist and learned to believe in myself and my intuition. I thank them for their belief in me and support regardless of the obstacles along the way. These labs have brought me close to many incredible scientists that I am now proud to call friends and colleagues. Specifically, I want to thank my co-author Joseph Benci for his insight, dedication, and friendship in developing our work together published here in Chapter 2. In addition, this work would not have been possible without the help and expertise of Ruth Choa and Taku Kambayashi. I owe a tremendous amount of gratitude to Minn lab comradery; Barzin, Tony, Bihui, Lisa, Jingya, and many others were always there for advice or to commiserate. Always be early. I also want to acknowledge Sangya, Chris, Avery and Robby from the June lab for their advice and friendship, as well as all members of the June and Minn lab families for their support over the past 5 years.

No thesis is possible without the help and support of good friends. The IGG community at Penn is a truly unique group of scientists that I am proud to be a part of. I would like to thank all of my fellow graduate students for their support and friendship over the past five years, and in particular my 2014/2015 classmates. We've shared unforgettable memories around the country and the world, but the most important are the days picking each other up and taking our minds off science. You all are my extended Philadelphia family and I could not have accomplished this without you. Finally, this would not have been possible without the support of my girlfriend Kelly. Your endless positivity

and encouragement always kept my spirits high and your support allowed me to keep pushing through nights, weekends, and holidays to accomplish my goals. We made it.

ABSTRACT

CELLULAR LOCALIZATION OF INFLAMMATORY SIGNALING AS A DETERMINANT OF TUMOR-IMMUNE BIOLOGY

Lexus R. Johnson

Andy J Minn & Carl H. June

Immune therapies have significantly improved outcomes for cancer patients with poor prognosis, but mechanisms that underlie response or resistance to therapy remain elusive. Inflammatory cytokines such as interferon-gamma (IFNG) augment immune function yet also promote T cell exhaustion through inhibitory ligands such as PDL1. How these opposing effects are integrated in the tumor microenvironment is unclear. We show that while inhibiting tumor IFNG signaling decreases interferon-stimulated genes (ISGs) in cancer cells, it increases ISGs in immune cells by enhancing IFNG produced by exhausted T cells (T_{EX}). In tumors with favorable antigenicity, these T_{EX} mediate rejection. In tumors with neoantigen or MHC-I loss, T_{EX} instead utilize IFNG to drive maturation of innate immune cells, promoting tumor clearance. Thus, interferon signaling in cancer cells and immune cells oppose each other to establish a regulatory relationship that limits both adaptive and innate immune killing. In melanoma and lung cancer patients, perturbation of this relationship is associated with response to immune checkpoint blockade independent of tumor mutational burden.

In addition to these suppressive mechanisms, tumor infiltration and antigen loss are common mechanisms that limit effectiveness of T cell responses in solid tumors, in particular chimeric antigen (CAR) T cells. Delivery of pattern recognition receptor agonists is one strategy to improve immune infiltration and prime adaptive immunity; however,

targeting these agonists to immune cells is challenging, and off-target signaling in cancer cells can be detrimental as described above. Here, we engineer murine CAR-T cells to deliver RN7SL1, an endogenous RNA that activates RIG-I/MDA5-dependent interferon signaling. RN7SL1 is deployed in extracellular vesicles and preferentially transferred to intratumoral immune cells. Unlike other RNA agonists, RN7SL1 restricts development of myeloid-derived suppressor cells and decreases TGFB expression. In dendritic cells, it fosters DC subsets with anti-viral and costimulatory features. Consequently, endogenous effector-memory $CD8^+$ T cells expand, while exhausted T cells contract. Armed with the ability to activate endogenous immune responses, these CAR-T cells effectively reject solid tumors and tumors with CAR antigen loss by drawing on our insights into tumor resistance mechanisms.

TABLE OF CONTENTS

LIST OF ILLUSTRATIONS

CHAPTER 1 - INTRODUCTION

Section 1.1 – Immunobiology of Cancer

The advent of immune-based therapies for the treatment of cancer has revolutionized patient outcomes in some highly refractory cancers. This is the realization of a concept famously pioneered by William Coley in the 19th century (Coley, 1991); and more recently carried forward by pioneers around the world focused on T cell growth factors, adoptive T cell therapies, and T cell checkpoint inhibitors (Riley et al., 2019). At a more fundamental level, these translational efforts have built on a foundation of basic research investigating the role of immunity in the context of cancer. This includes a role for T cells, ILC1/NK cells, Dendritic cells, Monocyte/Macrophages, and others.

Section 1.1.1 CD8$^+$ T cells in Tumor Immunity

CD8$^+$ T cells are the most well characterized anti-tumor effector immune cell described to date. These cells function to recognize and eliminate cells in the body that express non-self proteins. Generally, this occurs in the context of viral or bacterial infection in which infected cells alert CD8$^+$ T cells to infection through presentation of non-self peptide fragments on the cell surface. In the context of cancer, this occurs through the recognition of “neoantigens” presented via the MHC-I complex (HLA-A, B, C in humans) by the T cell receptor (TCR). Briefly, tumors arise from healthy cells in which mutations cause aberrant growth. These genomic mutations lead to the production of mutant proteins that are not a part of the natural self-repertoire on which CD8+ T cells are selected. Therefore, they are able produce immunogenic antigens that are recognized as “non-self” by CD8$^+$ T cells in some cases (Durgeau et al., 2018; Schumacher and Schreiber, 2015). Notably, peptide

affinity for the MHC-I complex (Roudko et al., 2020), and relative difference from the wild-type protein (Richman et al., 2019) are important determinants for T cell recognition of neoantigens. As these peptides arise from genomic mutations, there is a natural correlation between tumor immunogenicity and mutational burden (Cristescu et al., 2018; Hellmann et al., 2018; McGranahan et al., 2016; Riaz et al., 2017). Unsurprisingly then, immunotherapeutic strategies relying on the activation of these cells have seen the most success in tumor types with high levels of mutational burden such as melanoma and non-small cell lung cancer (NSCLC) (Reck et al., 2016; Wolchok et al., 2013).

Mutational burden and neoepitope recognition are not the only defining determinants of $CD8^+$ T cell activation in the tumor microenvironment (TME). T cells are activated and regulated by three important signals: Signal 1 being TCR recognition of a cognate peptide/MHC complex (in this case a neoantigen), Signal 2 being the ligation of costimulatory molecules such as CD28 and 41BB, and Signal 3 being the recognition of soluble cues such as IL-12 and Type I IFN (Chen and Flies, 2013; Curtsinger and Mescher, 2010; Smith-Garvin et al., 2009). Much research has elucidated the importance of signals 2 and 3 in the TME and ways in which tumor cells dampen $CD8^+$ T cell activation by limiting the strength of these signals.

TCR recognition of a cognate antigen induces the formation of an immune synapse that aggregates many relevant surface receptors and facilitates important interactions of the cytoplasmic portion of these proteins. The main consequence of these cytoplasmic interactions is the initiation of a phosphorylation signaling cascade initiated by the CD3 protein, particularly the zeta chain (Jordan and Koretzky, 2010). Aggregation of this co-receptor initiates a well characterized signaling cascade that includes phosphorylation of Lck, Zap70, Slp76, and PI3K among others. This is dependent on relevant costimulatory

receptors such as CD28 that also participate in this interaction at the immune synapse (Jordan and Koretzky, 2010). The end result of this cascade is the activation of NF-kappaB (NFkB) signaling and calcium flux that initiates gene programs for T cell activation and expansion. However, negative costimulatory molecules are also expressed on $CD8^+$ T cells. These include receptors such as PD1, Tim3, Lag3, and CTLA4, among others. These receptors function in various ways, but all converge on a function of limiting these signaling cascades, and therefore dampening T cell activation. The balance of these positive and negative signals, along with the strength of Signals 1 and 3 determines the strength and magnitude of anti-tumor $CD8^+$ T cell responses (Chen and Flies, 2013).

Signal 3 shapes the $CD8^+$ T cell response by integrating soluble cues present in the local environment. In the context of viral infection these cues are often inflammatory in nature (e.g. IL-12, Type I IFN) and signal through respective receptor complexes that generally converge on the STAT4 transcription factor in $CD8^+$ T cells (Crouse et al., 2015). This drives a transcriptional program for $CD8^+$ T cells that includes differentiation into effector cells able to recognize and kill target cells through the lytic Granzyme family of molecules and the pore-forming protein Perforin (Halle et al., 2017). However, in contexts such as wound-healing and tumorigenesis, suppressive Signal 3 cytokines such as TGF-beta (TGFB) may predominate. This activates an opposing transcriptional program in T cells through the SMAD family of transcription factors, and converges on programs of tolerance instead of effector function. In this case, the $CD8^+$ T cell response is again dampened, and is frequently compromised in the context of anti-tumor immunity (Batlle and Massague, 2019; Kloss et al., 2018; Mariathasan et al., 2018). Thus, tumors employ a number of mechanisms to suppress $CD8^+$ T cell responses that favor tumor growth.

Section 1.1.2 Dendritic Cells in Tumor Immunity

Anti-tumor T cell responses are most robustly primed by professional antigen presenting cells (APCs) known as dendritic cells (DCs). These cells are able to internalize dead or dying cells and process internalized proteins into 7-9 amino acid peptides that can subsequently be presented to $CD8^+$ T cells in the context of MHC-I in a process known as "cross-presentation" (Cruz et al., 2017; Gardner and Ruffell, 2016). Additionally, these cells express high levels of the costimulatory ligands CD80 and CD86 that are able to ligate CD28 and initiate the signaling cascade described above. Because of this capability to prime T cell responses, these cells have been identified in a number of studies to be crucial in the initiation of anti-tumor immunity (Gardner and Ruffell, 2016). In this context T cell priming may happen in the tumor microenvironment, draining lymph nodes, and tumor-associated tertiary lymphoid structures (Broz et al., 2014; Joshi et al., 2015; Roberts et al., 2016). Subsequently, activated T cells are able to expand and kill tumor cells that present a cognate antigen on their surface via MHC-I (Heath et al., 1989).

Because of this crucial role, much work has been done to characterize populations of DCs in the TME. This work has described several major populations thus far: DC1, DC2, DC3, and pDC. DC1 are thought to be the major cross-presenting APC in the TME, and are crucial for anti-tumor $CD8^+$ T cell responses. These cells are rare, and may be characterized by expression of the integrin CD103, and are dependent on the transcription factor BATF3 for differentiation (Broz et al., 2014; Murphy, 2013). Conversely, DC2 are poor activators of $CD8^+$ T cell responses, but have been hypothesized to drive $CD4^+$ T cell responses. These cells are much more prevalent in the TME than DC1, and can be defined by the transcription factor IRF4 and expression of the integrin CD11b (Binnewies et al., 2019; Murphy, 2013). The DC3 subset was recently defined as a migratory population that

is hypothesized to traffic from the tumor to local lymph nodes in order to interact with circulating immune cells. They may have features of both DC1 and DC2, making it unclear if these cells represent a unique lineage or an activation state; regardless, they appear to be important for T cell priming in draining lymph nodes (Zilionis et al., 2019). Finally, plasmacytoid DCs (pDC) have been observed in many tumors, but their role in anti-tumor immunity remains unclear. These cells are well-characterized in the context of viral infection to produce high levels of Type I IFN (IFN-I), and as such may represent a source of inflammatory signaling in the TME if activated (Musumeci et al., 2019).

Because of the key role for DCs, factors that drive recruitment (Spranger et al., 2015; Spranger et al., 2017), activation (Beatty et al., 2011; Salmon et al., 2016), and function (Carreno et al., 2013; Carreno et al., 2015) of DCs (and DC1 in particular) have been of intense interest to the field. To this end, chemokines such as CCL7 (Roberts et al., 2016) have been implicated in the recruitment of DCs to the TME. Similarly, soluble factors such as TGFB (Spranger et al., 2015) have been shown to depress the function of these cells when they arrive at the TME, and constitute additional resistance mechanisms employed by tumors to limit anti-tumor immunity.

Despite progress, endogenous signals that drive DC activation in the TME remain understudied. In the context of viral or bacterial infection, the recognition of pathogen associated molecular patterns (PAMPs) such as LPS, cytosolic DNA, and double stranded RNA (dsRNA) has been well characterized to drive activation of these cells and upregulation of antigen presentation machinery (Joffre et al., 2009; Kandasamy et al., 2016; Sprokholt et al., 2017b). In this way, DCs are critical bridges from innate to adaptive immunity. Yet how similar “non-self” molecular patterns might be present in the TME has not yet been well characterized.

Section 1.1.3 ILC1 Cells in Tumor Immunity

Group 1 innate lymphoid cells (ILC1s) can be split between classically defined natural killer (NK) cells and recently defined ILC1 cells by the expression of several surface markers (Spits et al., 2016). Regardless of classification, these cells act as major producers of IFNG and Perforin/Granzyme in viral and cancerous contexts (Chiossone et al., 2018). While functionally similar to T cells, these cells lack antigen-specific receptors and instead act on a balance of signaling inputs interpreting stress cues in their local environment. Specifically, these cells express activating receptors that recognize stress ligands such as MICA/MICB in humans and MULT1 in mice, as well as inhibitory receptors that recognize healthy expression of molecules like MHC-I. Stress receptors are generally activating (i.e. NKG2D), while receptors that recognize MHC-I tend to be inhibitory (i.e. Ly49a, KIR2DL2/3) (Lanier, 2005). In this way healthy cells that express high levels of MHC-I fail to activate these cells, while those that downregulate MHC-I or upregulate stress molecules are recognized and cleared from the body (Deng et al., 2015; Karre et al., 1986; Paczulla et al., 2019). These receptor families are extensive and capable of integrating many signaling inputs in a single cell (Cerwenka et al., 2001). By combining both activating and inhibitory signals ILC1/NK cells are able to recognize stressed cells by ligand expression as well as infected cells seeking to evade $CD8^+$ T cell recognition by downregulation of MHC-I. This role is particularly well studied in the context of antiviral immunity (van de Weijer et al., 2015), but has clear corollaries to anti-tumor immune evasion.

To date, research on the role of these cells in anti-tumor immunity has been restricted largely to liquid tumors in which experimental systems have been explicitly designed to lack MHC-I expression or express NKG2D ligands (Cerwenka et al., 2001; Deng et al., 2015; van den Broek et al., 1995). Clinically, this has resulted in a focus on leukemias and graft-vs-tumor effects (Boudreau et al., 2017; Mavers and Bertaina, 2018). However, loss of MHC-I is an emerging resistance mechanism to immunotherapies focused on the activation of $CD8^+$ T cells (Rooney et al., 2015; Sade-Feldman et al., 2017; Zaretsky et al., 2016). In this context we might expect ILC1/NK cells to play a role in tumor recognition and control based on a loss of inhibitory signaling regulated by normal levels of MHC-I. Further studies have also revealed the heterogeneity of the NK/ILC1 compartment in the TME, and identified TGFB as a key regulator of differentiation (Cortez et al., 2017; Gao et al., 2017). Thus, optimal priming of these cells may be a key regulator of anti-tumor immunity in tumors with low MHC-I expression.

Section 1.1.4 Macrophages and Monocytes in Tumor Immunity

Cells that provide suppressive cytokine signals such as TGFB are of intense interest to the field, as they impede optimal immune activation. Monocytes are cells of the myeloid lineage that circulate with high frequency and give rise to macrophages and MDSCs (myeloid-derived suppressor cells) in the TME (Laviron and Boissonnas, 2019). This is thought to be analogous to a similar role in wound-healing that is co-opted by tumors as an immune-suppressive mechanism (Muliaditan et al., 2018). Indeed, macrophages and MDSCs are largely immune-suppressive and are frequently the most prevalent immune cell type in the TME. Monocyte recruitment is achieved through enhanced expression of

chemoattractants such as CCL2 and CXCL1 by tumor cells followed by differentiation into macrophages or MDSCs in the TME (Quail and Joyce, 2013).

There are multiple mechanisms by which macrophages suppress anti-tumor T and ILC1/NK cell responses. The most well-characterized of these is differentiation into an “M2” macrophage phenotype. This phenotype is highly prevalent in tumors, and is associated with high levels of IL-10 and TGFB production that blunt activation of anti-tumor effector cells. In turn, M2 macrophage differentiation itself is thought to be regulated by IL10 and TGFB produced by tumor cells and pre-existing macrophages present in the local microenvironment (Batlle and Massague, 2019). This drives a forward-feeding loop that enforces a suppressive, non-inflammatory microenvironment within the tumor. A second major immune-suppressive mechanism deployed by macrophages in the TME is the high expression of PDL1 (PD1 ligand) (Benci et al., 2016). This ligates PD1 expressed on both T cells and ILC1/NK cells, inhibiting the full activation potential of these cells. This acts as a second pool of PDL1 on top of that expressed on tumor cells (Pesce et al., 2019; Sharpe and Pauken, 2018; Sun et al., 2018). Multiple studies have demonstrated that depletion, inhibition, or repolarization (Dammeijer et al., 2017; Hoves et al., 2018; Pyonteck et al., 2013) of macrophage function in the TME is an effective way to enhance anti-tumor immune responses, underscoring the crucial pro-tumor role that these cells play in regulating anti-tumor immunity.

MDSCs play a similar role to macrophages in the TME, albeit through slightly different reported mechanisms. These cells are well characterized suppressors of T cell function; unlike traditional M2 macrophages, MDSCs are thought exert pro-tumor function mainly through inhibitory soluble factors such as IDO, iNOS, and ARG1/2 (Gabrilovich, 2017). Thus, they enhance the immune-suppressive microenvironment that fosters malignant

tumor growth through orthogonal mechanisms. Similar to macrophages, many studies have characterized approaches that limit the function or prevalence of these cells in the TME and improve anti-tumor immunity (Anani and Shurin, 2017). Unfortunately, these approaches have yet to yield robust clinical benefits, demonstrating the need for novel approaches to modulate the emergence of these cells in the TME.

Section 1.1.5 $CD4^+$ T cells in Tumor Immunity

$CD4^+$ T cells will not be covered in depth in this thesis but are important contributors to the tumor-immune microenvironment. $CD4^+$ T cells come in a variety of subtypes, but most well-characterized in the TME are $CD4^+$ T regulatory cells (Tregs). These cells are thought to differentiate in response to TGFB in the TME and also to traffic to the TME in response to inflammation (Tanaka and Sakaguchi, 2017). They function to inhibit $CD8^+$ T and NK cell responses through a variety of proposed mechanisms including negative costimulatory ligation, TGFB secretion, and CD80/86 or IL-2 sequestration (Josefowicz et al., 2012). All of these mechanisms result in sub-optimal T cell priming and favor tumor growth. Other $CD4^+$ T cell subtypes such as Th1, Th2, and Th17 have been shown to influence the tumor immune microenvironment in various manners (Karin and Wildbaum, 2015), but will not be covered here.

Section 1.2 – Inhibitory Checkpoint Blockade

As mentioned above, T cells integrate costimulatory signals during priming and target recognition. These costimulatory receptors can be activating or inhibitory; the activating

CD28 signaling cascade was described briefly above, in which ligation of CD28 by CD80 or CD86 initiates the phosphorylation of SLP76, which eventually converges on NFkB signaling (Smith-Garvin et al., 2009). This process is antagonized by two key negative costimulatory receptors also expressed by T cells: PD1 and CTLA4. This section will describe the biology of inhibitory costimulatory molecules and clinical progress in the development of blocking antibodies for these pathways.

Section 1.2.1 PD1 and CTLA4 in T cell exhaustion

In response to acute viral and bacterial infections, T cells undergo rapid differentiation from a naïve cell type to a mature effector cell in order to clear the offending pathogen. This is followed by a contraction phase and the establishment of immune memory by a small pool of memory T cells (Kaech et al., 2002). The expansion of effector cells is required for clearance of many pathogens, and is a hallmark of productive immune responses. These cells are characterized by high levels of inflammatory cytokine production like IFNG and TNF, as well as robust killing capacity through expression of lytic molecules like Granzyme B (Kaech et al., 2002). This state is generally thought to be the product of effective integration of Signals 1, 2, and 3 described above and is associated with a wide variety of productive immune responses (Kaech and Cui, 2012). For this reason, some persistent or chronic infections and cancers employ mechanisms to limit this productive T cell expansion and instead drive a more dysfunctional T cell state termed T cell exhaustion (Wherry and Kurachi, 2015).

T cell exhaustion is a widely studied phenomenon that may be driven by chronic antigen stimulation, improper co-stimulation, suppressive cytokine exposure, or a combination of

these factors. This dysfunctional state is characterized by lower production of inflammatory cytokines like IFNG and TNF, as well as a diminished ability to kill target cells (Wherry and Kurachi, 2015). Extensive studies have demonstrated that this cell state is regulated by a core transcriptional program orchestrated by the transcription factor TOX1 (Alfei et al., 2019; Khan et al., 2019; Scott et al., 2019), which includes decreased chromatin accessibility of effector T cell genes and increased accessibility of inhibitory receptors such as PD1 and others (Pauken et al., 2016). This state is hypothesized to arise in viral infections as an evolutionary adaptation to limit immune pathology in chronic infections (Barber et al., 2006); however, many tumors impose this program to limit T cell function and favor tumor growth (Sun et al., 2018). For example, tumor cells frequently express high levels of PDL1 in order to limit T cell activation through the ligation of PD1 on T cells. Similarly, the secretion of the suppressive cytokine TGFB can act directly on cytotoxic T cells, while also recruiting regulatory T cells that utilize the inhibitory co-receptor CTLA4 to prevent optimal T cell priming as discussed above. Examples of these negative costimulatory regulators employed by tumor cells abound and will be discussed in this section.

PD1 (Programmed Death receptor 1) acts through the intracellular phosphatase SHP2 upon ligation with its cognate receptor PDL1. SHP2 dephosphorylates key components of the TCR signaling pathway such as ZAP70 and PI3K, effectively stopping TCR signaling and blunting activation of the T cell (Arasanz et al., 2017). This is thought to promote immune/pathogen stalemate in the context of infectious disease in order to limit immunopathology (Barber et al., 2006; Wherry and Kurachi, 2015); but in the context of the TME, it effectively renders T cells unable to kill tumor cells and promotes tumor growth (Benci et al., 2016; Sun et al., 2018). Thus, antibodies that block this PD1/PDL1 interaction

should effectively release this T cell inhibition and enhance T cell killing in the tumor. Indeed, this result has been achieved through a number of now clinically available antibodies (Mahoney et al., 2015), several of which have demonstrated impressive clinical efficacy.

Alternatively, CTLA4 acts by sequestering CD80 and CD86 from CD28 ligation through a higher affinity interaction. This effectively deprives the T cell of positive costimulatory signaling and achieves a similar result to PD1 ligation by limiting the level of TCR pathway activation. This leads to poor T cell priming and enforces the T cell exhaustion program (Esensten et al., 2016). While the major PD1/PDL1 interaction is thought to occur mainly between T cells and tumor cells, this CTLA4/CD80-86 interaction is thought to happen mostly at the level of DC/T cell priming and Treg/T cell intratumoral interactions (Dyck and Mills, 2017). In this way, tumors limit the priming of cytotoxic T cells at multiple checkpoints in the activation process and impose a state of T cell exhaustion that favors tumor growth.

Section 1.2.3 Clinical Successes Utilizing Checkpoint Inhibitors

Treatment of cancer with antibodies that block these inhibitory checkpoint molecules has been termed inhibitory checkpoint blockade (ICB), and has fundamentally changed the treatment of some advanced cancers. The first major clinical results demonstrating the efficacy of this approach were published roughly 10 years ago now, with the major conclusion that remissions achieved after treatment with these ICB therapies were extremely durable (Wolchok et al., 2013). This is reminiscent of immunological memory observed in murine experiments (Leach et al., 1996), and represents a level of tumor control rarely achieved by small-molecule therapies.

Unfortunately, the most dramatic responses have been limited to specific subsets of cancers. Notably, responses in melanoma and NSCLC appear particularly robust following ICB therapy (Gandhi et al., 2018; Wolchok et al., 2013). This may be explained by high levels of previous immune infiltration (Hellmann et al., 2018), as well as high levels of tumor mutational burden (Alexandrov et al., 2013). However, even tumor types with relatively high levels of mutational burden, such as NSCLC, respond to therapy in a durable fashion only ~20% of the time (Gandhi et al., 2018). This may be attributed to several factors; first, many tumors simply exist as immune deserts. In this case, no T cells are present to become activated following ICB therapy, and therefore the therapy is ineffective (Teng et al., 2015). A similar scenario has also been described in which T cells are limited to the margins of the tumor; these tumors are known as “T cell excluded” (Mariathasan et al., 2018). In other cases, adaptive resistance mechanisms such as MHC-I loss, TGFB suppression, or metabolic rewiring may prevent T cells from becoming properly activated even in the context of enhanced priming facilitated by ICB (Bengsch et al., 2016; Kloss et al., 2018; Sade-Feldman et al., 2017). Finally, a tumor may have no recognizable mutant T cell neoantigens; in this case there is simply nothing for the T cells to recognize and ICB is priming T cells that have no relevant target (Alexandrov et al., 2013). For these reasons, more innovation is required to expand the clinical benefit being realized from the basic understanding of T cell biology and tumor-immune interactions.

Section 1.2.3 Additional Negative Costimulatory Receptors

Since the discovery of PD1 and CTLA4, many additional T cell inhibitory costimulatory receptors have been identified. Tim3, Lag3, and TIGIT, among others have been

demonstrated to be of particular relevance to enforcing the T cell exhaustion phenotype. These receptors bind various ligands associated with T cell/APC interactions, and generally converge on intracellular ITIM motifs to suppress TCR pathway signaling through phosphatase activation. While these receptors will not be covered in detail in this thesis, significant work has been done to elucidate the importance of these receptors in the context of anti-tumor immunity. Despite the insight gained, clinical blockade strategies targeting these receptors have shown significantly less efficacy than anti-PD1 and anti-CTLA4 strategies. This may imply that PD1 and CTLA4 act as master regulators of T cell activation in the TME, and that there is additional underlying biology that we have yet to understand (Chen and Flies, 2013).

Section 1.3 – Interferon signaling in cancer

Both IFN-gamma (IFNG) and Type I IFN (IFN-I) are known to have critical roles in anti-tumor immunity. IFN enhances immune function by inducing expression of MHC-I (Dighe et al., 1994), which is constitutively expressed on many tissues, and by enabling dendritic cells to cross-prime T cells (Diamond et al., 2011; Fuertes et al., 2011). In this way, IFNs are important in the early phase of antigen recognition and are crucial to the interaction between adaptive and innate immunity. Accordingly, loss-of-function mutations and genomic alterations in the IFN/JAK signaling pathway have been associated with clinical ICB resistance and/or relapse (Gao et al., 2016; Shin et al., 2017; Zaretsky et al., 2016), and unbiased genetic screens have identified this same pathway as being important for immunotherapy response in certain mouse models (Manguso et al., 2017; Mezzadra et al., 2017). In contrast, some patients with mutations in the IFN pathway still respond to

ICB (Hellmann et al., 2018; Sade-Feldman et al., 2017) or have high serum levels of IFNG that associates with ICB progression (Huang et al., 2017). These paradoxical observations may represent immunosuppressive properties of the IFN pathway.

Section 1.3.1 IFNG in the Tumor Microenvironment

IFNG is an immune-stimulatory cytokine that is produced at high levels by activated T and NK cells during viral and bacterial infections. This cytokine signals to a variety of other immune and non-immune cell types through a dedicated IFNG-receptor (IFNGR), which is made up of a heterodimer consisting of IFNGR1 and IFNGR2. Upon ligation of IFNG, a complex of 2 IFNGR heterodimers is formed, creating an active signaling complex of two heterodimer receptors and two IFNG molecules (Mendoza et al., 2019). This active complex phosphorylates the transcription factor STAT1 via JAK1/JAK2 kinases, inducing STAT1 dimer formation and nuclear translocation. This signaling converges on a well-studied set of genes termed “interferon stimulated genes” (ISGs), that are critical to anti-viral and bacterial immunity (Castro et al., 2018).

Since the discovery that T and NK cells are also able to recognize tumor cells (Asjo et al., 1977; Schick and Berke, 1977), there has been much interest about how IFNG affects the TME. Several studies have demonstrated the importance of IFNG in DCs that cross-prime anti-tumor $CD8^+$ T cells (Diamond et al., 2011; Frasca et al., 2008), as well as a crucial role for initiating and enforcing inflammatory gene programs in macrophages (Ivashkiv, 2018; Kaneda et al., 2016). In DCs, IFNG is crucial for activation of antigen-processing machinery that facilitates cross-presentation to $CD8^+$ T cells (Matsuo et al., 2004). This process is particularly crucial in anti-tumor contexts, as dead or dying tumor cells must be

internalized and processed by DCs in order to prime $CD8^+$ T cells to recognize tumor neoantigens (Roberts et al., 2016). Moreover, costimulatory molecules CD80 and CD86 are well-defined ISGs that enhance T cell priming when upregulated in DCs (Castro et al., 2018). In macrophages, IFNG enforces an inflammatory gene program and chromatin state that is actively repressed by intracellular PI3K in the TME (Kaneda et al., 2016). Thus, IFNG may represent a crucial regulator of macrophage polarization in the TME, and a key determinant of immune activation. This suggests an important role for IFNG in activating anti-tumor gene programs in the myeloid compartment. Interestingly, recent evidence has suggested an opposing role in T cells in which high levels of IFNG signaling may lead to activation-induced cell death (Pai et al., 2019). This may represent another evolutionary mechanism for limiting immune pathology during pathogenic infections, but could limit T cell expansion in tumors.

Further supporting the pleiotropic role for this cytokine in the TME, conflicting reports have described both positive and negative roles for IFNG signaling in tumor cells. As mentioned above, IFNG is a strong stimulus for the upregulation of MHC-I, which is crucial for $CD8^+$ T cell responses. However, signaling also drives expression of inhibitory ligands such as PDL1 and Galectin-9, among others, on the surface of cancer cells (Benci et al., 2016). This enforces T cell dysfunction and favors tumor growth. Further, high MHC-I expression limits the activation of NK cells in the tumor, which favors tumor growth in contexts of low neoantigen prevalence. These opposing outcomes are seemingly contradictory, and the outcome of tumor/immune interactions in this setting are likely context dependent.

Section 1.3.2 Type I IFN in the TME

Unlike IFNG, IFN-I is mainly a product of innate immunity. During viral infections, it is produced at high levels by macrophages, DCs, and epithelial cells that recognize infection and seek to alert neighboring immune cells. This family of cytokines includes IFN-beta (IFNB), and multiple subtypes of IFN-alpha (IFNA), both of which signal through a shared IFN-I receptor (IFNAR). IFNAR signaling leads to the formation of heterodimers of phosphorylated STAT1 and STAT2 that translocate to the nucleus and upregulate ISGs that are overlapping, but not identical to those triggered by IFNG signaling (Lee and Ashkar, 2018). Interestingly, IFNA was proposed and tested as one of the first recombinant protein therapeutics for induction of anti-tumor immunity (Borden, 2019). In recent years our understanding of the pleiotropic role of this pathway in the TME has improved and suggests more targeted therapeutic approaches may improve this paradigm.

IFN-I target ISGs play a variety of roles depending on cell type. For example, in macrophages IFN-I is strongly associated with M1 macrophage polarization (Park et al., 2017; Snell et al., 2017), and drives differentiation of monocytes to an inflammatory phenotype instead of a pro-tumor MDSC phenotype (Dangi et al., 2018; Santini et al., 2000). Similar to IFNG, IFN-I drives upregulation of costimulatory molecules and antigen presentation machinery in DCs that facilitate T cell activation. During this priming process, IFN-I in the local microenvironment acts as an important Signal 3 molecule, priming effector $CD8^+$ T cell responses and Th1 $CD4^+$ T cell responses (Longhi et al., 2009; Wiesel et al., 2012). In mice that lack IFNAR, antiviral (Kolumam et al., 2005) and anti-tumor (Diamond et al., 2011) T cell responses are severely curtailed, leading to ineffective clearance and enhanced morbidity. These IFN-I primed T cells are characterized by an upregulation of survival programs that include BCL-XL, as well as induction of TBET, a

master regulator of T cell differentiation. Accordingly, T cells that lack IFNAR are unable to differentiate into short-lived effector cells and control viral infections (Marrack et al., 1999; Wiesel et al., 2012). Similar studies have not yet been carried out in tumors, but consistencies between anti-viral and anti-tumor T cell studies would suggest a similar role for IFN-I in anti-tumor T cell priming.

Consistent with the pleiotropic role of many cytokines in the TME, IFN-I signaling in tumor cells has been additionally correlated with resistance to therapy. This was first described as a broad resistance signature to chemotherapy, radiation, or a combination of the two (Weichselbaum et al., 2008). However, in recent years a more nuanced understanding has been reached in which some core ISGs predict resistance to therapy (Boelens et al., 2014; Nabet et al., 2017), while others that are more critical to immune activation predict response to therapy (Manguso et al., 2017; Patel et al., 2017). This is unsurprising given the nature of IFN-I target genes; for example, BCL-XL upregulation in tumor cells is likely to favor tumor growth and survival (Boise et al., 1993; Kumar et al., 1996), while upregulation of MHC-I and antigen processing will favor immune recognition, cell death, and responsiveness to therapy (Patel et al., 2017). Thus, a central hypothesis of this thesis is that the relative cellular localization of inflammatory signaling is a key determinant to the activation of these pathways in the TME. Since the source of these signaling pathways is generally thought to be the recognition of viral or bacterial infection, how the production of IFN-I is initiated in the TME is of significant interest.

Section 1.4 – PAMPS in the TME

Pathogen associated molecular patterns (PAMPS) have (unsurprisingly) been most well described in the context of pathogenic infections. Generally, this term refers to molecular patterns that are “foreign” to the eukaryotic immune system. For example, the detection of double-stranded or structured RNA/DNA in the cytoplasm by pattern recognition receptors (PRRs) alerts the host to viral infection. Similarly, detection of bacterial cell wall components activates anti-bacterial immunity and aid in the clearance of infections (Kawasaki and Kawai, 2014; Schlee and Hartmann, 2016). However, in recent years a budding literature has emerged around a role for pattern recognition receptors in anti-tumor immunity and tumor-associated inflammation (Zitvogel et al., 2015). This implies that tumors are producing pathogen-like molecules in some contexts and suggests a role for innate immune pathways in the discrimination of self vs non-self in anti-tumor immunity.

Section 1.4.1 STING signaling in the TME

STING is a cytoplasmic DNA sensor that works in concert with its partner protein cGAS. Upon recognition of cytoplasmic DNA cGAS becomes activated and produces the messenger molecule cyclic guanine adenosine monophosphate (cGAMP). cGAMP is then recognized by STING, which initiates a signaling cascade that converges on phosphorylation of the IRF3 transcription factor and a core ISG gene program (Chen et al., 2016). This process is normally associated with recognition of DNA viruses, but in recent years it has become appreciated that genome instability in tumor cells allows for release of DNA into the cytoplasm as free-floating DNA or microsatellites (Barber, 2015; Li and Chen, 2018). In this way, STING may act as genomic stress sensor, similar to the RNA sensor PKR, that alerts surrounding cells to decreased cellular fitness.

In contrast to the paradigm described above for IFN-I and IFNG, DNA damage and activation of the STING pathway seem uniformly pro-immunogenic and enhance response to ICB. In general, chromosomal instability or microsatellite formation leads to immune activation (Harding et al., 2017) or senescence (Dou et al., 2017) that synergize with checkpoint blockade strategies. On this basis, several interventional approaches have been investigated to trigger STING activation in the TME. These may involve the use of ionizing radiation that causes double-stranded DNA breaks (Deng et al., 2014), or injection of STING agonist molecules directly in the TME (Ager et al., 2017; Corrales et al., 2015; Ramanjulu et al., 2018). However, it is worth noting that DNA damage is associated with increased rates of mutation which can confer resistance to many therapeutic modalities (Vasan et al., 2019).

STING agonists seek to trigger the STING pathway in immune cells present in the TME, leading to enhanced anti-tumor immunity. Encouragingly, strategies such as radiation combined with ICB have demonstrated some clinical efficacy (Twyman-Saint Victor et al., 2015), although it is difficult in this setting to attribute that benefit to any one specific molecule or pathway. The outlook is less positive for strategies utilizing direct STING agonist molecules, usually in the form synthetic di-nucleotides. Thus far, systemic delivery of these molecules either alone or in liposome-encapsulated formulations has not been able to achieve relative concentrations high enough to generate robust clinical anti-tumor responses (Riley et al., 2019). This is associated with general inflammatory toxicity from systemic delivery (Hu et al., 2019), as well as localization of liposomes to liver and kidneys instead of sites of disease (Sercombe et al., 2015). Alternatively, direct injection at tumor sites has shown robust responses in preclinical models (Corrales et al., 2015), but is not necessarily appropriate for patients with difficult to reach or multiple metastatic sites. Thus,

deeper understanding of PRR biology in the TME and novel targeted approaches are needed to leverage these pathways for improving outcomes following ICB therapy.

Section 1.4.2 dsRNA signaling in the TME

Like cytoplasmic DNA, double-stranded or highly structured RNA is a common viral nucleic acid motif. In recent years such RNAs have also emerged as a potent inducer of ISGs in both tumor and immune cells in the TME. This RNA motif is detected in the cytoplasm by the PRRs MDA5 and RIG-I, and in endosomes by TLR3 (Schlee and Hartmann, 2016). In the cytoplasm, MDA5 is thought to recognize foreign RNAs through a structural mechanism that favors longer RNAs, while RIG-I activation is triggered by shorter RNAs that contain a 5' tri-phosphate moiety that is less dependent on structure (Brisse and Ly, 2019). This 5' tri-phosphate serves as distinguishing feature of foreign RNA, as eukaryotic mRNA transcripts are transcribed by RNA Polymerase-II which cleaves this 5' tri-phosphate and leaves instead a 5' -OH. Additionally, the majority of non-messenger RNA in eukaryotic cells contains a 5'-monophosphate. Viral polymerases are not able to create these motifs, and so even short and non-structured viral RNAs may be recognized by eukaryotic hosts (Phatnani and Greenleaf, 2006; Vignuzzi and Lopez, 2019). Both RIG-I and MDA5 signal through the adaptor protein MAVS that acts as a signaling platform located on the mitochondria and translates this recognition of foreign RNA into phosphorylation and activation of transcription factors IRF3 and IRF7. This results in the upregulation of an antiviral ISG signature including robust production of IFN-I (Schlee and Hartmann, 2016).

Frequently the RNAs that are recognized by these PRRs in tumors are endogenous retroviral elements that have been incorporated into the human genome, but are repressed in the steady state. They may be de-repressed by epigenetic changes associated with cancerous transformation (Sheng et al., 2018), or through therapeutic interventions such as DNMT inhibitors (Chiappinelli et al., 2015), and radiation (Lee et al., 2020). Regardless of how they become derepressed, the recognition of these stimulatory RNAs generates an inflammatory IFN-I genomic signature in a variety of experimental systems. And again, reports differ on the effect of these elements in the TME. This underscores that further study is required to understand the determinants of survival outcomes, despite many of these inflammatory processes converging on similar gene programs (Boelens et al., 2014; Sheng et al., 2018).

To this point, most studies have focused on cancer or immune-specific effects of such RNAs, while ignoring potential competition or interplay between these two cellular compartments. For example, several papers have demonstrated that intratumoral administration of dsRNA ligand Poly I:C improves anti-tumor immunity and response to ICB both in mice and human (Hammerich et al., 2019; Salmon et al., 2016). These papers largely ignore effects on tumor cell signaling, while papers that have characterized tumor recognition of endogenous dsRNA elements focus mainly on tumor cell-intrinsic effects of PRR activation (Boelens et al., 2014; Nabet et al., 2017). In this case, pro-tumor effects of intratumoral inflammation and IFN-I signatures are highlighted. Given that both instances give rise to robust phenotypes, more work is needed to understand the interaction between these populations.

Of particular interest is the endogenous non-coding RNA RN7SL1 (7SL). This RNA is derived from an ancient retroviral element and is conserved from mammals to bacteria

(Denks et al., 2014). It has significant secondary structure and functions as a scaffold for the signal recognition particle (SRP) complex, which facilitates translation of transmembrane proteins (Halic and Beckmann, 2005). Transcription of this RNA is controlled by an RNA Pol-III promoter, and unlike mRNA produced by RNA Pol-II, the 5' tri-phosphate of the RNA is not processed (Phatnani and Greenleaf, 2006). Additionally, this promoter is sensitive to MYC and so is intrinsically linked to cellular growth signals (Campbell and White, 2014). In homeostatic conditions, the SRP complex decorates the RNA and shields 7SL from recognition by the cytoplasmic dsRNA sensors described above. However, in some cancerous contexts with high levels of Notch and MYC signaling, the stoichiometry of 7SL RNA and SRP complex proteins can be dysregulated in such a way that that 7SL RNA is over-produced and will not bound by SRP proteins. In this case, unshielded 7SL RNA becomes available for recognition by PRRs. This drives a tumor-cell intrinsic ISG program that enhances tumor growth and resistance to ICB therapy (Nabet et al., 2017). The effect that such an RNA might have on immune cells in the TME would be of significant interest to the field and could elucidate context-specific effects for these inflammatory stimuli.

Section 1.5 – Extracellular RNA Transfer and Communication

While soluble cytokines such as IFN-I often act as the extracellular messengers that communicate PRR activation to neighboring cells, PAMPs themselves may also be transferred between cells via extracellular vesicles. Extracellular vesicles (EVs) are a class of sub-cellular lipid vesicles that are characterized by a lipid membrane and are sub-classified by size into categories including microvesicles, exosomes, and large EVs,

among others. EVs are derived from the endosomes or plasma membranes of living cells, maintain surface expression of some surface receptors, and are loaded with biological cargo including nucleic acids and proteins, but are unable to independently replicate. In general, EVs favor smaller cargo including miRNAs, lncRNAs, small peptides, and secondary messengers, raising an intriguing possibility that these vesicles may serve as important cell-to-cell communication vehicles (Raposo and Stoorvogel, 2013).

Section 1.5.1 Tumor Extracellular Vesicle Communication

Tumors are well-known to utilize EVs for the purpose of altering extracellular processes, first characterized in the context of miRNAs. In many cases, tumors export miRNAs in complex with DICER/AGO processing machinery; this has been reported to promote EMT mesenchymal differentiation (Whiteside, 2018), enhanced fibroblast differentiation (Yang et al., 2017), and immune suppression (Whiteside, 2016), among other processes. Subsequent studies have confirmed that tumor-derived miRNAs can limit DC (Yu et al., 2007) and T cell (Curtale et al., 2010) activation, further favoring tumor growth. Additional evidence for EV-mediated transfer of protein cargo was demonstrated by observing Cre-recombinase mediated genetic deletion in mixed populations such that no cell expressed all necessary components internally (Pucci et al., 2016). This evidence is particularly compelling because it necessitated the transfer of EV cargo from the cell surface into the nucleus to affect the genome of the acceptor cell. This opens the possibility that tumor cells may export malignant proteins that are produced in abundance like MYC or RAS to neighboring cells, further enhancing their proliferative potential. This a powerful tool for cancer cells to export proteins and complexes that modulate transcriptional programs and

phenotypes of neighboring cells in the TME to their advantage. Indeed, many groups have suggested that exosomal secretion is required for metastatic niche preparation and drives metastatic potential of tumors (Becker et al., 2016).

Conversely, tumor-derived EVs may also contain immunogenic molecules due to the structured nature of many lncRNAs and nucleotide based secondary messengers. For example, cGAMP is often transferred between cells via gap junction (Ablasser et al., 2013; Schadt et al., 2019) and EVs (Bridgeman et al., 2015; Gentili et al., 2015) in order to propagate recognition of DNA viruses by activating STING in neighboring cells. Indeed, DNA microsatellites in tumor cells were able to initiate cGAS-mediated production of cGAMP which enhanced anti-tumor immunity (Harding et al., 2017). Crucially in this case, host STING was required for anti-tumor immunity, implying that cGAMP was being transferred from tumor cells to neighboring immune cells in the TME in some way. Similarly, RN7SL1 was identified as an inflammatory stimulus by studying EV RNA that was transferred from fibroblasts to tumor cells (Nabet et al., 2017). This highlights the complex nature of EV cargo and multitude of pathways that it may influence in acceptor cells.

Finally, many tumor-derived EVs retain surface molecules such as PDL1 and TGFB (Chen et al., 2018; Shelke et al., 2019). Similar to tumor cell surface ligands, these suppress anti-tumor immunity, such that even with immunogenic cargo the uptake of these EVs may represent an immunosuppressive event. The confluence of these pathways are a microcosm for the TME as a whole, and point to a need for understanding of the factors that mediate EV uptake as a driver of signal localization within the TME.

Section 1.5.2 Extracellular Vesicle Sorting

As EVs bud from the cellular membrane, it is clear that cargo is loaded into these bodies. However, whether this is a passive or active process remains a subject of significant debate. Given that many EV-enriched surface receptors contain intracellular domains, it is an attractive possibility that these proteins direct cargo sorting and enrich for specific molecules or motifs, similar to clathrin-coated vesicles. Indeed, the receptor ALIX is thought to sort some protein cargo specifically into EVs in a ubiquitin-dependent manner (Bebelman et al., 2018). Similarly, it has been hypothesized that integrin inclusion on the surface of EVs targets vesicles to specific acceptor cells based on reciprocal integrin expression. This is supported by the specification of tumor metastases to specific anatomic sites given tumor-EV integrin expression independent of tumor type (Hoshino et al., 2015).

A competing school of thought places more emphasis on passive localization than active sorting in these processes. In this case, cargo that is nearest the plasma or endosomal membrane as EVs are incorporated is included in the vesicle. Thus, size and frequency of a given molecule are the key determinants of EV inclusion. This hypothesis can be supported by the frequency of common miRNAs and ncRNAs found in EVs, as well as the amount of small protein cargo found in these vesicles as compared to larger molecules (i.e. cGAMP vs Cre-recombinase) (Abels and Breakefield, 2016). Similarly in this view, acceptor cells are specified more by proximity to secretor cells than specific EV/cell interactions. This may be supported the importance of tumor/stroma exosomal communication, as these cells frequently reside in tight proximity within the TME (Yang et al., 2017). Importantly, these possibilities are not mutually exclusive, and likely both play a role in EV distribution and cargo content.

Section 1.6 – CAR-T cell biology

Chimeric antigen receptor (CAR) T cells are engineered *ex vivo* to recognize and kill tumor cells. This is achieved through viral transduction of T cells in order to express a CAR molecule that contains two major subunits. The first is a single chain variable fragment of an antibody (scFv) that allows for recognition of tumor cells; this is connected to intracellular signaling domains derived from either the 41BB or CD28 costimulatory proteins along with the intracellular CD3-zeta chain. This construct as a whole translates binding of the scFv to a target antigen into the TCR signaling cascade described in detail above, and facilitates killing of the target cell by the engineered T cell (Lim and June, 2017). This section will outline CAR-T biology and current clinical approaches utilizing this novel therapeutic modality.

Section 1.6.1 Current scFv Targets

scFv recognition and binding of a target antigen is the functional equivalent of TCR/MHC interaction in natural T cell target recognition. However, the use of an antibody domain in this case allows the CAR-T cell to target stable proteins on the surface of a target cell instead of peptide/MHC complexes. The affinity of this scFv/target binding event has important implications for CAR-T cell killing. CAR molecules with high affinity kill target cells in a more robust fashion (Richman et al., 2018), although this has also been shown to result in decreased cellular persistence (D'Angelo et al., 2018). The overall avidity of the scFv/target interaction is also related to the copy number of the target antigen, and is

an important determinant for the feasibility of targeting a given antigen (Ramakrishna et al., 2019). Thus, there must be a balance between expression level and scFv avidity in order to achieve optimal CAR-T cell activation. In general, highly expressed proteins have been the most popular CAR targets to date, but improved development of scFv and camelid nanobody binding domains may change this paradigm moving forward (Jackson et al., 2016; Xie et al., 2019). In total, scFv selection must be based on actionable target antigen density that is paired with scFv affinity high enough to trigger cytolysis, but low enough so as to not drive exhaustion and poor persistence.

The first and most clinically developed CAR-T target is the B cell lineage protein CD19. Anti-CD19 CAR-T cells have been in clinical testing for nearly a decade and have achieved ongoing complete response (CR) rates as high as 50% in refractory B-ALL (B cell acute lymphoblastic leukemia) (Maude et al., 2018). This is a remarkable achievement in a previously devastating disease and has sparked trials in additional indications such as B-CLL, Non-Hodgkin Lymphoma, DLBCL, and AML. Accordingly, this has sparked the development of other blood-focused targets such as CD20, CD22, and CD33 which have showed similar levels of pre-clinical efficacy and are currently undergoing clinical testing (MacKay et al., 2020).

There is considerable interest in expanding this treatment paradigm to solid tumors that comprise the majority of cancer incidence throughout the world. Targets for common solid tumors include PSMA (prostate-specific membrane antigen) in refractory prostate cancer (Zhong et al., 2010), HER2 in breast cancer (Ahmed et al., 2007), GD2 in glioblastoma (Pule et al., 2008), and mesothelin in lung and pancreatic cancers (Carpenito et al., 2009). While extensive pre-clinical research has suggested that such targets may provide viable strategies for targeting these cancers, convincing clinical data has not yet emerged to

support this idea. Alternatively, strategies have been developed that focus on cancer-specific mutations instead of wild-type proteins. These include unique glycosylation isoforms (Posey et al., 2016), and receptors (EGFRvIII) (Morgan et al., 2012). Again, preclinical results in this case are promising but clinical data are not yet available.

While ICB therapies have shown significantly more clinical efficacy in solid tumors than CAR-T cells thus far, CAR-T therapy possesses a crucial advantage that can be leveraged in the majority of cancer incidences. While endogenous T cells rely on chemokine cues and antigen processing of mutated proteins to enter and kill tumors (Fu and Jiang, 2018), CAR-T cells will enter and expand in previously un-infiltrated tumors on the basis of engineered target recognition (Posey et al., 2016). In this way, CAR-T cells may have the capacity to fundamentally alter the tumor microenvironment in a way that ICB therapies are not able to. Beyond this, the localized production of stimulatory cues and/or chemotactic molecules within the TME is likely to generate higher effective concentrations of relevant molecules than would be tolerable via systemic delivery (Sercombe et al., 2015). In this way, an engineered T cell might act as a signaling platform with the potential to fundamentally restructure the TME through delivery of beneficial cues that are specified by the engineer. Thus, one could envision many approaches that leverage underlying biology to improve the efficacy of both therapies in combination.

Section 1.6.2 Relevance of Costimulatory Domain

After physically binding an antigen target through the scFv, CAR-T cells must become activated to proliferate and kill target cells. In non-engineered T cells this is accomplished through a cascade revolving around the intracellular ITAM domains of the CD3 proteins

and relevant costimulatory Signal 2 proteins discussed in Section 1.1 and 1.2. This is mimicked in CAR-T cells through the addition of the ITAM domains of either 41BB or CD28 along with CD3-zeta. By connecting these intracellular domains in a single chimeric protein to the receptor-target synapse formed at the cell surface between scFv and target antigen, CAR-T cells are able to effectively mimic the naturally occurring antigen-recognition process hardwired into T cells during development (June et al., 2018).

Important differences have been identified between the T cell activation programs that are driven by differential use of the CD28 or 41BB intracellular costimulatory domain, despite superficially similar cellular functions. Notably, 41BBz CAR-T cells persist more robustly than CD28z counterparts (Kawalekar et al., 2016) and control tumors more effectively in some circumstances (Long et al., 2015). In contrast, CD28z-based CAR-T cells kill target cells more quickly and produce higher levels of inflammatory cytokines (Zhao et al., 2015). This has been associated with higher levels of cytokine release syndrome in the clinical setting (Davila et al., 2014) along with higher rates of fatal neurological complications (2018). However, this may point to a paradigm in which utilization of different intracellular domains can effectively tailor T cell function to individual tumor characteristics on a patient-by-patient basis. This is supported by research on additional costimulatory domains such as ICOS (Guedan et al., 2018) and MyD88 (Mata et al., 2017), which impose subtly different transcriptional programs following scFv/target recognition.

Differences in persistent or immediate inflammatory activation seem to be well-correlated to metabolic function. 41BBz signaling has been shown to impose a metabolic program of oxidative phosphorylation, while CD28z signaling favors glycolysis (Kawalekar et al., 2016). Indeed, this is consistent with published T cell biology in which oxidative phosphorylation is associated with long-lived central memory cells (Cui et al., 2015),

whereas glycolysis and its production of useful macromolecules is associated with the highly inflammatory expansion phase of T cell activation (Buck et al., 2016). Therefore, signaling strategies that favor aspects of both effector function and also persistence may capture beneficial aspects of both signaling modules.

Section 1.7 – CAR-T Limitations and Advances

Currently, there are many approaches to create “next-generation” CAR-T cells that have been proposed. Several strategies utilize engineered T cells as a source for the production of inflammatory molecules, while a number of additional genetic manipulations have been proposed to improve intrinsic function of the CAR-T cell itself. Finally, approaches targeting multiple tumor antigens have also been proposed to improve efficacy in both solid and liquid tumors. Importantly, the vast majority of these approaches are focused on improving function of the engineered cells as the primary effector cell for tumor clearance.

Section 1.7.1 Persistence and Functional Deficiencies

A major barrier to T cell function in solid tumors is a suppressive microenvironment characterized by anti-inflammatory cytokines, hypoxia, poor nutrient availability, and inhibitory ligands (Thommen and Schumacher, 2018). All of these factors enforce a state of T cell dysfunction on both endogenous and engineered T cells, and generally favor tumor growth. This is a major barrier to CAR-T cell efficacy and is the focus of a number

of engineering strategies designed to enhance persistence of CAR-T cells and therefore efficacy of the therapy itself.

Suppressive cytokines like TGFB and IL10 are produced by Tregs and tumor cells in order to limit T cell activation. Novel engineering approaches have demonstrated that the presence of these cytokines in the TME may be leveraged through the engineered expression of dominant negative or “switch” receptors. In the case of dominant negative receptors, suppressive signaling through the wild-type receptor is reduced by sequestering the active cytokine in a signaling-dead complex (Kloss et al., 2018). This is taken a step further in the case of switch receptors; here a chimeric protein is designed in which an inhibitory receptor such as PD1 is connected to an ITAM-containing intracellular domain of a costimulatory receptor such as CD28 (Liu et al., 2016a). In this way, a naturally suppressive signaling event is converted into a costimulatory signal for the T cell and the suppressive environment is interpreted by the cell in a different manner. This is a novel strategy, and one could imagine utilizing extracellular domains of suppressive cytokine receptors like IL10R or TGFBR (Roth et al., 2020), as well as inhibitory receptors like Tim3 or Lag3 with stimulatory intracellular domains of IL12R, MYD88, ICOS, or others. While this approach has yet reached the clinic, it represents an elegant solution to several adaptive immune resistance mechanisms.

Beyond switch receptors, genetic deletion of inhibitory proteins has emerged as another solution to T cell suppression. The elimination of inhibitory receptors such as PD1 and CTLA4 via CRISPR is an attractive and straightforward approach to limit these proteins’ effect on engineered T cell activation. Indeed, the first patients were recently treated with PD1-edited NYESO-1 T cells in a landmark study for the genome editing field (Stadtmauer et al., 2020); these cells were tolerated and demonstrated some increased efficacy,

showing this approach may be viable moving forward. In order to affect whole transcriptional networks, some groups have proposed that deletion of core transcription factors may be even more effective. Notably, the transcription factor Tox, and its' relatives NRA3/NRA4, have been recently shown to control core T cell exhaustion programs (Chen et al., 2019; Seo et al., 2019; Yao et al., 2019). Further, deletion of these transcription factors in models of adoptive cell therapy (ACT) improved anti-tumor T cell responses, demonstrating that such approaches may be translatable to clinical settings. Similar results were achieved by deletion of the ribonuclease REGNASE-1, demonstrating that multiple pathways contribute to the T cell exhaustion state (Wei et al., 2019). The absence of these factors enforces an effector-like state in transferred T cells, which can be similarly achieved through overexpression of transcription factors are positively correlated with effector T cell function such as c-jun (Lynn et al., 2019). In all, the major goal of these strategies is to block the exhausted T cell fate and to instead enforce a more functional effector-like transcriptional program with the goal of enhanced function for transferred T cells and therefore enhanced efficacy of ACT.

In addition to direct T cell suppression, solid tumors create poor nutrient environments by consuming necessary molecules like glucose at supraphysiological rates. This prevents neighboring cells from obtaining normal levels of these molecules. This competition for nutrients is exacerbated by irregular blood vessel networks that create zones of poor nutrient penetration that favor transformed tumor cells (De Palma et al., 2017). Typically, T cells upregulate glycolysis following activation, regardless of nutrient or oxygen availability. This is thought to generate both ATP and other macromolecules necessary for rapid proliferation and expansion, but requires the consumption of high levels of glucose (Buck et al., 2016). Interestingly, this phenomenon was first described in cancer

cells, and is known as the “Warburg effect” (Warburg, 1956). Thus, T cells are competing with tumor cells for limited nutrients to expand and persist within the TME in order to carry out effector functions and control tumor growth.

A number of strategies are emerging to tilt this competition in favor of T cells. Treatment with metabolism-altering drugs such as metformin, which favors fatty acid metabolism, improves persistence of T cells (Pearce et al., 2009). In theory this could be used either *ex vivo* during T cell expansion or *in vivo* following infusion. Similarly, expansion with IL-15 instead of IL-2 during the expansion phase of CAR-T cell manufacturing favors memory-like phenotypes that utilize oxidative phosphorylation (ox-phos) over glycolysis and persist more robustly *in vivo* (Alizadeh et al., 2019), this may also be recapitulated by enforcing STAT5-dependent IL7 signaling in engineered cells (Shum et al., 2017). Finally, genomic edits in genes such as PPARG and mTOR converge on similar functions and enhance ox-phos metabolism and persistence *in vivo* (Henriksson et al., 2019). A combination of these strategies may be optimal, and should be tested for their ability to improve engineered T cell function through orthogonal pathways.

Section 1.7.2 Target Heterogeneity

While strategies to improve T cell function have dramatically advanced in recent years, target heterogeneity in solid tumors remains difficult to address and represents a significant bottleneck in achieving long-term remissions for patients through cell therapy. This problem was not addressed in early CAR-T indications, as CD19 is expressed on almost all B cells, both malignant and healthy. Thus, successful CD19-directed CAR-T therapy eliminates the healthy B cell repertoire as well as malignant cells (Maude et al.,

2018). B cell aplasia is a tolerable side-effect given the disease, but this is not the case for most solid tumor CAR targets. This is the basis for concern about “on-target, off-tumor” toxicity for targets such as mesothelin and Her2. In this case, critical healthy tissues express the target antigen, and are attacked by CAR-T cells, which has led to serious toxicities (Morgan et al., 2010). Thus, target selection in solid tumors is generally a trade-off between these toxicities and identification of targets that are not expressed on healthy tissues, but are only expressed on a subset of cancer cells (Posey et al., 2016). This is of particular concern because multiple cases of CD19-negative leukemic relapse have been reported following CD19-directed CAR-T therapy (Gardner et al., 2016; Sotillo et al., 2015). This antigen-negative relapse mechanism is likely to be much more pronounced in solid tumors where a significant number of tumor cells will not be recognized by CAR-T cells. Therefore, addressing this problem of target heterogeneity is critical to successful therapeutic outcomes, as T cells optimally engineered for persistence and efficacy still will not eliminate cells that they do not recognize.

Strategies to solve this problem thus far have centered around combinatorial targeting. For example, “AND-gate” approaches aim to increase safety by requiring two input signals to trigger T cell activation. This has been accomplished through inducible promoters (Roybal et al., 2016), separation of activation domains (He et al., 2020), and pharmacological triggers (Wu et al., 2015). Alternatively, many groups have developed so-called “universal” CAR-T cells that recognize a common domain added to a repertoire of antibodies with varying specificity. For example, replacing the scFv domain of a CAR molecule with a domain that recognizes biotin (Lohmueller et al., 2017), an engineered Fc region (Rodgers et al., 2016), or leucine zipper (Cho et al., 2018) will trigger CAR-T activation. Engineered antibodies that bind several different tumor targets can then be

administered and antibody-bound tumor cells will be recognized by a single CAR-T cell product specific to the engineered constant region of the antibody. This approach seeks to overcome the heterogeneity problem by targeting multiple antigens at once, but is still limited by target validation, engineering capacity, and antibody diffusion kinetics. Finally, approaches centered around CAR-T infusion products containing multiple CAR-T specificities might overcome heterogeneity problems, but regulatory hurdles make this approach unlikely in the clinic. Even with optimal engineering, these approaches are limited to a repertoire on the order of 10^1 targets, and are therefore unlikely to achieve clearance of highly heterogenous tumors. Alternatively, the endogenous T cell repertoire can theoretically encode 10^{15} specificities (Laydon et al., 2015); this makes strategies that leverage endogenous immunity a particularly attractive approach for solving the heterogeneity problem.

Section 1.8 – Unresolved questions

Because of conflicting reports around the role of inflammation in the TME, a central goal of the field is to identify contexts that determine whether the activation of inflammatory pathways such as IFNG and IFN-I drives tumor resistance or response to ICB therapy. The existing data on this subject reviewed here suggest that this is likely dependent on a combination of antigen availability, MHC-I expression, and effector cell activation. Chapter 2 of this thesis will outline a mechanistic framework for how we believe IFNG affects these pathways, and how they compete and cooperate to determine outcomes following ICB therapy.

IFNG is produced mainly by the adaptive immune system. This response becomes engaged when the innate immune system is alerted to danger, a process traditionally mediated by PRR activation. Similar to inflammatory responses generated by the adaptive immune system, the role for context and localization of PRR signaling has not been well defined in the regulation of anti-tumor immune responses. In Chapter 3, we provide a framework based on cellular localization of these signals to explain pro- and anti-tumor effects of PRR signaling. Further, we outline a novel cell therapy approach to leverage these findings in syngeneic solid tumor models. These experiments provide a rationale for novel cell engineering approaches and provide insight into a crucial role for localization of PAMP signaling in the TME. In total, this thesis will outline a framework for understanding the contexts in which inflammatory signaling is beneficial or detrimental to anti-tumor immunity depending on cellular localization, and how this influences therapeutic survival outcomes.

CHAPTER 2 – OPPOSING FUNCTIONS OF INTERFERON COORDINATE ADAPTIVE AND INNATE IMMUNE RESPONSES TO CANCER IMMUNE CHECKPOINT BLOCKADE

Section 2.1 – Introduction

Immune checkpoint blockade (ICB) of the inhibitory receptors CTLA4 and PD1 can result in durable responses in multiple cancer types (Ribas and Wolchok, 2018). Resistance and relapse are common and can be influenced by factors inherent to immune cells, cancer cells, or both (Patel and Minn, 2018). Important immune features include the status of T cell infiltration and the differentiation or activation state of T cells and innate immune cells. Features intrinsic to cancer cells that can impact ICB outcome include their repertoire of neoantigens, the ability to present antigens on major histocompatibility complex class one (MHC-I), and the expression of inhibitory receptor ligands. The clinical relevance of these immune and cancer cell factors is highlighted by common biomarkers for ICB response such as type I or II interferon (IFN) stimulated genes (ISGs) (Ayers et al., 2017; Harlin et al., 2009), tumor mutational burden (TMB) (Rizvi et al., 2015; Snyder et al., 2014), and expression of PDL1 (Taube et al., 2012; Tumeh et al., 2014).

Both IFN-gamma (IFNG) and Type I IFN (IFN-I) are among the known pathways that have critical roles in anti-tumor immunity. IFN enhances immune function by inducing expression of MHC-I (Dighe et al., 1994), which is constitutively expressed on many tissues including cancer cells, and by enabling dendritic cells (DCs) to cross prime T cells (Diamond et al., 2011; Fuertes et al., 2011). In this way, IFNs are important in the early phase of antigen recognition and the interaction between adaptive and innate immune cells. Accordingly, loss-of-function mutations and genomic alterations in the IFN signaling pathway have been associated with clinical ICB resistance and/or relapse (Gao et al.,

2016; Shin et al., 2017; Zaretsky et al., 2016), and unbiased genetic screens have identified this same pathway as being important for immunotherapy response in certain mouse models (Manguso et al., 2017; Mezzadra et al., 2017). In contrast, some patients have tumors with mutations in the IFN pathway that nonetheless respond to ICB (Hellmann et al., 2018; Sade-Feldman et al., 2017) or have high serum levels of IFNG that associates with ICB progression (Huang et al., 2017). These apparently "paradoxical" observations may represent feedback inhibition properties of IFN signaling (Snell et al., 2017). In the context of chronic pathogen infection, persistent IFN signaling and ISGs dampen immune responses to prevent immune-mediated pathology while allowing for a host-pathogen stalemate (Cheng et al., 2017; Teijaro et al., 2013; Wilson et al., 2013). In cancer, this dichotomous function of IFN is exploited through chronic signaling by tumor cells that can promote resistance to ICB (Benci et al., 2016). IFN-driven resistance can be inhibited by genetic ablation of the IFNG receptor (IFNGR) and/or IFN-I receptor (IFNAR) in cancer cells, resulting in a decrease in PDL1, other inhibitory ligands, and the GzmB antagonist SERPINB9 (Jiang et al., 2018). Expansion of exhausted T cells (T_{EX}) can then ensue to restore ICB response through unknown mechanisms. Together, these observations highlight the importance of understanding how the opposing functions of IFN signaling impact cancer immunotherapy.

Loss of the beta-2 microglobulin (B2M) subunit of MHC-I appears to be a common resistance mechanism to ICB (Sade-Feldman et al., 2017). However, diminished expression or loss of B2M can also occur in patients who respond to ICB (Rizvi et al., 2018; Rodig et al., 2018), suggesting that innate immune cells might contribute to ICB response in some cases. Indeed, conventional NK cells and innate lymphoid cells (ILCs) are capable of destroying cancers through either perforin-mediated cytotoxicity or TNF-

family death receptors such as TRAIL (Spits et al., 2016). NK/ILC effector function is regulated through cellular maturation, combinations of activating and inhibitory receptors, and possibly immune checkpoint receptors like PD-1, TIM3, and TIGIT (Gao et al., 2017; Zhang et al., 2018). Recent evidence indicates that type one ILCs (ILC1s) can participate in anti-tumor immunity or cancer immune surveillance. This includes ILC1-like populations (Dadi et al., 2016) and intratumoral ILC1s that are generally poorly cytotoxic (Cortez et al., 2017; Gao et al., 2017). Although the ability of NK/ILC1s to eradicate tumors with diminished MHC-I and/or a poor neoantigens is of significant interest, how to mobilize these innate immune cells to facilitate tumor response is unclear.

Section 2.2 – ISGs Expressed by Cancer Cells Predict Resistance to Immune Checkpoint Blockade while ISGs Expressed by Immune Cells Predict Response

A large proportion of human cancers differentially express a subset of ISGs that can predict resistance to radiation and chemotherapy (Weichselbaum et al., 2008). Coincidentally, this ISG resistance signature (ISG.RS) is also associated with resistance to ICB, as demonstrated by elevated expression in murine tumors from Res 499 melanoma cells (Benci et al., 2019), which were derived from an ICB-resistant B16-F10 tumors (Twyman-Saint Victor et al., 2015). In contrast, ISGs can also predict clinical ICB response, especially ISGs typically associated with IFNG signaling (Ayers et al., 2017). To begin reconciling these seemingly disparate observations, we examined the ISG.RS and genes from the IFNG hallmark gene set (IFNG.GS) by dividing them into two non-overlapping subsets (Figure 2.1A) and creating a metagene (the average scaled expression of all genes in the set). The expression of these ISG metagenes was then examined across different cellular populations in human melanomas using previously

published single-cell RNA-seq data (Tirosh et al., 2016). This revealed that the IFNG.GS is predominantly expressed by intratumoral immune cells such as T cells, NK cells, and macrophages. In contrast, the ISG.RS is predominantly expressed in cancer cells, albeit with variable expression (Benci et al., 2019).

To understand the potential consequences of these differences in IFNG.GS and ISG.RS expression patterns, we analyzed bulk RNA-seq data combined from two cohorts of melanoma patients treated with anti-PD1 (Hugo et al., 2017; Riaz et al., 2017). As expected, the majority of genes in the IFNG.GS are depressed in the majority of tumors from non-responders to anti-PD1. However, like ICB-resistant murine Res 499 tumors, most ISG.RS genes are enriched in tumors from non-responders. Consistent with the importance of $CD8^+$ T cells in response, tumors with high IFNG.GS but low ISG.RS also have the greatest proportion of $CD8^+$ T cells as inferred by CIBERSORT (Newman et al., 2015). The higher frequencies of $CD8^+$ T cells are accompanied by increased number of activated NK cells, which also has been associated with clinical ICB response (Riaz et al., 2017). To understand how these immune and interferon-related variables independently contribute to ICB response, we utilized a multivariable logistic regression model. This revealed that while higher IFNG.GS increases the odds ratio for response, ISG.RS independently decreases the likelihood. The significance of both of these variables are independent of tumor mutational burden (TMB) status, which expectedly correlates with response. In contrast, neither the abundance of $CD8^+$ T cells nor NK cells are significant in the model. In total, these data suggest that while expression of IFNG.GS by immune cells is associated with $CD8^+$ T cell abundance, accumulation of activated NK cells, and ICB response, all of these effects are opposed by high levels of ISG.RS in cancer cells (Benci et al., 2019).

Although the IFNG.GS and ISG.RS predict opposite clinical outcomes, their expression is positively correlated, consistent with IFN controlling both metagenes (Figure 2.1B). An explanation for this apparent ‘‘paradox’’ lies in the relative expression of each metagene. When expression of the ISG.RS exceeds the IFNG.GS, resistance is favored (Figure 2.1B, left plot, red circles below diagonal). In contrast, most responses occur when IFNG.GS is similar to or greater than ISG.RS (Figure 2.1B, blue circles). Based on these findings, we combined the two metagenes into a ratio of IFNG.GS over ISG.RS (or, the difference of these two metagenes in log transformed space). By logistic regression, this composite variable (dISG) is strongly associated with response and is independent of TMB (Figure 2.1B, right plot and inset). Specifically, the probability of response is low when either the ratio or TMB is low but increases when either increase. Furthermore, random forest machine learning and bootstrapping revealed that the ISG ratio has the highest robustness and average variable importance compared to TMB and multiple immune features (data not shown, (Benci et al., 2019)).

In total, the single-cell and bulk RNA-seq analysis suggests that distinct ISGs differentially expressed by cancer and immune cells can oppose each other to influence $CD8^+$ T cell infiltrate and NK activation and can be combined into a ratio that predicts ICB response independent of TMB (Figure 2.1C). Motivated by these findings, we sought to understand the mechanistic underpinnings inferred by these statistical relationships.

Section 2.3 – Models Differing in MHC-I, TMB, and Neoantigen Status for Examining the Effect of Blocking Tumor IFN Signaling on ICB Response

If the probability of ICB response is influenced by the ratio of IFNG-related ISGs expressed by immune cells to inhibitory ISGs expressed by cancer cells, one way to enhance the ratio in favor of response is to prevent IFN signaling in cancer cells. We first confirmed whether the ISG.RS, which is elevated in ICB-resistant Res 499 tumors, is regulated by IFN signaling in cancer cells (hereafter referred to as tumor IFN signaling). Indeed, CRISPR knockout of IFNGR and/or IFNAR significantly diminishes ISG.RS levels (Benci et al., 2019). However, loss of tumor IFN signaling can render cancers less responsive to immunotherapy due to compromised MHC-I and antigen processing (Manguso et al., 2017; Zaretsky et al., 2016) suggesting that the impact from ablating tumor IFN signaling might be context dependent. In light of this, we surmised two situations whereby the benefit of inhibiting IFN-driven resistance could outweigh the potential negative impact on MHC-I. The first is when constitutive MHC-I is high, minimizing effects that loss of IFN-inducible MHC-I has on CTL-mediated killing. A second situation is when tumors have depleted or poor neoantigens. Here, diminished CTL recognition presumably makes MHC-I status less consequential for T cell-mediating killing, but interference with IFN-driven resistance might improve killing by NK or other innate lymphoid cells.

We first characterized various mouse tumor models for differences in MHC-I expression, TMB, and predicted neoantigen status (Figure 2.1D). Of these, CT26 colorectal cancer has the highest TMB, and maintains high MHC-I in the absence of IFNG signaling (Figures 2.1E and 2.1F). Similarly, TSA-derived Res 237 breast cancer cells also have high IFNG-independent baseline MHC-I but exhibit lower TMB (Figure 2.1D). In contrast, B16 and/or Res 499 melanoma have intermediate TMB and low constitutive MHC-I and rely on IFNG for high MHC-I expression (Figure 2.1D-F). Since Res 499 originated from an abscopal B16 tumor that relapsed several weeks after radiation (RT) plus anti-CTLA4 (Twyman-

Saint Victor et al., 2015), we surmised that Res 499 may additionally have undergone immunoediting prior to relapse. Recent evidence suggests that neoantigens that have clonal or near-clonal representation are predominantly targeted by the immune system, while neoantigens at low clonal fractions can remain immunologically silent (Gejman et al., 2018; McGranahan et al., 2016). In accord with this notion, there is a significant decrease in the cumulative frequency of predicted high affinity (< 100 nM) neoantigens with clonal (near-heterozygous or greater) frequencies in Res 499 compared to B16 (Benci et al., 2019). Together, these data define several tumor models that differ in reliance on IFNG for high MHC-I and in predicted neoantigen availability.

Figure 2.1

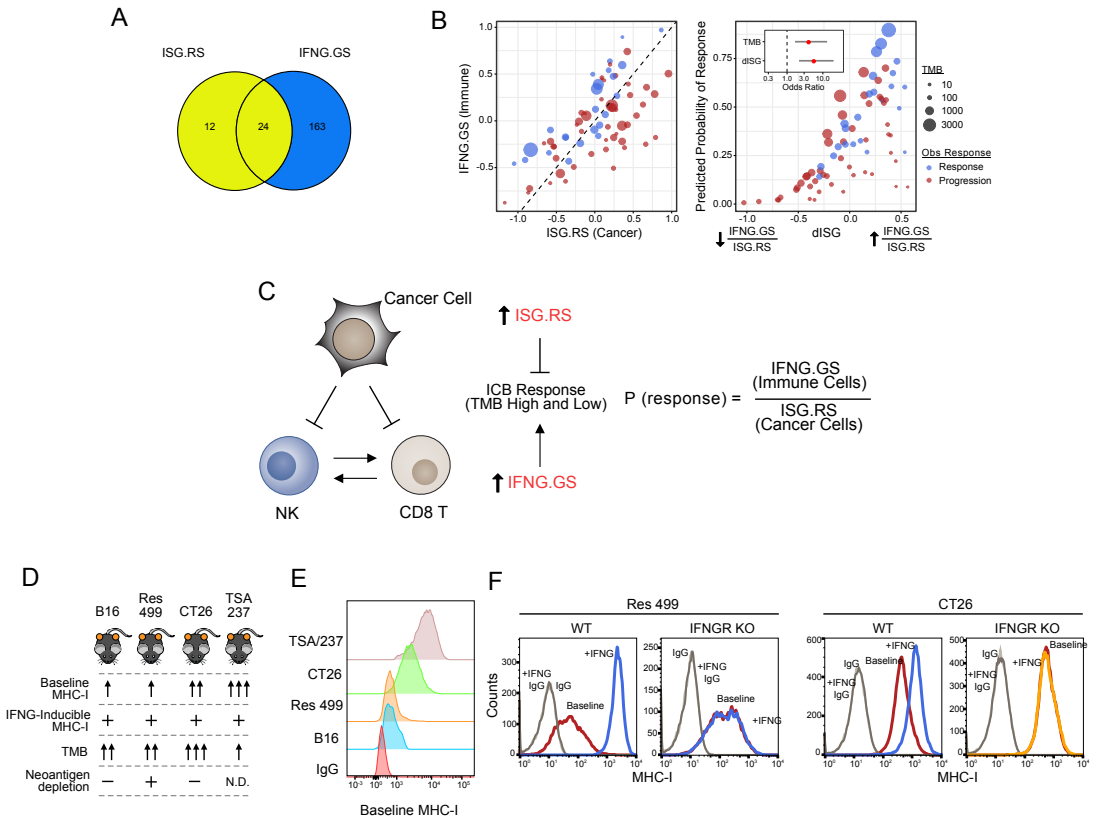

Figure 2.1. Distinct ISGs are differentially expressed in cancer and immune cells and have opposing functions in predicting clinical ICB response. A) Venn diagram of genes in the cancer-associated ISG.RS along with immune-associated hallmark IFNG-related genes (IFNG.GS) partitioned into non-overlapping gene sets (color-coded) and used to create individual metagenes. **B)** Expression of each metagene (left plot), and the predicted probability of anti-PD1 response (right plot) from a model using TMB and the ratio of IFNG.GS over ISG.RS (dISG). Odds ratios are shown in the inset. Circle color indicates response and size indicates TMB. **C)** Summary of cancer and immune cell relationships inferred by statistical modeling and how ISGs impact probability of ICB response. **D)** Summary of key properties of mouse tumor models. N.D. is not determined. **E)** Constitutive (baseline) and **F)** IFNG-inducible (+IFNG) MHC-I on indicated tumor cells with or without IFNGR KO.

Section 2.4 – Blocking Tumor IFN Signaling Broadly Improves ICB Response through $CD8^+$ T and Innate Immune Cells

We first used the CT26 model to examine whether tumors with high constitutive MHC-I and TMB demonstrate improved response when ISG.RS is decreased by blocking tumor IFN signaling. Remarkably, when IFNGR or both IFNGR and IFNAR are ablated, mice either show markedly slower tumor growth or spontaneous regression that is $CD8^+$ T cell dependent (Figure 2.2A), as determined by antibody-mediated depletion (Figure S2.2A). The addition of anti-PD1 further improves anti-tumor effects and survival. Both spontaneous regression and durable response to anti-PD1 requires B2M and hence MHC-I. All mice with complete response are also resistant to tumor rechallenge (8 out of 8 mice), further indicative of a T cell dominant response. Thus, decreasing ISG.RS by preventing IFN signaling in tumors with high baseline MHC-I does not interfere with CTL-mediating killing and markedly enhances immunogenicity.

Unlike CT26, B16 cells are reliant on IFN for high MHC-I expression. B16 tumors respond poorly to anti-PD1 but respond to RT + anti-CTLA4, a combination that enhances T cell repertoire diversity and improves response over anti-CTLA4 alone (Twyman-Saint Victor et al., 2015). Surprisingly, knockout of IFNGR and IFNAR in B16 tumors does not negatively impact the efficacy of RT + anti-CTLA4 (Figure 2.2B, top left plots, red versus orange), suggesting that other immune-mediated killing mechanisms may compensate for low MHC-I and compromised CTL recognition in this context. Indeed, partial response of IFNGR + IFNAR knockout tumors to RT + anti-CTLA4 is maintained even after B2M is ablated (Figure 2.2B, top left plots, gray versus light blue). However, when B2M knockout is accompanied by depletion of $NK1.1^+$ cells (Figure S2.2A), which are typically conventional NK cells and ILC1s, response is completely eliminated (Figure 2.2B, left top

and bottom plots, gray versus red). In contrast to B16, Res 499 tumors are resistant to RT + anti-CTLA4 and have relative depletion of predicted neoantigens. Despite this, knockout of IFNGR and IFNAR restores Res 499 response to levels at least as high as parental B16 tumors (Figure 2.2B, right plots). Consistent with loss of neoantigens and reliance on innate immune killing, co-ablation of B2M has no discernible effect, while depletion of $NK1.1^+$ cells alone abrogates the benefit from IFNGR + IFNAR knockout (Figure 2.2B, right top and bottom plots). However, if the requirement for high MHC-I and antigen is bypassed by using a murine chimeric antigen receptor (CAR) T cell against ectopically expressed human CD19 (Figure S2.2B), blocking tumor IFN signaling similarly improves response of both B16 and Res 499 tumors (Figure 2.2C). In the absence of CAR-T cells, IFNGR + IFNAR knockout tumors grow similarly to control (Figure S2.2C). Thus, blocking tumor IFN signaling can impact both $CD8^+$ T cell and NK/ILC1 effector function.

In total, these data suggest that blocking tumor IFN signaling can improve T cell-mediated killing when antigen recognition is not limited by inhibiting IFN function, as in the case of CT26 tumors or use of CAR-T cell therapy. In tumors with low MHC-I, preventing tumor IFN signaling may compromise CTL-mediated recognition but anti-tumor effects of NK/ILC1s can compensate to maintain response, as in the case of B16 tumors. In tumors such as Res 499 that are highly resistant and otherwise poorly recognized by T cells, the dispensability of MHC-I allows for restored response through NK/ILC1-mediated killing.

Section 2.5 – Inhibition of Tumor IFNG Signaling Enables $CD8^+$ T cells to Support NK/ILC1-Mediated Killing

To understand how blocking tumor IFN signaling restores ICB response in resistant or relapsed tumors and to avoid conflating effects of type I and II IFN, we focused on how IFNGR knockout restores response in the Res 499 model. We also opted to use

anti-CTLA4 monotherapy given that addition of RT does not significantly improve response over anti-CTLA4 alone (Figure 2.2D versus 2.2B). As expected for NK/ILC1-mediating killing, IFNGR knockout improves response to anti-CTLA4 in the absence of B2M and requires NK1.1^{+} innate immune cells (Figures 2.2D and S2.2D, credit-Joseph Benci). Interestingly, this response is also abrogated in the absence of CD8^{+} T cells, despite a lack of B2M on tumor cells. Thus, like with inhibition of both type I and II IFN signaling, blocking tumor IFNG signaling can restore ICB response by enhancing NK/ILC1-mediated effector function, likely through enhanced effector function supported by CD8^{+} T cells.

A similar requirement for both CD8^{+} T cells and NK/ILC1s is also observed after IFNGR knockout in the resistant TSA/237 breast cancer model that exhibits relatively low TMB and a paucity of predicted strong neoantigens (Figures 2.1D and S2.2E). These observations suggest that although CD8^{+} T cells do not directly kill IFNGR knockout Res 499 tumors, they may have a supportive role.

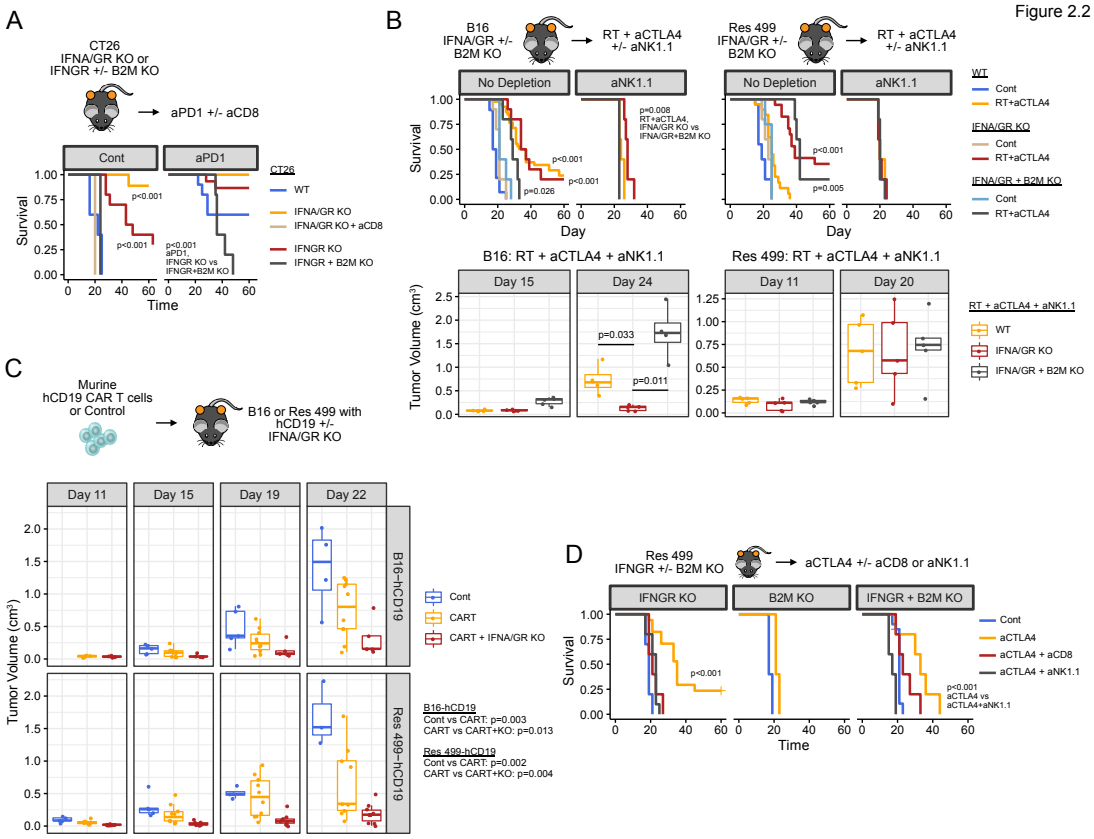

Figure 2.2. Preventing tumor IFN signaling promotes CD8$^+$ T cell-dependent and/or NK/ILC1-dependent ICB response. A) Survival of mice bearing CT26 tumors with KO of IFNGR +/- B2M or of both IFNGR and IFNAR (IFNA/GR) after no treatment (Cont), CD8 depletion (aCD8), or anti-PD1 (anti-PD1). For each group, n=5-15. **B)** Survival (top) and tumor volumes (bottom) after treatment with RT + anti-CTLA4 or control (Cont) for mice bearing B16 or Res 499 tumors with the indicated KO. Unless indicated, displayed p-values are for comparisons within each genotype (legend). For tumor volumes, only groups of interest are shown. Groups with no depletion: WT, n=20-28; IFNA/GR KO, n=10-20; IFNA/GR + B2M KO, n=4-5. For aNK1.1 groups, n=5. **C)** Tumor volumes for B16 and Res 499 tumors expressing human CD19 (hCD19) with or without IFNA/GR KO after a single infusion with primary murine T cells transduced with a CAR (CART) against hCD19. **D)** Survival of mice bearing IFNGR KO Res 499 tumors with or without concurrent B2M KO after treatment with anti-CTLA4. Effect of immune cell depletion with anti-CD8 or anti-NK1.1 is shown. IFNGR KO, n=5; B2M KO, n=5; IFNGR + B2M KO, n=10-20.

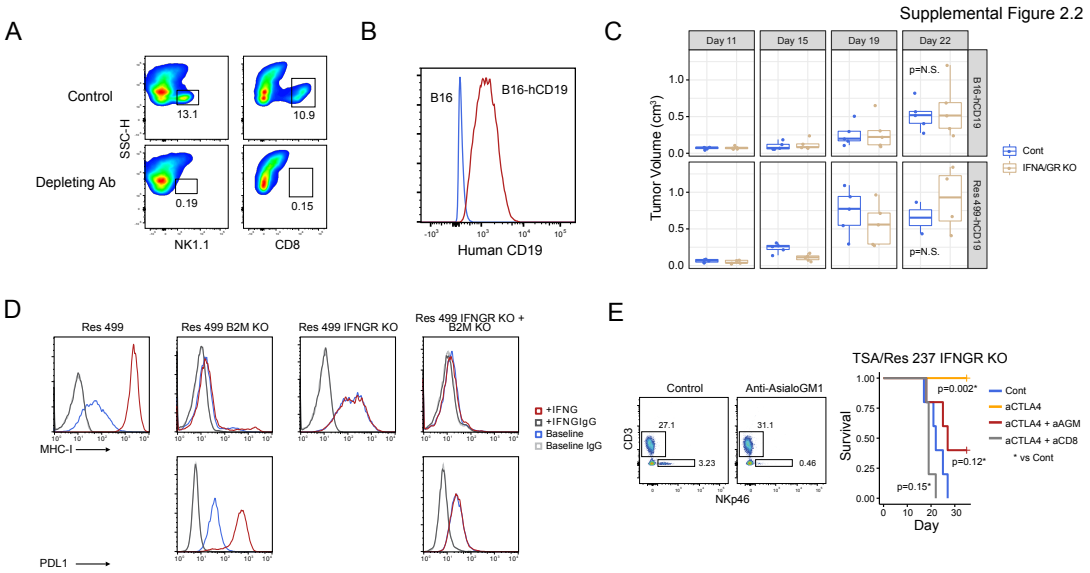

Supplemental Figure 2.2. Immune cell requirements for response after IFNGR knockout, Related to Figure 3. A) Representative density plots of tumor infiltrating CD45$^+$ lymphoid cells that are either NK1.1$^+$ or CD8$^+$ after control (top) or depletion with anti-NK1.1 (bottom left) or anti-CD8 (bottom right). **B)** Ectopic expression of human CD19 on B16 and Res 499 melanoma cells. **C)** Tumor growth of B16 and Res 499 tumors expressing human CD19 with (IFNA/GR KO) and without (Cont) concurrent IFNGR + IFNAR knockout. **D)** Baseline and IFNG-inducible expression of MHC-I and PDL1 on Res 499 cells with or without knockout of IFNGR and/or B2M. **E)** Survival of mice bearing TSA/Res 237 tumors with IFNGR knockout after anti-CTLA4 and prior depletion of CD8$^+$ T cells or NK/ILCs with either anti-CD8 (aCD8) or anti-Asialo-GM1 (aAGM), respectively. For all groups, n=5-10. On the left is a representative scatter plot of CD3$^-$ NKp46$^+$ intratumoral immune cells after control and depletion with anti-Asialo-GM1.

Section 2.6 – Preventing Tumor IFNG Signaling Enhances Immune Cell IFNG Signaling, $CD8^+$ T_{EX} Function, and Maturation of NK/ILC1 Cells

To examine how $CD8^+$ T cells might support NK/ILC1s, we employed single-cell RNA-sequencing (scRNA-seq) and 28-color flow cytometry. Analysis of intratumoral $CD45^+$ immune cells by scRNA-seq revealed that a dominant effect of tumor IFNGR knockout is an increase in the proportion of $CD8^+$ T cells (Figure 2.3A). Intratumoral $CD8^+$ T cells are typically exhausted and reside in either a progenitor exhausted or terminally exhausted population (Miller et al., 2019). Although terminally exhausted $PD1^+$ $CD8^+$ T cells have limited long-term proliferative potential, they can carry out various effector functions such as cytotoxicity and IFNG production (Miller et al., 2019; Paley et al., 2012). Gene set enrichment analysis (GSEA) using transcriptional signatures of these exhausted subsets (defined using the LCMV infection model) revealed that the expanded $CD8^+$ T cells resulting from IFNGR knockout show a marked increase in terminal exhaustion genes (e.g., Pdcd1, Eomes, Cd38) and a decrease in progenitor exhaustion genes (e.g., Tcf7) (Figures 2.3B and S2.3A). Accordingly, there is a per cell increase in the amount of IFNG protein produced by $PD1^+$ $CD8^+$ T cells, and after anti-CTLA4 there is a large increase in IFNG per gram of tumor (Figures 2.3C and S2.3B), which is not observed with cytokines such as IL-6 (Figure S2.3C, credit-Joseph Benci). Depletion of $CD8^+$ T cells largely abrogates this intratumoral increase in IFNG, highlighting the importance of exhausted $CD8^+$ T cells in generating this cytokine. Accompanying the increase in IFNG is a marked increase in the IFNG.GS primarily from myeloid/DC populations (Figure 2.3D). Among various IFNG.GS genes that increase include Cxcl9 and Cxcl10 (Figure 2.3E), which are chemokines implicated in NK cell recruitment, activation, or maturation (Pak-Wittel et al., 2013). Thus, disrupting tumor IFNG signaling not only decreases the ISG.RS in cancer cells but also increases production of IFNG by terminally exhausted $CD8^+$ T

cells. As an apparent consequence, myeloid/DC populations increase expression of IFNG.GS that include chemokines important in innate immune function.

In order to investigate how preventing IFNG signaling in tumor cells impacts NK/ILC1 status, we re-clustered NK/ILC1 populations identified by scRNA-seq (Figure 2.3F-G). This revealed NK populations differing in maturity and effector function (Chiossone et al., 2009), including an immature CD11blow population, an intermediate CD11bint population, and a mature CD11bhigh cluster that typically possesses the greatest effector function. Moreover, recently described ILC1 and intermediate ILC1 (intILC1) populations (Cortez et al., 2017; Gao et al., 2017) were also identified (Figure S2.3D). Knockout of tumor IFNGR results in a large shift in the NK populations toward the mature CD11b-high cluster and an additional shift toward the ILC1 cluster (Figure 2.3F, density plots). These ILC1s exhibit relatively high levels of Pd1 (*Pdcd1*) and TRAIL (*Tfnsf10*) (Figure 2.3G), consistent with previously reported properties for this population. Using 28-color flow cytometry (Figures S4E and S4F), we confirmed that tumor IFNGR knockout leads to an increase in the proportion of NK/ILC1s that are CD11bhigh NK cells or PD1+ TRAIL+ ILC1s (Figures 2.3H–4I and S2.2G). Flow cytometry also confirmed that this is accompanied by an increase in the proportion of terminally exhausted $CD8^+$ T cells, particularly after anti-CTLA4, as indicated by an increase in $PD1^+$ $Eomes^+$ $CD8^+$ T cells that express multiple inhibitory receptors and relatively high levels of Ki67 and GzmB (Figures 2.3H and S2.3G).

Together, these results indicate that preventing tumor IFNG signaling expands $CD8^+$ T_{EX} toward terminal exhaustion and increased production of IFNG. In this way, disrupting tumor IFNGR not only decreases ISG.RS in cancer cells but conversely increases IFNG.GS expression by immune cells. This enhanced IFNG signaling in immune cells

might then drive maturation and function of NK/ILC1 subsets, including a PD1+ TRAIL+ ILC1 population that potentially contributes to ICB response.

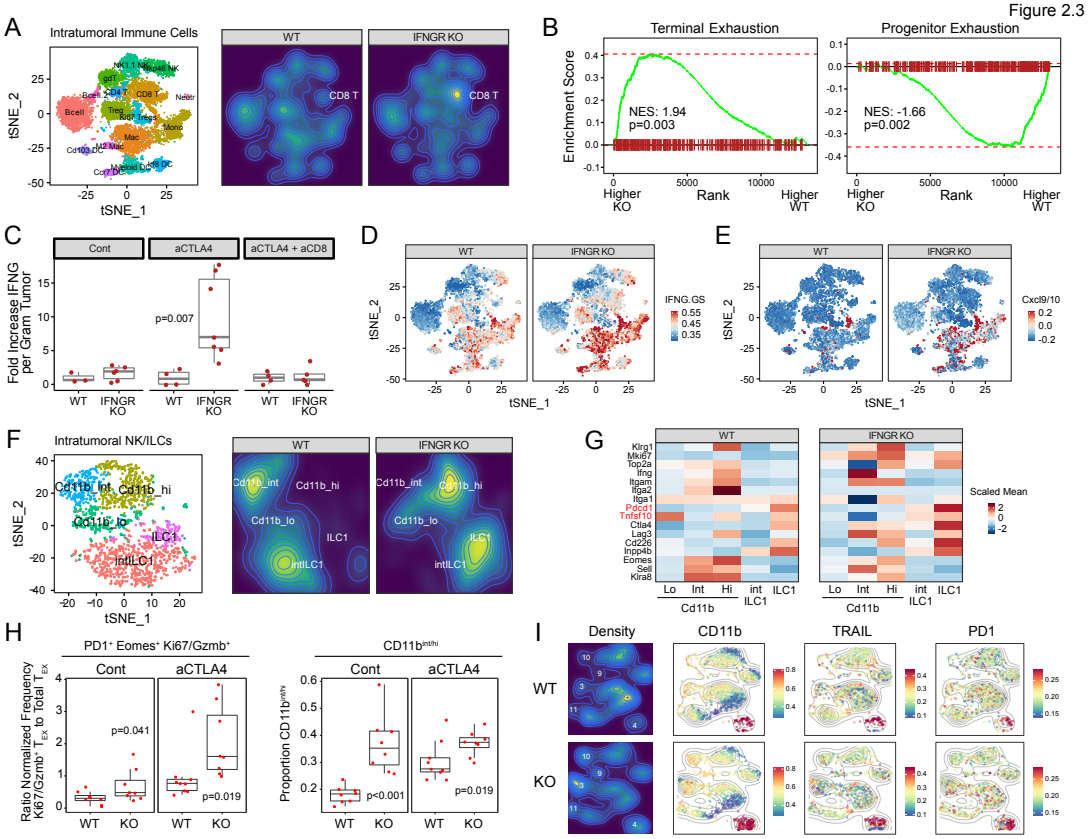

Figure 2.3. Blockade of tumor IFNG signaling promotes CD8$^+$ T$_{EX}$ expansion, IFNG production, immune cell IFNG signaling, and maturation of NK and PD1$^+$ TRAIL$^+$ ILC1 cells. CD45$^+$ immune cells from Res 499 tumors with or without IFNGR KO were profiled by scRNA-seq. **A)** tSNE plot with identified immune populations (left) and corresponding density plots (right). The percent of CD8$^+$ T cells is 6.4% and 16.8% in wild type (WT) and IFNGR KO tumors, respectively. **B)** GSEA on CD8$^+$ T cell clusters using T cell terminal exhaustion and progenitor exhaustion gene sets. **C)** Intratumoral IFNG protein levels from wild type or IFNGR KO Res 499 tumors treated with or without anti-CTLA4. Effect of CD8$^+$ T cell depletion (aCD8) is also shown. **D)** Expression of IFNG.GS or **E)** average expression of *Cxcl9* and *Cxcl10* across intratumoral immune cells from wildtype or IFNGR KO tumors overlaid on the tSNE map shown in (A). **F)** NK1.1$^+$ and NKp46$^+$ NK cell clusters from (A) were re-clustered. Shown is a tSNE plot with identified NK and ILC1 populations (left) and corresponding density plots (right). **G)** Average expression of select NK/ILC1 genes for each of the indicated NK or ILC1 maturation stage. **H)** CD8$^+$ T cells and NK/ILC1 populations were identified by 28-color flow cytometry. Shown is ratio of PD1$^+$ Eomes$^+$ CD8$^+$ T$_{EX}$ that belong to Ki67$^+$ GzmB$^+$ clusters over total PD1$^+$ Eomes$^+$ CD8$^+$ T$_{EX}$ (left) or the proportion of CD11b^{hi} NK and PD1$^+$ TRAIL$^+$ ILC1 cells relative to total NK/ILC1s (right). **I)** Density plots of NK/ILC1 clusters and expression of indicated markers overlaid onto a tSNE plot. Points are colored by scaled MFI and overlaid with a contour plot. Clusters 3, 9, 10, and 11 are CD11b^{hi} NK cells, and cluster 4 is PD1$^+$ TRAIL$^+$ ILC1 cells. See also Supplemental Figure 2.3.

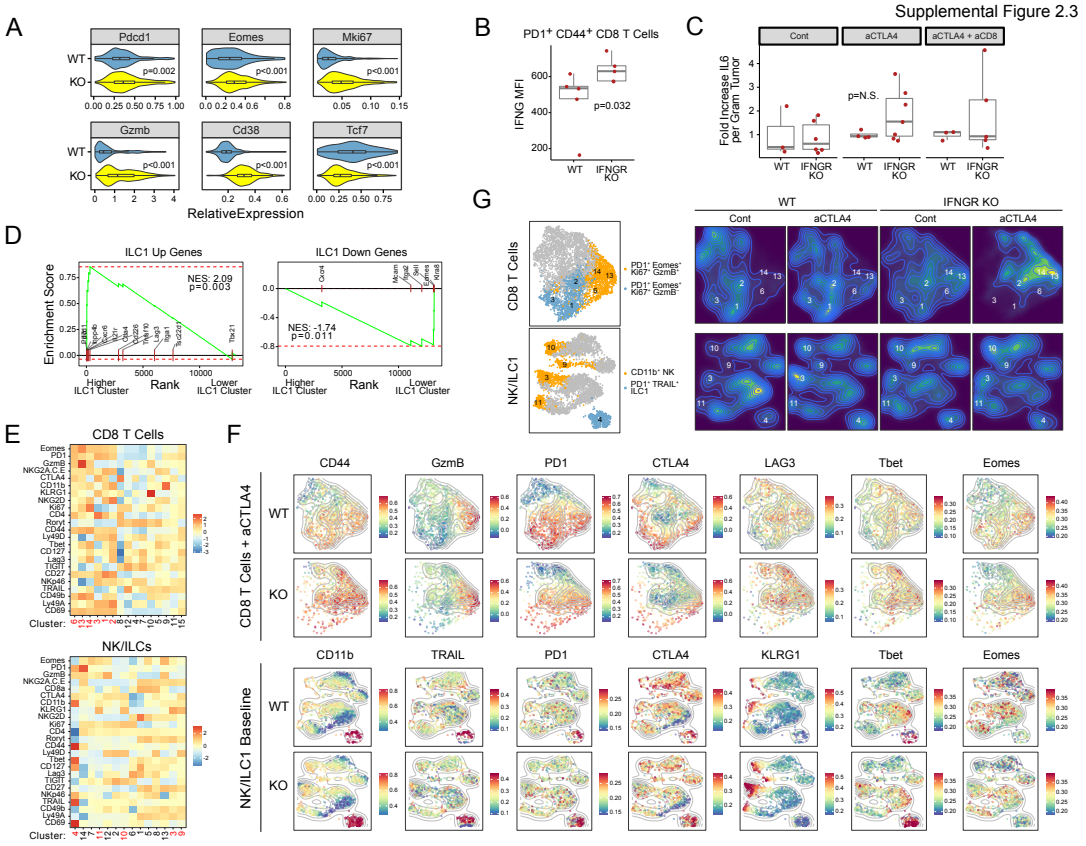

Supplemental Figure 2.3. Improved T_{EX} function and NK/ILC1 maturation after blocking tumor IFNG signaling, Related to Figure 2.3. A) Violin plots showing expression of the indicated genes in $CD8^+$ T cells from Res 499 wild type (WT) or IFNGR knockout (KO) tumors. **B)** Intracellular IFNG expression in tumor-infiltrating $CD44^+$ $PD1^+$ $CD8^+$ T cells and **C)** intratumoral IL6 protein levels from wild type or IFNGR knockout Res 499 tumors treated with or without anti-CTLA4. Effect of antibody-mediated $CD8^+$ T cell depletion (aCD8) on IL6 levels was also examined. **D)** GSEA comparing ILC1 cluster to other NK cell clusters using genes increased or decreased in ILC1s relative to conventional NK cells. **E)** Dimensionality reduction and cluster identification were performed on $TCRB^+$ $CD8^+$ T cells or $TCRB^-$ $NK1.1^+$ NK/ILC1s. Shown are heatmaps of the scaled MFI for each of the indicated markers across the identified clusters (labels below heatmap). For $CD8^+$ T cells, clusters representing $PD1^+$ $Eomes^+$ T_{EX} are denoted in red. For NK/ILC1s, clusters in red denote $CD11b^{high}$ innate immune cells. **F)** Contour plots showing the distribution of $CD8^+$ T cells after anti-CTLA4 (top) or of NK/ILC1s at baseline (bottom) in either wildtype or IFNGR knockout Res 499 tumors. Individual cells corresponding to the contour plot are overlaid and colored by the scaled MFI of the indicated marker. **G)** Density plots of $CD8^+$ T cells or NK/ILC1s in wildtype or IFNGR knockout Res 499 tumors treated with or without anti-CTLA4. The left plot is a tSNE map. For $CD8^+$ T cells, clusters for $PD1^+$ $Eomes^+$ T_{EX} with low or high expression of GzmB and Ki67 are color-coded and numbered. For NK/ILC1s, clusters enriched for $CD11b^{high}$ NK cells or $PD1^+$ $TRAIL^+$ ILC1 cells are color-coded and numbered. Cluster numbers correspond to cluster labels shown in (E).

Section 2.7 – Preventing Tumor IFNG Signaling Enables IFNG from CD8$^+$ T_{EX} to Drive NK/ILC1 Function while Removing Inhibitory Feedback from PD1/PDL1

Given the single-cell findings, we sought to investigate whether IFNG produced by CD8$^+$ T_{EX} is involved in NK/ILC1-mediated killing and whether the PD1/PDL1 pathway can contribute to response after IFNGR knockout. To test the role of IFNG produced by CD8$^+$ T cells, we adoptively transferred CD8$^+$ T cells from wild-type or IFNG knockout mice into RAG-deficient hosts and then implanted the mice with Res 499 IFNGR knockout tumors. This revealed that IFNG production by CD8$^+$ T cells is required for anti-CTLA4 response (Benci et al., 2019). Conversely, when CD8$^+$ T cells are depleted, there is a decrease in the proportion of mature CD11b$^+$ NK/ILC1s, as well as total NK/ILC1s (Figure 2.4A). However, direct intratumoral injection of IFNG or CXCL10 can rescue or partially rescue the loss in NK/ILC1 cells (Figure 2.4B). NK/ILC1-dependent ICB response and survival that is also compromised after depleting CD8$^+$ T cells is similarly rescued by injection of IFNG (Benci et al., 2019). Thus, these results suggest NK/ILC1-dependent response resulting from blocking tumor IFNG signaling relies on IFNG produced by CD8$^+$ T_{EX} and on downstream chemokines such as CXCL10.

Although IFNG has a critical role in promoting NK/ILC1 function, it also induces high levels of PDL1 on tumors. Given that PD1 is expressed on ILC1 cells, this suggests that the PD1/PDL1 axis may normally function as an IFNG-directed feedback inhibition mechanism to antagonize innate immune function, similar to its role in regulating T cell responses. If so, removal of this feedback inhibition by IFNGR knockout may contribute to the improved response resulting from blocking tumor IFNG signaling. To examine this, we ectopically expressed PDL1 in PDL1 knockout Res 499 tumors to make PDL1 levels independent of IFNG signaling. In contrast to wild-type or B2M-deficient Res 499 tumors,

the ability of IFNGR deletion to improve anti-CTLA4 response is lost when PDL1 levels are fixed (Benci et al., 2019). To remove effects of PD1 from $CD8^+$ T cells, we depleted $CD8^+$ T cells but restored NK/ILC1 function in IFNGR-deficient Res 499 tumors by intratumoral administration of IFNG (Figure 2.4C, red boxplots). Consistent with tumor PDL1 inhibiting NK/ILC1 killing, fixing high PDL1 expression despite IFNGR knockout blunted NK/ILC1-dependent ICB response. The notion that PD1/PDL1 can directly inhibit NK/ILC1 killing was also corroborated by using $CD49a^+PD1^+$ liver NK cells cultured with IFNGR-deficient Res 499 cells with and without ectopic PDL1 (Benci et al., 2019). In total, these results suggest that tumor IFNG signaling normally drives feedback inhibition through tumor PDL1 to regulate NK/ILC1 function. Thus, ablating tumor IFNGR not only increases immune cell IFNG signaling but also enhances innate immune killing by interfering with the PD1/PDL1 inhibitory axis.

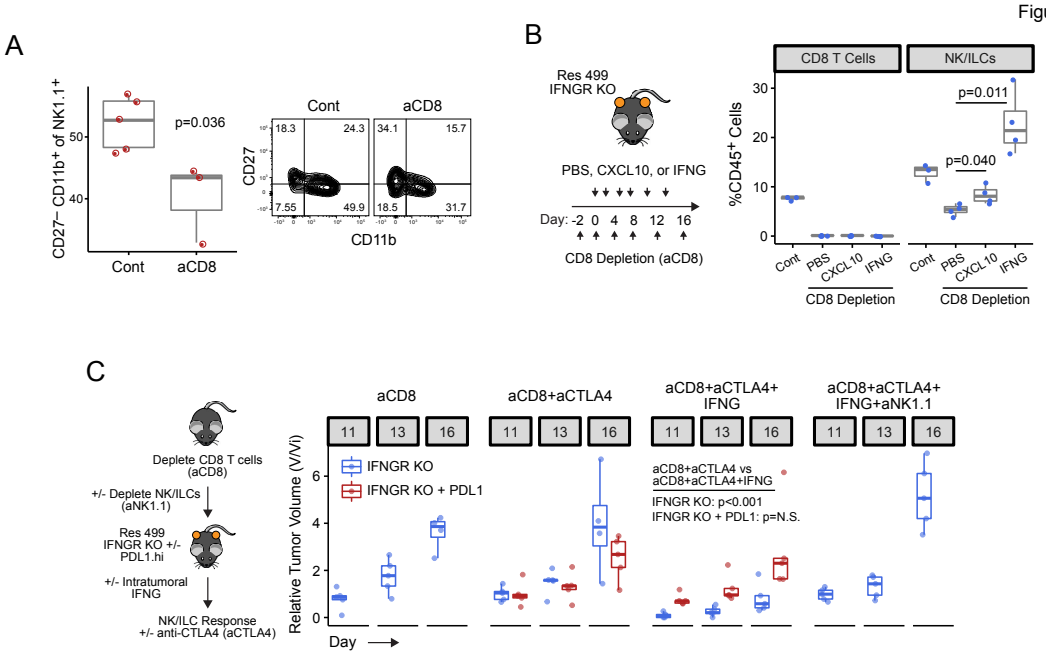

Figure 2.4. NK/ILC1-mediated killing from blocking tumor IFNG signaling is regulated by IFNG produced by T_{EX} and PDL1. A) Proportion of mature $CD27^{-}$ $CD11b^{+}$ NK/ILC1s in Res 499 tumors after $CD8^{+}$ T cell depletion (aCD8). Representative flow cytometry contour plots are shown. **B)** Mice bearing IFNGR KO Res 499 tumors were depleted of $CD8^{+}$ T cells followed by intratumoral injection of the indicated cytokine. Shown is the percentage of intratumoral $CD8^{+}$ T cells and NK/ILC1s. **C)** Response of IFNGR KO Res 499 tumors in $CD8^{+}$ T cell-depleted mice. Mice were treated with anti-CTLA4 with or without intratumoral injection of IFNG. Effect of concurrent depletion of NK/ILC1s with anti-NK1.1 is also shown as well as effect of high constitutive PDL1 on IFNGR KO tumors (red boxplots). Tumor volumes are relative to initial control tumor volume.

Section 2.8 – Adaptive Immune Cell Requirements for Innate Immune Cell Killing After Blocking Tumor IFNG Signaling

Despite our findings that response after IFNGR knockout of Res 499 tumors requires IFNG produced by $CD8^+$ T cells, the dispensability of tumor MHC-I argues that antigen presentation by tumor cells is not necessary for $CD8^+$ T_{EX} to support NK/ILC1 function. To corroborate this, we implanted Res 499 tumors deficient in both IFNGR and B2M in either wild-type mice or OT-1 mice expressing a transgenic T cell receptor to OVA antigen, which is not expressed by Res 499 tumors. The accumulation of both intratumoral $CD8^+$ T cells and NK/ILC1s is reduced and ICB response is lost in OT-1 mice compared to wild-type mice. However, intratumoral injection of OVA peptide rescued the compromised $CD8^+$ T cell frequency and partially restored NK/ILC1 levels. Moreover, despite the absence of tumor MHC-I, response to anti-CTLA4 was also partially rescued. Thus, the ability of IFNGR knockout to enhance NK/ILC1-dependent ICB response need not depend on antigen presentation by tumor cells themselves. Rather, cross-primed and/or activated bystander T cells can suffice (Benci et al., 2019).

Section 2.9 – Tumor Mutations in IFN Pathway Genes Predict Clinical Response to Dual Blockade of PD1 and CTLA4

Our findings suggest that mutations predicted to reduce tumor IFN signaling might associate with decreased ISG.RS and improved clinical response to ICB. To investigate this, we extended the analysis of recently described exome-sequencing data of non-small cell lung cancer (NSCLC) patients from either TCGA or a clinical trial using anti-PD1 plus anti-CTLA4 (Hellmann et al., 2018). After excluding common non-disease single-nucleotide variants, pathogenic missense and nonsense mutations were predicted using two algorithms, CADD and DANN, that were trained on a catalog of benign and pathogenic

variants from the ClinVar database. Indels were also evaluated as damaging or neutral using SIFT. In the TCGA, there is an 8.6% incidence of patient tumors with at least one predicted pathogenic variant in a core set of 11 type I and II IFN pathway genes (Benci et al., 2019). These tumors exhibit a decrease in ISG.RS genes, consistent with an enrichment for IFN pathway variants with defective signaling (Figure 2.5A). In the patients treated with anti-PD1 plus anti-CTLA4, 14.7% of patients have at least one IFN pathway variant and these patients have improved progression-free survival (PFS) with dual ICB (Figures 2.5B). In contrast, only 0.58% of random gene sets of similar size yield PFS differences that are as significant, and IFN pathway variants do not associate with survival in TCGA patients (data not shown), arguing that variant status is not a general prognostic marker. Notably, despite a higher likelihood of response, variant-positive tumors exhibit lower percent tumor PDL1 expression (5.4% versus 20.3%; Figure 2.5C, credit-Wolchok laboratory), consistent with variants having a negative impact on tumor IFN signaling. In contrast, stratification by variant status of random genes rarely yields a difference in % PDL1 this large (data not shown). Notably, one patient had a tumor with multiple alleles of B2M with a frameshift indel or predicted pathogenic missense mutations who nonetheless had a PR to ICB (Benci et al., 2019). This is consistent with previous reports describing a NSCLC patient responding to anti-PD1 despite deleterious B2M mutations and loss of B2M expression confirmed by immunohistochemistry (Rizvi et al., 2018). Thus, genetic alterations of the IFN pathway in human NSCLC are associated with decreased ISG.RS, decreased tumor PDL1, and improved ICB response independent of TMB status.

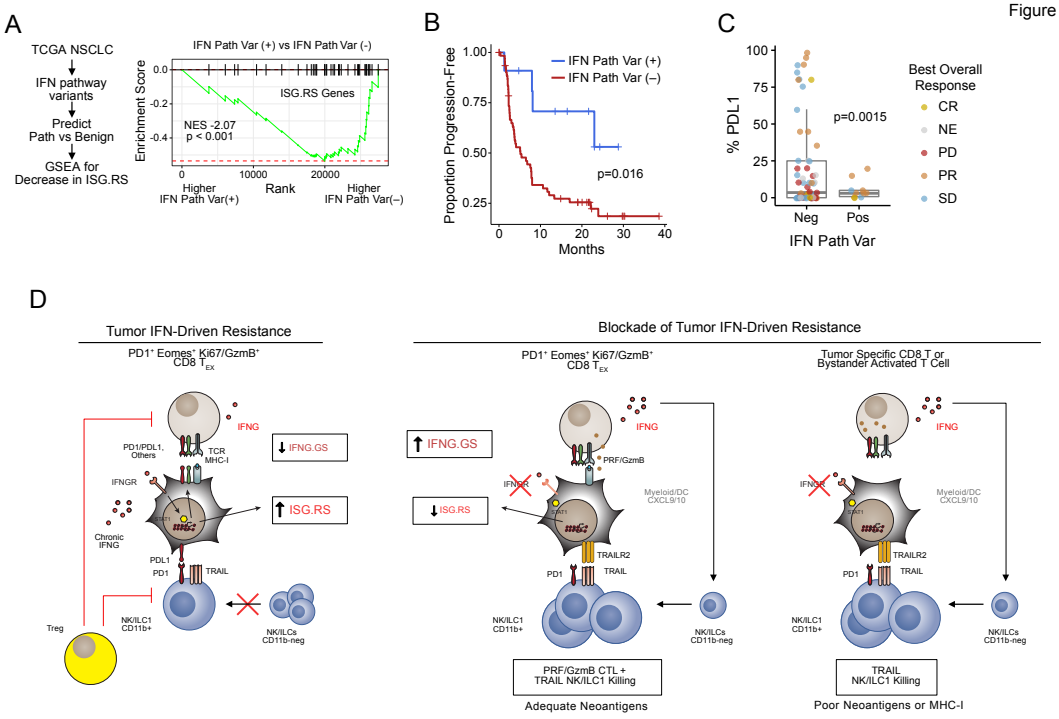

Figure 2.5. Tumor mutations in the IFN pathway predict decreased ISG.RS and increased survival in lung cancer patients treated with anti-CTLA4 and anti-PD1. **A)** GSEA of ISG.RS genes comparing TCGA NSCLC patients with and without a predicted pathogenic variant in the IFN pathway (IFN Path Var). **B)** Progression-free survival after anti-CTLA4 and anti-PD1. **C)** Boxplot of %PDL1 staining and response. **D)** Model for how the opposing roles of IFN signaling in immune and tumor cells regulate ICB response in tumors differing in neoantigen and MHC-I status.

Section 2.10 Discussion

In this study, we describe how IFNG signaling in tumor cells antagonizes both T cell and innate immune responses. This is accomplished through an inhibitory feedback circuit orchestrated by tumor cells whereby IFNG from immune cells not only regulates its own inhibition but tightly controls adaptive and innate immunity (Figure 7G). Our current and previous findings suggest several main components to this IFNG circuit. First, we previously reported that persistent IFNG signaling can initiate epigenetic changes in cancer cells characterized by enhanced STAT1-associated open chromatin (Benci et al., 2016) that includes loci for ISGs belonging to ISG.RS genes (unpublished data). Since resistance caused by persistent IFNG signaling can take several weeks to establish, these results suggest that the first component of the feedback circuit is the establishment of an epigenetic landscape in cancer cells that is permissive for enhanced ISG.RS expression. The second component is enforcing T cell exhaustion through high levels of PDL1 and likely other inhibitory ligands, which may include HVEM, LGALS9, and others (Benci et al., 2016). How the increase in these inhibitory ligands are mechanistically related to the epigenetic changes is currently unclear. Nonetheless, the end result is interactions between cancer and immune cells that favor an exhausted T cell state characterized by decreased IFNG and CTL function. The third component is inhibition of innate immunity by impeding NK/ILC1 effector function and differentiation. IFNG signaling in cancer cells not only increases PDL1 but decreases TRAILR2, which is the receptor for TRAIL expressed on some ILC1 cells (Benci et al., 2019). Consequently, cytotoxicity from $PD1^{+}$ $TRAIL^{+}$ NK/ILC1 cells is antagonized. Additionally, the decreased production of IFNG by T cells further safeguards against innate immune killing by stalling NK/ILC1 recruitment and/or maturation. This may be at least partly due to diminished expression of CXCL9/10

from myeloid cells. Thus, IFNG signaling in cancer cells orchestrates feedback inhibition on multiple levels to limit both adaptive and innate immune function.

By preventing tumor IFNG signaling, both adaptive and innate immune functions are unleashed (Figure 7G). However, the degree to which each of these effector arms contribute to response is context dependent. In tumors that are less reliant on IFNG for high MHC-I expression and antigen presentation (e.g., CT26 and TSA), blocking tumor IFNG signaling enables T_{EX} to coordinate both CTL- and NK/ILC1-mediated responses. For tumors with low baseline MHC-I that are reliant on IFNG to elevate MHC-I expression (e.g., B16), a decrement in CTL killing is likely; however, the presence of innate immune killing can help to maintain overall response. For tumors such as Res 499 with poor neoantigens and low MHC-I, or for tumors that have lost B2M, compromised IFN-inducible MHC-I is likely inconsequential. Here, enhanced IFNG production by cross-primed T_{EX} or possibly activated bystander T cells increases IFNG signaling in immune cells and maturation of NK/ILC1s. Ablating tumor IFNG signaling may particularly help activate otherwise poorly cytotoxic $PD1^+$ $TRAIL^+$ ILC1 cells by increasing tumor TRAILR2, decreasing PDL1, and/or altering other inhibitory pathways present on NK cells and/or ILC1s (Figure 2.3G). Thus, preventing tumor IFNG signaling enhances both adaptive and innate immune effector function but the magnitude that each contributes to response is context-dependent – in particular, MHC status and antigen availability are likely key determinants.

Even if $CD8^+$ T cells are not able to effectively mediate direct cytolytic tumor killing, the ability of T_{EX} to generate IFNG is important to promote NK/ILC1 function. Preventing tumor IFNG signaling both enhances $CD8^+$ T cell abundance and drives them toward terminal exhaustion, a state characterized by high IFNG production compared to progenitor T_{EX}.

Our studies also suggest that IFNG produced by cross-primed and/or activated bystander T cells might be sufficient to sustain NK/ILC1 maturation and NK/ILC1-dependent tumor killing. These findings have relevance for bystander T cells to common viruses and other non-tumor antigens that not only are abundant in human tumors (Simoni et al., 2018) but can be leveraged for immunotherapy (Rosato et al., 2019). One reason why antigen-restriction may not be required is because the stimulatory effects of IFNG on NK/ILC1s are indirect. IFNG from $CD8^+$ T cells appear to increase IFNG.GS expression predominantly in DC and myeloid cells, and IFNG.GS genes such as *Cxcl10* then influences intratumoral NK/ILC1 abundance. In melanoma patients, IFNG.GS is also highest in macrophages and positively correlates with the proportion of activated intratumoral NK cells (Benci et al., 2019). Thus, tumor-specific T_{EX} or activated bystander T cells can enhance innate immune responses against cancer when tumor IFNG signaling is blocked.

CHAPTER 3 - Delivery of Immunostimulatory RNA by CAR-T Cells Activates RNA Pattern Recognition Receptors and Endogenous Immunity to Overcome Tumor Resistance

Section 3.1 – Introduction

Cell therapies such as chimeric antigen receptor (CAR) T cells have generated remarkable outcomes in a small subset of liquid cancers. Unfortunately, these therapies remain ineffective in the majority of solid tumors. Among the factors that contribute to poor efficacy in solid tumors are poor expansion and persistence of transferred cells in the tumor microenvironment (Martinez and Moon, 2019). However, even if CAR-T cells do successfully engage cancer cell targets, a fundamental limitation of singly-targeted adoptive cell therapies is the outgrowth of tumors arising from cells that have lost expression of CAR-specific antigen (Gardner et al., 2016; Sotillo et al., 2015). In contrast to adoptive cell therapy, immune checkpoint blockade (ICB) stimulates endogenous T cells of multiple specificities and/or activates innate immune cells to potentially yield a polyclonal anti-tumor response (Keskin et al., 2019; Wu et al., 2020). However, due to a low mutational burden and immunoediting in most cancers, the lack of strong neoantigens can make this endogenous T cell repertoire ill-equipped for effective tumor eradication. For both CAR-T cell and ICB therapy, expression of negative immunoregulatory genes such as PDL1 (Liu et al., 2016a) and production of suppressive cytokines like TGFB (Kloss et al., 2018; Tang et al., 2020) within the tumor microenvironment (TME) are additional barriers that impede immunotherapy response. Thus, strategies that simultaneously employ CAR-T cells, enhance endogenous T cell function, and counteract common suppressive mechanisms may offer effective approaches to improve solid tumor response.

Damage-associated and pathogen-associated molecular patterns act as ligands for pattern recognition receptors (PRRs) that signal tissue injury and/or pathogen invasion. The activation of PRRs can initiate an innate immune response that is a prerequisite for mounting successful adaptive immunity. RIG-I and MDA5 are cytoplasmic PRRs that typically recognize virus-encoded double stranded RNA (dsRNA) with a 5'-triphosphate. Upon activation, these PRRs aggregate with the MAVS signaling platform (Reikine et al., 2014) to enhance production of interferon (IFN) and induce transcription of interferon stimulated genes (ISGs). Such innate immune signaling is particularly important for myeloid and/or dendritic cells (DCs) to effectively prime and/or activate T cells (Kandasamy et al., 2016; Sprokholt et al., 2017a). For example, viral RNA or synthetic mimetics such as poly I:C can promote anti-tumor T cell responses by improving co-stimulation and antigen presentation in T cell/DCs interactions (Hammerich et al., 2019; Salmon et al., 2016). However, recent evidence demonstrates that endogenous nucleic acids can also serve as damage-associated molecular patterns (DAMPs) to activate PRRs. RN7SL1 (7SL) is a highly structured noncoding RNA that is present in all cell types and conserved from humans to bacteria (Denks et al., 2014). Under homeostatic conditions, 7SL functions as a molecular scaffold crucial for protein translation. In this role, it is decorated by a number of RNA binding proteins that shield it from recognition by cytosolic RNA sensors such as RIG-I and MDA5 (Halic and Beckmann, 2005). However, under pathological conditions, decreased interaction with RNA binding proteins enables 7SL to become unshielded and secreted via extracellular vesicles (EVs) such as exosomes. Consequently, unshielded 7SL now mimics viral RNA to activate a RIG-I-dependent inflammatory response in cancer cells and myeloid cells (Nabet et al., 2017).

Although DAMPs can activate PRRs in cancer cells and immune cells, the consequences of inducing a type I IFN (IFN-I) or type II IFN response in each cell type for mounting an effective anti-tumor immune response can be complex and even opposing. While PRR activation and IFN signaling in DCs can be immunostimulatory, PRR and IFN signaling in cancer cells can drive cancer progression and enhance immunosuppression that leads to immunotherapy resistance (Benci et al., 2016; Boelens et al., 2014; Liu et al., 2016b). The immunosuppressive effects of tumor-intrinsic activation of ISGs is thought to occur through multiple mechanisms that include induction of immune inhibitory genes and genes that influence immune-mediated tumor killing. Thus, directing PRR and IFN signals toward immune cells and away from cancer cells may improve cancer immunotherapy (Benci et al., 2019).

In this study, we engineer CAR-T cells to deploy 7SL to selectively activate PRR signaling in immune cells as opposed to cancer cells. As a consequence, this enables CAR-T cells to productively activate myeloid and dendritic cells, recruit endogenous T cells, and generate effective immunity against solid tumors.

Section 3.2 – Biasing PRR activation through 7SL RNA away from cancer cells improves immunotherapy response

We produced *in vitro* transcribed 7SL and a control RNA with the same nucleotide composition as 7SL but scrambled in its sequence (Scr). Additionally, a ribozyme sequence was used to generate a uniform 3' end. The 7SL RNA has extensive RNA secondary structure, while the Scr RNA is predicted to lack widespread dsRNA regions (Nabet et al., 2017). Both RNAs have a 5'-triphosphate, which is a feature that promotes

recognition by RIG-I. Compared to cellular RNA, which is primarily comprised of ribosomal RNA with a 5'-monophosphate, transfection of 7SL into B16-F10 melanoma cells or human DCs induces ISGs such as MHC-I, PDL1, or CD86 (Fig. 3.1A and S3.1A-B). ISG induction also occurs after transfection with poly I:C, which served as a positive control, or with the Scr RNA. Interestingly, the ability of 7SL to stimulate ISGs is dependent on both RIG-I and MDA5. In contrast, Scr RNA and Poly I:C only require one PRR or the other. Thus, although 7SL and Scr RNA both induce ISGs, 7SL RNA utilizes and/or relies on both RIG-I and MDA5, indicating that its' signaling requirements may be distinct.

To determine the consequence of 7SL and Scr RNA recognition *in vivo* we implanted B16 tumors into the flanks of wildtype mice and injected liposome-encapsulated RNA intratumorally. While cellular and Scr RNA have minimal effect compared to a liposome-only control, intratumoral injection of 7SL enhances tumor growth and decreases survival in mice unable to mount a T cell-dependent adaptive immune response due to T cell depletion (Fig. 3.1B). These results are consistent with our previous findings demonstrating that the activation of RIG-I by 7SL in cancer cells can promote tumor growth and metastasis in an immunocompromised setting (Nabet et al., 2017). To determine the effect of 7SL when the immune system is intact and activated, mice were treated with immune checkpoint blockade using anti-PD1 plus anti-CTLA4 rather than $CD8^+$ T cell depleting antibodies. In this context, intratumoral injection of 7SL improves ICB response, while Scr and cellular RNA continue to have minimal effect (Fig. 3.1C). Accordingly, 7SL RNA also augments infiltration of proliferating and activated T cells, as well as enhances the frequency of intratumoral DCs (Fig 3.1D-E, Fig S3.1D). Thus, these results suggest that although stimulation of cancer cell-intrinsic RIG-I can promote tumor growth, this deleterious effect can be offset by the ability of 7SL to also promote immune activation.

Considering that activating cancer cell-intrinsic RIG-I can have unfavorable effects on tumor growth, we reasoned that stimulation of cancer cell RIG-I by 7SL might also negatively impact immune function even in the presence of ICB. Indeed, when B16 melanoma cells with RIG-I knockout are implanted into flanks of mice and then treated with intratumoral 7SL RNA plus ICB, tumor response is improved compared to control wildtype B16 tumors (Fig 3.1F). In contrast, treatment with ICB alone does not favor response in RIG-I knockout tumors, suggesting that cancer cell RIG-I does not impact immunotherapy response in the absence of stimulatory RNA. In total, these results suggest that although 7SL can enhance immunotherapy, RIG-I activation in cancer cells can contribute to suboptimal response. Thus, strategies that bias delivery of 7SL away from cancer cells in favor of immune cells might improve the efficacy of immunotherapy.

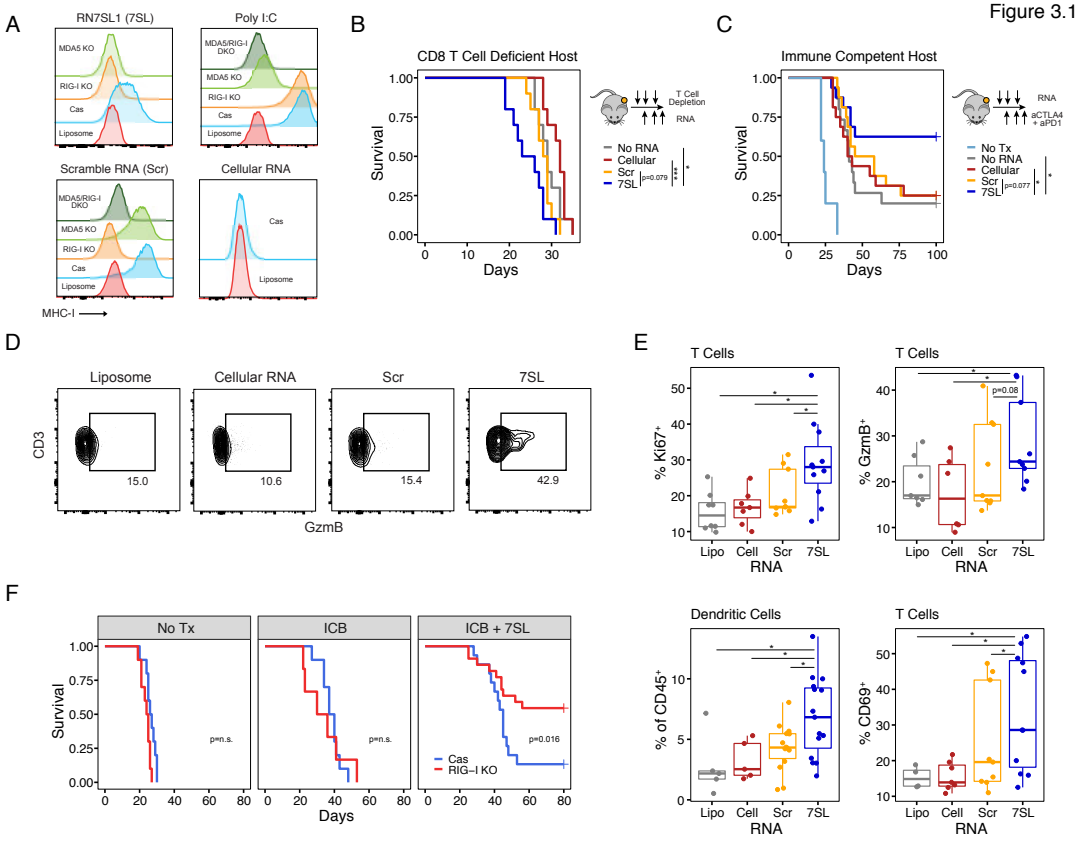

Figure 3.1. Localization of 7SL signaling dictates pro-tumor and pro-immune outcomes. A) B16-F10 cells of indicated genotypes were stimulated by transfection with *in vitro* transcribed 7SL RNA. 48 hours later, MHC-I levels were assessed by flow cytometry. **B)** C57BL/6 mice were treated with CD4 and CD8 depleting antibodies and then injected subcutaneously with B16-F10 tumors. Mice were then treated with indicated RNAs at days 5, 8, and 11. Tumors were monitored for growth until sacrifice criteria was reached. **C)** Mice were implanted with tumors as in B) and treated with RNA at days 5, 8, and 11 and anti-PD1 + anti-CTLA4 at days 8, 11, and 14. Tumors were again monitored for growth until sacrifice criteria was reached. **D)** C57BL/6 mice were implanted with B16-F10 tumors s.c. and then treated with indicated RNA at days 5, 8, and 11. Tumors were harvested at day 15 and T cells were assessed for Granzyme B expression by flow cytometry. **E)** Frequency of intratumoral T cells expressing Ki67, Granzyme B, and CD69 as well as DC infiltration after treatment with indicated RNAs. **F)** Mice were implanted with indicated genotypes of B16 tumors and then treated as in C), survival is shown.

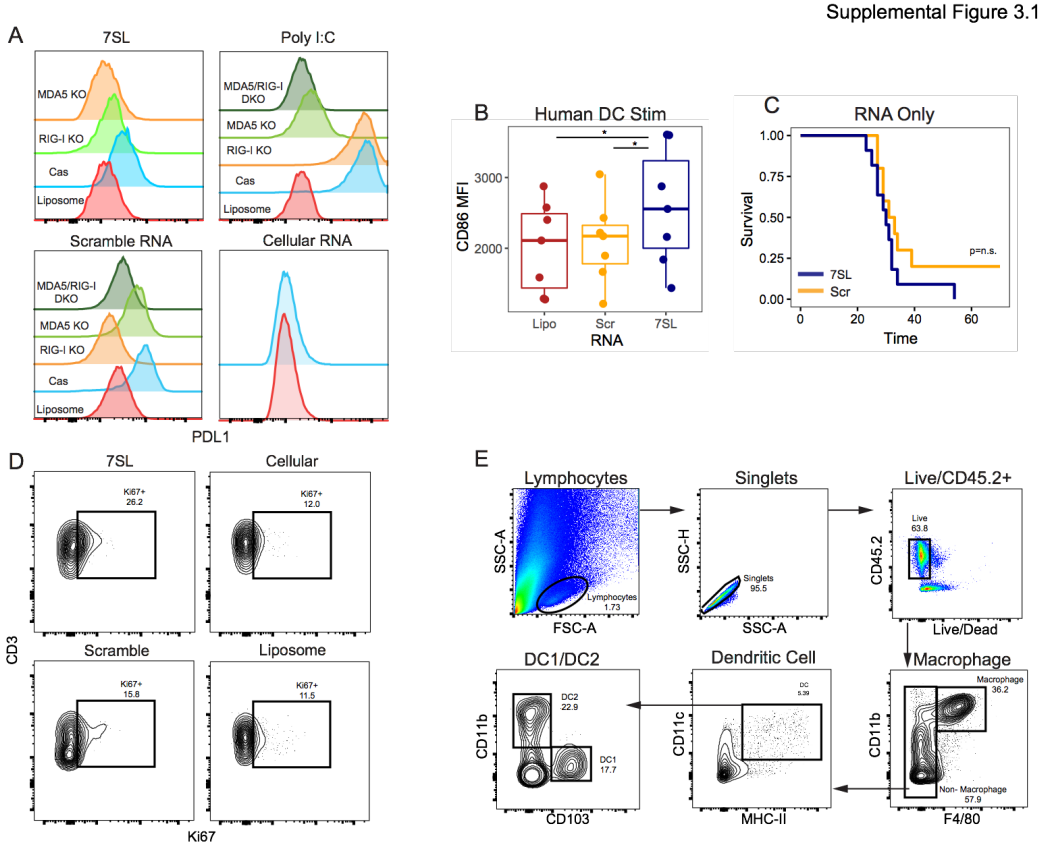

Supplemental Figure 3.1. 7SL stimulates immune activation in vitro and in vivo. **A)** B16-F10 cells of indicated genotypes were stimulated by transfection with indicated RNAs. 48 hours later, PDL1 levels were assessed by flow cytometry. **B)** Healthy donor human PBMCs were stimulated with indicated *in vitro* transcribed RNA and CD86 expression on DCs was analyzed 48 hours later. **C)** C57BL/6 mice were implanted with B16-F10 tumors s.c. and treated with indicated RNAs at days 5, 8, and 11. Survival is shown. **D)** Mice were treated as in C) and tumors were harvested at day 15 to perform flow cytometry. Expression of Ki67 in T cells is shown. **E)** Gating strategy to identify macrophages and DC subsets.

Section 3.3 – CAR-T Cells Can Preferentially Deliver 7SL RNA to Immune Cells Via Extracellular Vesicles

In order to devise an approach to deliver 7SL RNA to tumors that biases uptake by immune cells instead of cancer cells, we investigated the potential for using CAR-T cells. We surmised that CAR-T cells not only can be engineered with these properties but doing so could arm CAR-T cells with unique functions. To test this hypothesis, we designed a base syngeneic CAR-T cell system in which murine T cells are transduced with a human CD19BBz CAR construct (Fig. 3.2A), and B16-F10 melanoma cells expressing human CD19 (B16-h19) are used as a solid tumor model (Fig. 3.2B). We then incorporated a U6 promoter downstream of the CAR sequence to transcribe a 5'-triphosphate RNA of interest (Fig 3.2A). Here, 19BBz is combined with either human RN7SL1 RNA (19BBz-7SL), which only differs from the murine sequence at bases 18-20, or a scrambled control RNA (19BBz-Scr). Transduction of primary mouse T cells with either chimeric construct reveals that surface expression of the CAR is comparable (Fig. S3.2A) and both human 7SL and Scr RNA are constitutively detected (Fig. S3.2B).

Since our previous work demonstrated that 7SL is transferred between different cell types in the TME through exosomes (Nabet et al., 2017), we reasoned that CAR-T cells might also export 7SL through extracellular vesicles (EVs) that can then be transferred to immune cells in the tumor. Indeed, 7SL RNA was detected in purified EVs from CAR-T cells using species-specific primers, as was the Scr RNA (Fig 3.2C). To determine if RNA contained in CAR-T cell EVs can be transferred to other cells in the TME, we utilized a fluorescent RNA-specific dye (SytoRNA Select) to label the RNA of congenically marked $CD45.1^+$ CAR-T cells prior to transfer into $CD45.2^+$ mice bearing

B16-h19 tumors. Indeed, a significant fraction of endogenous CD45.2$^+$ immune cells, including myeloid cells, DCs, and endogenous T cells, are labeled with the SytoRNA dye indicating transfer from CAR-T cells (Fig. 3.2D). Consistent with EV-mediated delivery, transfer of CAR-T cell RNA is diminished in all immune populations examined after inhibiting EV secretion with GW4869, a neutral sphingomyelinase inhibitor known for limiting exosomal production (Trajkovic et al., 2008). To verify that 7SL or Scr RNA is among the RNA transferred from 19BBz-7SL or 19BBz-Scr CAR-T cells to endogenous immune cells, we sorted SytoRNA$^+$ CD45.2$^+$ endogenous immune cells from B16-h19 tumors and performed qRT-PCR for 7SL and Scr RNAs. Both 7SL and Scr RNA are detected in endogenous immune cells (Fig. 3.2E). Moreover, uptake of RNA from 19BBz-7SL CAR-T cells in DCs and macrophages led to upregulation of the activation marker CD86 in these populations (Fig S3.2E). Finally, RNA from CAR-T cells is preferentially taken-up by CD45.2$^+$ immune cells compared to cancer cells as measured by flow cytometry in individual tumors (Fig. 3.2G). In total, these results suggest that CAR-T cells can be used to preferentially transfer stimulatory RNAs such as 7SL to endogenous immune cells instead of cancer cells.

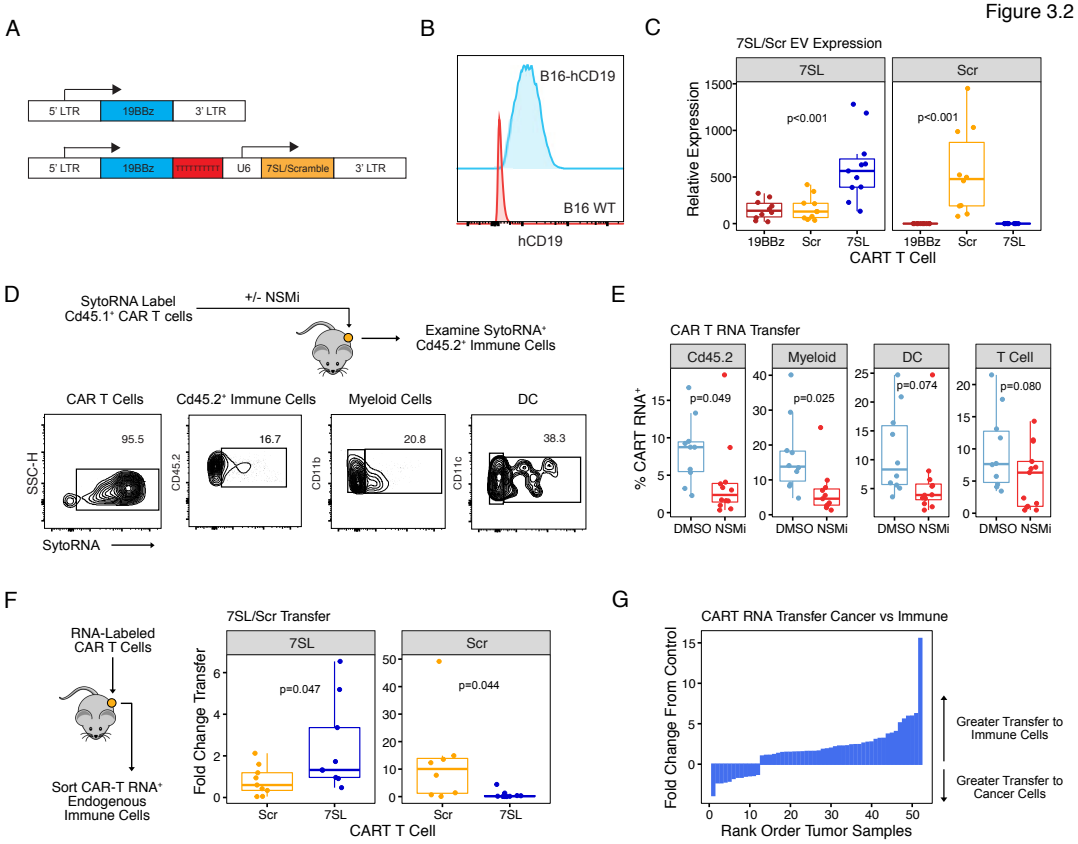

Figure 3.2. CAR-T cells localize therapeutic RNA delivery to immune cells over cancer cells. A) Construct design for 19BBz-7SL and 19BBz-Scr CAR-T cells. **B)** B16-F10 cells were stably transduced to express the human CD19 antigen, stable expression shown by flow cytometry. **C)** EVs were purified from CAR-T cell culture media by ultracentrifugation. qPCR for indicated RNAs was performed on purified RNA. **D)** B16-h19 tumors were injected i.t. with SytoRNA-labeled CD45.1^{+} CAR-T cells at day 14. 24 hours later tumors were harvested and CAR-T derived RNA was observed by flow cytometry. **E)** RNA transfer in indicated populations was measured after pre-treatment of CAR-T cells with exosome inhibitor GW4869 (NSMi) or DMSO. **F)** CD45.2^{+} immune cells positive for SytoRNA dye were sorted and cellular RNA was isolated. qPCR was then performed for RNAs of interest. **G)** The frequency of CAR-T RNA-labeled 45.2^{+} immune cells and 45.2^{-} tumor cells was quantified by flow cytometry in individual tumors. Fold change from equal transfer is shown.

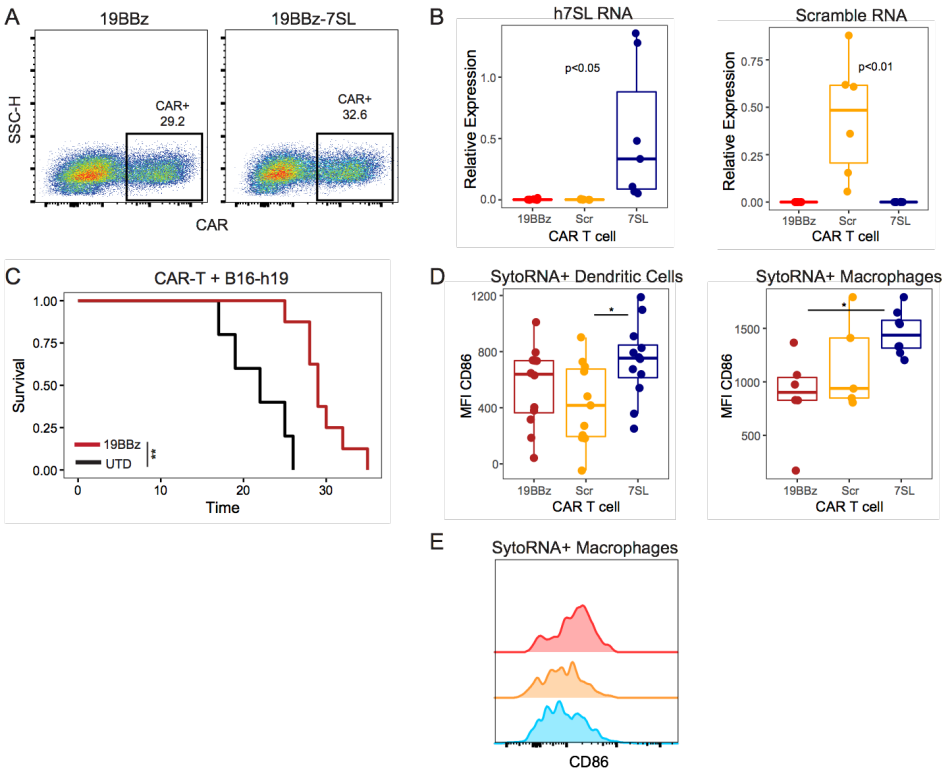

Supplemental Figure 3.2. 19BBz-7SL CAR-T cells as a model for immune activation. A) Expression of the h19BBz CAR molecule was assessed on the surface of murine T cells transduced with h19BBz or h19BBz-7SL CAR constructs following T cell expansion. **B)** RNA was harvested from murine T cells transduced with the relevant CAR constructs. qPCR for RNAs of interest is shown. **C)** C57BL/6 mice were implanted with B16-h19 tumors and then treated with h19BBz or untransduced mCAR-T cells at days 5 and 12. Survival is shown. **D)** Mice were implanted with B16-h19 tumors and then injected i.t. with SytoRNA-labeled CAR-T cells. CD86 expression in RNA-labeled cells was quantified as a measure of activation in indicated populations. **E)** Representative plot of CD86 expression SytoRNA+ macrophages.

Section 3.4 – CAR-T Cell Delivery of 7SL to Solid Tumors Controls Tumor Growth

In order to investigate if selective delivery of stimulatory RNA to immune cells is associated with improved CAR-T cell efficacy, we examined the survival of mice bearing B16-h19 tumors after treatment with 19BBz-7SL, 19BBz-Scr, 19BBz, or untransduced (UTD) murine T cells. Although 19BBz-7SL CAR-T cells resulted in the best survival (Fig. 3.3A), this improvement is modest, since the delivery of 7SL to immune cells would be expected to primarily improve endogenous immune function. Therefore, to unveil the impact of 7SL RNA on the endogenous immune compartment, anti-CTLA4 was added to the CAR-T cell regimen. Under these conditions, delivery of 7SL by CAR-T cells markedly enhances tumor response compared to UTD or 19BBz-Scr CAR-T cells (Fig 3.3B), a result that is also observed in a Kras/p53 lung cancer model that is typically refractory to immunotherapy (Fig S3.3A). Although anti-CTLA4 also increases efficacy of 19BBz or 19BBz-Scr CAR-T cells, this impact is modest compared to 19BBz-7SL CAR-T cells (Fig. 3.3A-B), further suggesting that 7SL impacts the endogenous immune system. Indeed, the intratumoral delivery of 7SL by CAR-T cells is accompanied by greater infiltration of both CAR-T and endogenous immune cells even in the absence of ICB (Fig. 3.3C-D). Examination by single-cell RNA-sequencing (scRNA-seq) reveals that this increase in endogenous immune infiltration associated with 7SL primarily results from an increase in subsets of $CD8^+$ T cells (Fig. 3.3E). By comparison, the main effect from intratumoral delivery of the Scr RNA is an altered immune composition characterized by enrichment of myeloid subsets. Thus, by engineering CAR-T cells to deploy 7SL selectively to immune cells, infiltration of both CAR-T and endogenous immune cells are enhanced. Upon addition of ICB, marked improvement in anti-tumor response ensues.

Immune infiltrate and tumor response after CAR-T cell therapy is improved with delivery of 7SL but not with Scr RNA, despite the fact that both RNAs induce ISGs after cellular transfection in vitro. To corroborate that differences between 7SL and Scr RNA are not simply due to gross differences in inducing ISGs in vivo, we examined ISG enrichment in $CD45.2^{+}$ immune populations from B16-h19 tumors. Immune cells with the highest ISG expression include subsets of monocytes, macrophages, DCs, and a small population of T cells (Fig. 3.3F). These same immune cell populations can further induce ISGs after CAR-T cell delivery of 7SL or Scr RNA, with Scr RNA showing a slightly broader effect compared to 7SL (Fig. 3.3G). Notably, the expression of *Rig-I* (*Ddx58*) and *Mda5* (*Ifih1*) are similar to each other and also follow a similar pattern to ISGs in general (Fig. 3.3H). Thus, these results suggest that the ability of 7SL to improve immune function after CAR-T delivery compared to Scr RNA likely involves more complex mechanisms than activating IFN-I signaling or differences in PRR expression.

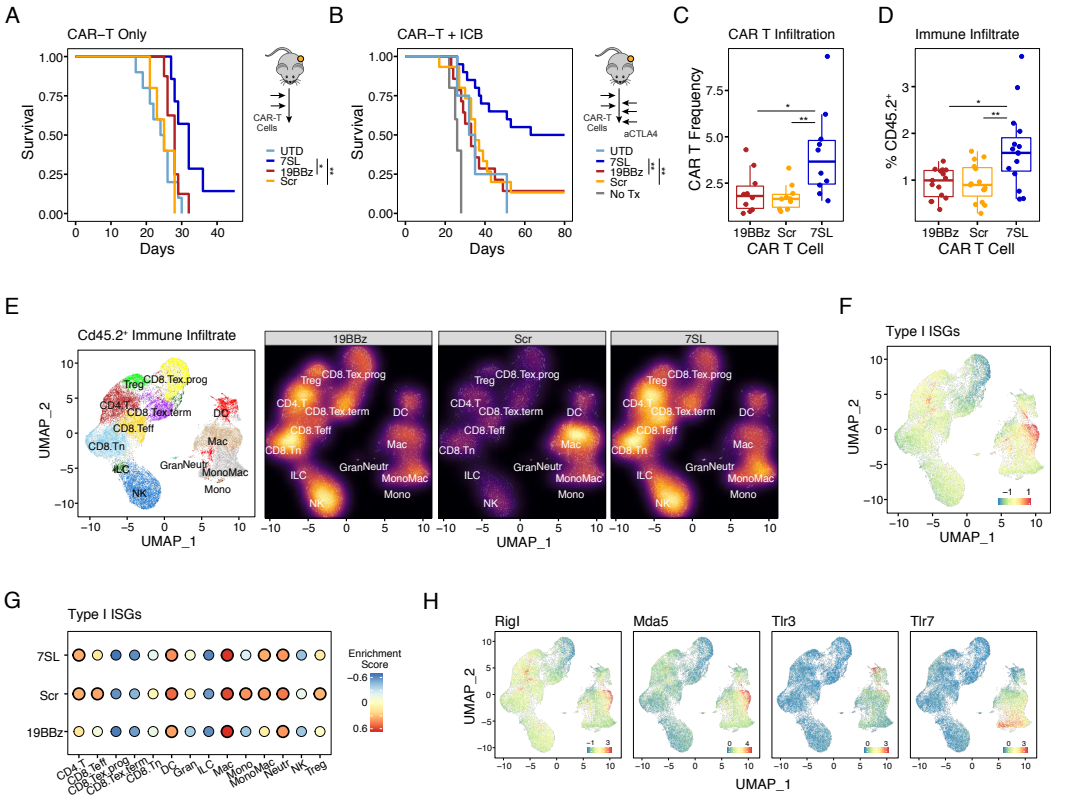

Figure 3.3. 19BBz-7SL CAR-T cells improve endogenous immune activation and survival. A) Mice were implanted with B16-h19 tumors and then treated with CAR-T cells at days 5 and 12 or **B)** CAR-T cells plus ICB at days 8, 11, and 14. **C)** Mice were implanted with tumors and treated with indicated CAR-T cells at days 5 and 12. Tumors were harvested at day 15 and flow cytometry was performed, shown is frequency of live CD45.1^{+} CAR-T cells or **D)** CD45.2^{+} events. **E)** 45.2+ endogenous immune cells were sorted at d15 from B16-h19 tumors treated with indicated CAR-T cells and then subjected to single-cell RNA sequencing. Shown are identified clusters and density heat maps indicating frequency of labeled clusters. **F)** A metagene comprised of the Hallmark Type-I IFN geneset mapped onto the UMAP of all 45.2+ cells. **G)** Enrichment in individual clusters separated by CAR-T treatment group. Dark circles represent statistically significant enrichment as compared to enrichment of random genesets. **H)** Expression of relevant RNA PRRs mapped onto 45.2+ UMAP.

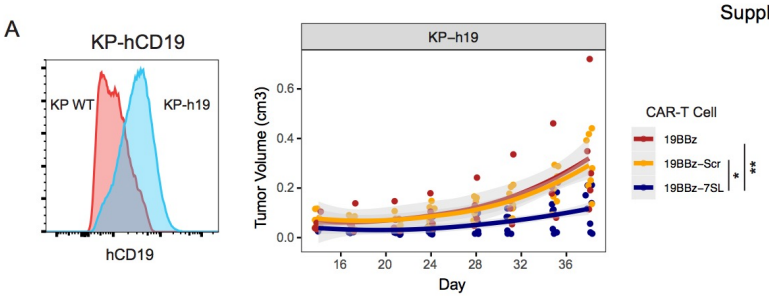

Supplemental Figure 3.3. 7SL- CAR-T cells improve KP lung tumor control. A) KP lung cancer cells were transduced to express hCD19 and treated with indicated mCAR-T cells on day 5 and 12 plus anti-CTLA4 and anti-PD1. Tumor growth shown.

Section 3.5 – 7SL RNA delivered by CAR-T cells improves immunostimulatory properties of myeloid and DC subsets

Since the ability to increase IFN signaling in immune cells does not obviously account for the different immunostimulatory effects of 7SL versus Scr RNA, we sought to more closely interrogate how each RNA differentially impacts immune cell properties. Given that *Rig-I*, *Mda5*, and ISGs show high expression in myeloid and DC subsets (Fig. 3.3H), we elected to first examine these innate immune cell types. Using Monocle and scRNA-seq data for CD45.2$^+$ intratumoral immune cells, we inferred a differentiation trajectory and different cell states and then used genesets for various myeloid subsets to assign each state (Fig. 3.4A-B). To define cells with immunosuppressive properties, genes for myeloid derived suppressor cells (MDSCs) and for *Tgfb1* were evaluated (Alshetaiwi et al., 2020). As expected, delivery of either 7SL or Scr RNA by CAR-T cells increases ISGs across multiple myeloid states (Fig. 3.4C). However, delivery of the Scr but not 7SL RNA leads to higher frequencies of myeloid states enriched in MDSC genes, particularly the Mdsc.2 state, which exhibits the greatest enrichment in MDSC genes that include *Cd84* and *Arg2* (Fig. 3.4D). This was confirmed at a broad level using flow cytometry which revealed a higher frequency of Ly6C$^+$ monocytes in 19BBz-Scr CAR-T treated tumors (Fig. S3.4A). Conversely, delivery of 7SL RNA decreases levels of *Tgfb1*, which is highly expressed in myeloid states that are largely distinct from the Mdsc.2 state. Together, these results suggest that although 7SL and Scr RNA both stimulate an IFN response, only delivery of 7SL by CAR-T cells limits expression of MDSC genes and/or *Tgfb1* across multiple myeloid cell types.

To better define changes in DCs, DCs and monocytic DCs were re-clustered and assigned using genesets for established DC populations. Potential stimulatory properties

of each subset were also evaluated using several gene regulatory modules that change in response to DC activation (Zilionis et al., 2019). This includes a co-stimulatory module (*Cd80*, *Cd86*, *Cd40*, *Relb*, *Cd83*) and an inhibitory immunoregulatory module (*Cd274*, *Pdcd1lg2*, *Cd200*). Four major DC subsets including DC1 (characterized by *Xcr1*, *Clec9a*), DC2 (characterized by *Itgam*, *Sirpa*), DC3 (characterized by *Ccr7*), and plasmacytoid DC (pDC) (characterized by *Siglech*, *Cd7*, and *Cd209a*) were identified along with a fifth cluster primarily comprised of monocytic DCs (Fig. 3.4F-G). As with the myeloid states, delivery of either 7SL or Scr RNA by CAR-T cells increases ISG expression to varying degrees in some but not all subsets (Fig. 3.4H). However, only delivery of 7SL RNA increases the frequency of a pDC-like cluster (Fig. 3.4I), which we also confirmed by flow cytometry using CD209a as a representative marker (Fig. 3.4J, S3.4B). pDCs typically produce IFN-I in the context of viral infections (Webster et al., 2016), suggesting a similar viral-like response is elicited by intratumoral delivery of 7SL RNA. 7SL RNA leads to a more modest increase in frequency for the DC1 subset known to stimulate $CD8^+$ T cell responses (Broz et al., 2014); however, this subset in particular exhibits reciprocal changes in key regulatory gene modules. Specifically, DC1 cells show an enrichment of the co-stimulatory module but a decrease in the inhibitory immunoregulatory module (Fig. 3.4K). This favorable change in the ratio of costimulatory to inhibitory genes was confirmed using flow cytometry by showing an increase in DCs expressing CD86 in favor of PDL1 (Fig. 3.4L, S3.4C).

In total, these findings suggest that delivering an RNA that simply mounts an IFN response is not adequate to enable CAR-T cells to favorably enhance innate immune cells in the TME. Rather, the ability of 7SL RNA to improve CAR-T cell function is associated

with limiting the development of suppressive myeloid states and promoting DCs to adapt greater anti-viral or costimulatory properties.

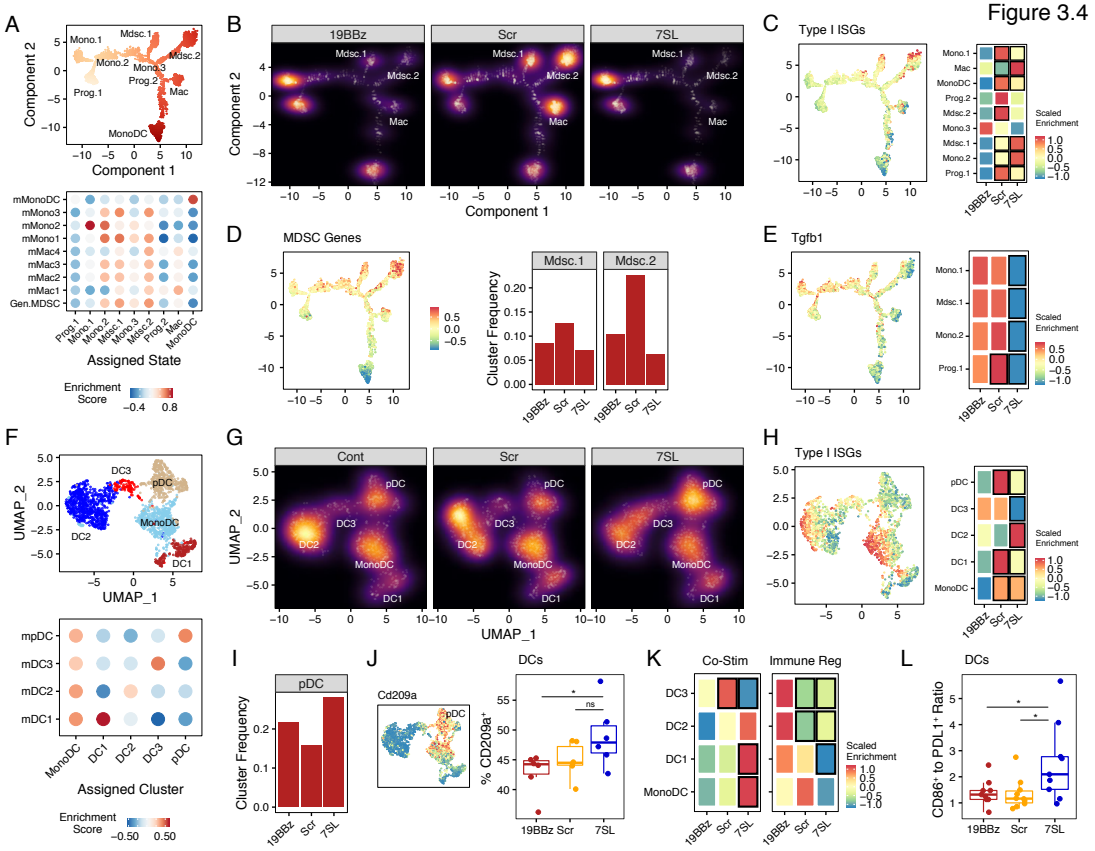

Figure 3.4. Single cell sequencing reveals improved DC and myeloid activation by 19BBz-7SL CAR-T cells. A) Non-DC myeloid clusters were isolated from the total 45.2+ single cell dataset and subjected to pseudotime analysis using Monocle (top). Cluster identification was performed using previously defined genesets for myeloid populations (bottom). **B)** Cluster frequency is represented by brightness mapped onto the pseudotime trajectory, panels are split by CAR-T treatment. **C)** Hallmark IFN-I geneset mapped onto pseudotime trajectory. Enrichment in individual clusters shown, statistical significance determined by comparison to enrichment of random genesets. **D)** General MDSC geneset mapped onto pseudotime trajectory (left) and frequency of cells in MDSC clusters split by CAR-T treatment (right). **E)** TGFB expression mapped onto pseudotime trajectory. Enrichment in individual clusters shown, statistical significance indicated by outlined boxes. **F)** The DC cluster from total 45.2+ dataset was isolated and subjected to reclustering using Seurat (top). Cluster identification was performed using previously defined genesets for DCs (bottom). **G)** Cluster frequency is represented by brightness mapped onto the DC UMAP, panels are split by CAR-T treatment. **H)** Hallmark IFN-I geneset mapped onto DC UMAP. Enrichment in individual clusters shown, statistical significance indicated by outlined boxes. **I)** Frequency of DC clusters in different CAR-T treated tumors. **J)** CD209a expression mapped on DC UMAP and quantified by flow cytometry in CAR-T treated B16-h19 tumors. **K)** Expression of costimulatory or immune regulatory genes in DC clusters, significance indicated by outlined boxes. **L)** DCs from B16-h19 tumors were assessed for CD86 and PDL1 by flow cytometry. A ratio of single-positive events is shown (see S3.4C).

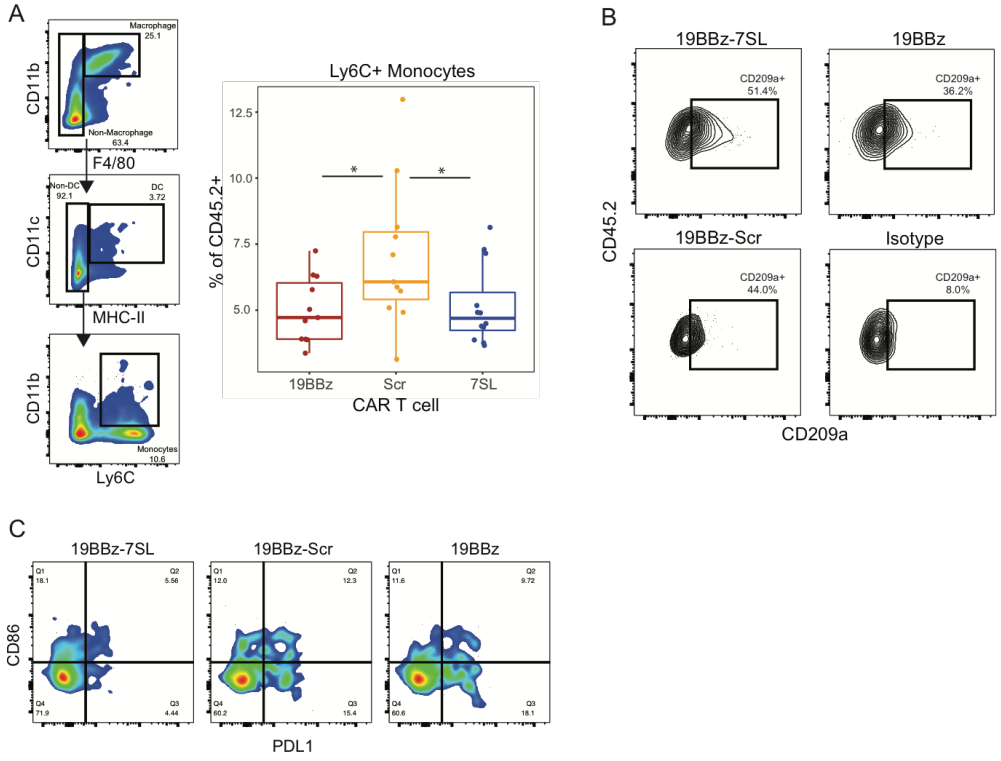

Supplemental Figure 3.4. Single-cell sequencing reveals altered myeloid differentiation patterns mediated by RNA CAR-T cells. A) Gating strategy to identify Ly6C+ monocytes from 45.2+ cells. Frequency of monocytes following treatment with indicated CAR-T cells is shown. **B)** Expression of CD209a on DCs from B16-h19 tumors treated with indicated CAR-T cells. **C)** Representative expression of CD86 and PDL1 on DCs from B16-h19 tumors treated with indicated CAR-T cells. Ratio in Fig 3.4L is derived from single-positive events in quadrant 1 and quadrant 3.

Section 3.6 – Delivery of 7SL RNA by CAR-T cells improves the function of endogenous CD8$^+$ T cells

Treatment with 19BBz-7SL CAR-T cells improves both the infiltration of endogenous T cells and stimulatory properties of DCs and myeloid cells in the tumor. To more deeply understand how these intratumoral T cells are affected, we extended our scRNA-seq analysis of CD45.2$^+$ immune cells to non-naïve CD8$^+$ T cells (Fig. 3.5A). Similar to the myeloid cell analysis, differentiation states and trajectories were inferred and genesets for CD8$^+$ T cell subsets were used to assign the individual T cell states (Beltra et al., 2020). Using a set of core CD8$^+$ T cell exhaustion genes, each state was first defined as exhausted or non-exhausted. Then, the exhausted and non-exhausted states were further refined using additional genesets for T cell subsets (Miller et al., 2019). This revealed that compared to tumors treated with 19BBz CAR-T cells, tumors treated with 19BBz-7SL CAR-T cells show an increase in effector-like T cells (T_{EFF}) and in effector/memory-like T cells (T_{EM}) that express *Klrg1* and/or *Tcf7* (Fig. 3.5B-D). Conversely, there is a decrease in *Tox*-expressing exhausted T cells (T_{EX}), particularly exhausted T cells belonging to the progenitor 2 subset (T_{EX}^{prog2}). In comparison, delivery of Scr RNA results in effects that are intermediate between 19BBz and 19BB-7SL CAR-T cells. These changes in CD8$^+$ T cell subsets are also corroborated by flow cytometry using ITGB7 as a marker for T_{EFF} and T_{EM} cells and TOX as a marker for T_{EX} (Fig. 3.5C, 3.5E-F, S3.5A). Thus, these findings suggest that improved myeloid and DC function resulting from delivery of intratumoral 7SL fosters development of CD8$^+$ T cells with effector/memory-like properties rather than features of T cell exhaustion.

To more directly test the requirements for 7SL RNA stimulation of myeloid cells and DCs to promote improved CD8$^+$ T cell function, we utilized mouse BMDCs stimulated with or

without RNA and assayed their capacity to activate OT-I $CD8^+$ T cells against the ovalbumin (OVA, SIINFEKL) peptide (Fig. 3.5G, left). This revealed that stimulation of BMDCs with liposome-encapsulated 7SL RNA is sufficient to enhance proliferation of OT-I T cells and their production of effector proteins such as GzmB and IFNG (Fig. 3.5G, right). A similar effect is also observed using EV RNA isolated from 19BBz-7SL CAR-T cell cultures (Fig. 3.5H). In contrast, the stimulatory effects of 7SL RNA are largely abrogated when BMDCs from MAVS knockout mice are used, consistent with 7SL activating RIG-I and/or MDA5 in myeloid/DC subsets (Fig. 3.5G, S3.5B). Indeed, 7SL stimulation of BMDCs also enhances production of IFNB and two assayed subtypes of IFNA (Fig. 3.5I) and blocking IFN-I receptor signaling with an anti-IFNAR antibody during T cell priming also interferes with T cell activation (Fig. 3.5J). Thus, these results suggest that when CAR-T cells deploy 7SL RNA, 7SL can directly elicit favorable changes in myeloid/DC subsets that help activate $CD8^+$ T cells.

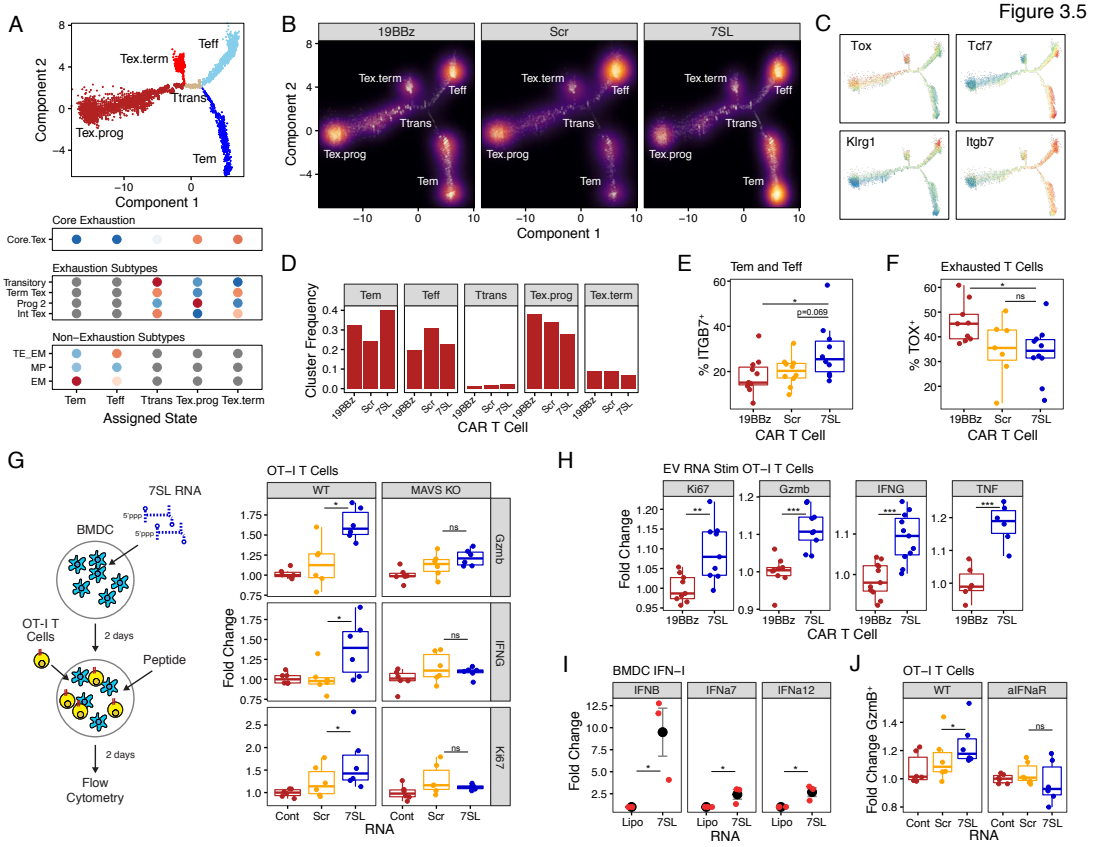

Figure 3.5. 7SL CAR-T cells enhance CD8$^+$ T cell activation and differentiation through DC/T cell interactions. A) Non-naïve CD8$^+$ T cells were isolated from the 45.2+ single cell dataset and subjected to pseudotime analysis using Monocle. Trajectory (top) and cluster identification using previously defined genesets (bottom) is shown. **B)** Cluster frequency represented by brightness mapped onto psuedotime trajectory. **C)** Expression of relevant genes mapped onto pseudotime trajectory. **D)** Cluster frequency quantified from B16-h19 tumors treated with indicated CAR-T cells. **E)** Itgb7$^+$ or **F)** Tox$^+$ intratumoral CD8$^+$ T cells were quantified by flow cytometry following treatment with indicated CAR-T cells. **G)** BMDCs from MAVS KO or matched C129/J mice were stimulated with *in vitro* transcribed 7SL or Scr RNA and co-cultured with OT-I T cells for 48 hours. Expression of Granzyme B, IFNG, and Ki67 was measured by flow cytometry. **H)** The same experiment was performed with EV RNA from 19BBz-7SL or control CAR-T cell culture media. Data normalized to 19BBz control EV RNA stimulation. **I)** BMDCs were stimulated with 7SL RNA and harvested 48 hours later to perform qPCR for Type I IFN transcripts. **J)** aIFNAR blocking antibody MAR1-5A3 was added to BMDC cultures concurrently with OT-I T cells. Granzyme B expression was assayed by flow cytometry 48 hours later.

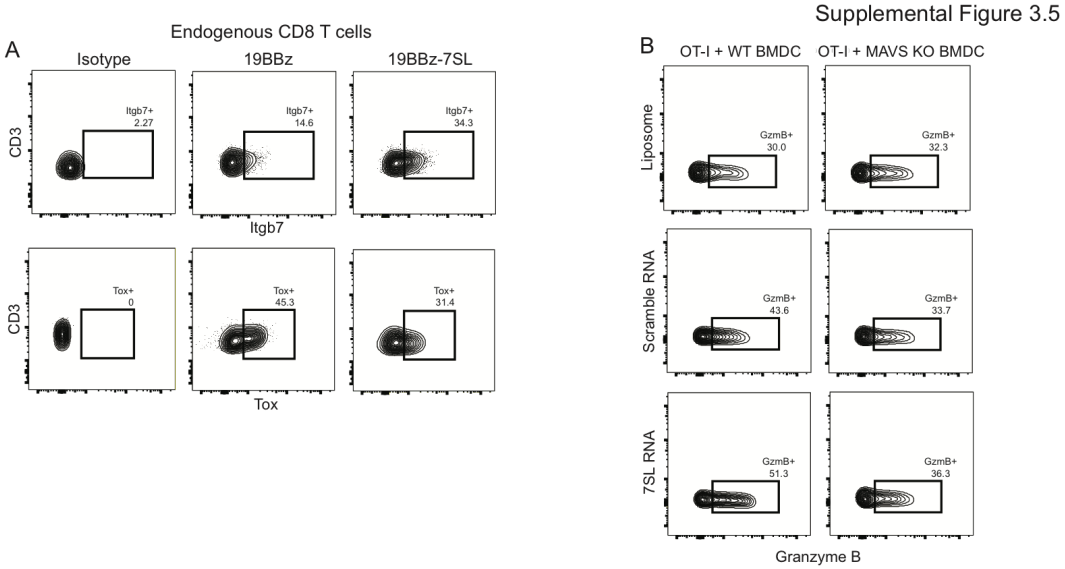

Supplemental Figure 3.5. 7SL enhances CD8$^+$ T cell differentiation while limiting exhaustion. A) B16-h19 tumors treated with indicated CAR-T cells were harvested at day 15 and CD8$^+$ T cells were analyzed for Itgb7 and Tox expression by flow cytometry. **B)** BMDCs from MAVS KO or matched C129/J mice were stimulated with *in vitro* transcribed RNAs and co-cultured with OT-I T cells for 48 hours. Representative flow cytometry plots for OT-I expression of Granzyme B are shown.

Section 3.7 – Type I IFN Production is Critical to the Activation of 19BBz-7SL CAR-T Induced Anti-Tumor Immunity

The ability of 7SL RNA to recruit and mitigate dysfunction of endogenous T cells suggests that 19BBz-7SL CAR-T cells might be armed with unique properties that can overcome resistance due to CAR antigen loss. To investigate this notion, we first determined if improved response with 19BBz-7SL CAR-T cells plus ICB requires endogenous T cells and DCs. Indeed, when *Trac*$^{-/-}$ mice are implanted with B16-h19 tumors, the difference between 19BBz-7SL and 19BBz CAR-T cells is abrogated (Fig. 3.6A), indicating that endogenous T cells are required for the therapeutic effect of 7SL. Next, we investigated the role of DCs, particularly DC1 cells that exhibit preferential expression of costimulatory versus inhibitory genes after 19BBz-7SL CAR-T cell treatment. For this, we used BATF3 knockout mice, which lack the DC1 population (Fig S3.6A). In the absence of DC1s, treating tumor-bearing *Batf3*$^{-/-}$ mice with 19BBz-7SL CAR-T cells increases the frequency of the DC2 subtype (Fig. 3.6B). This suggests that although infiltration of endogenous CD8^{+} T cells and CAR-T cells are diminished in *Batf3*$^{-/-}$ mice (Fig. 3.6C-D), CAR-T cells can still infiltrate the tumor and exert effects on endogenous immune cells. Nonetheless, when mice are treated with CAR-T cells plus ICB, survival with 19BBz-7SL CAR-T cells is identical to 19BBz CAR-T cells (Fig. 3.6E) and mirrors the results from *Trac*$^{-/-}$ mice. This is further supported by a lack of endogenous T cell activation despite 7SL delivery in the absence of DC1 (Fig S3.6B). Thus, the specific benefit of intratumoral delivery of 7SL to enhance CAR-T cell responses requires both endogenous T cells and the DC1 subset of DCs.

Our in vitro results suggest that 7SL activates RIG-I/MAVS and IFN-I signaling in DCs to facilitate T cell activation. To corroborate these findings, we utilized RIG-I knockout

mice. Although *Ddx58*$^{-/-}$ mice exhibit embryonic lethality and rare offspring are born at sub-Mendelian ratios, we procured a small cohort and treated mice bearing B16-h19 tumors with 19BBz-7SL CAR-T cells plus ICB. In contrast to the effects from knocking out RIG-I in cancer cells (Fig. 3.1D), the absence of host RIG-I decreases survival, suggesting host RIG-I signaling is required for the therapeutic benefit of 7SL (Fig. 3.6F). Accordingly, anti-IFNAR antibody similarly interferes with 19BBz-7SL CAR-T cell efficacy (Fig. 3.6G). This is accompanied by only a modest decrease in the proportion of endogenous intratumoral $CD8^+$ T cells (Fig. 3.6H), but a failure by 7SL to enhance the frequency of the DC1 subset after 19BBz-7SL CAR-T cell therapy (Fig. 3.6I, Fig S3.6C). As a consequence, blocking IFN-I signaling also prevents the increase in $ITGB7^+$ $T_{EFF\text{-}like}$ and $T_{EM\text{-}like}$ cells, GzmB expression, and proliferation typically observed after 19BBz-7SL CAR-T treatment (Fig 3.6J-K, S3.6D-E). Together, these results corroborate that intratumoral delivery of 7SL by CAR-T cells activates RIG-I and IFN signaling to improve DC and hence T cell function.

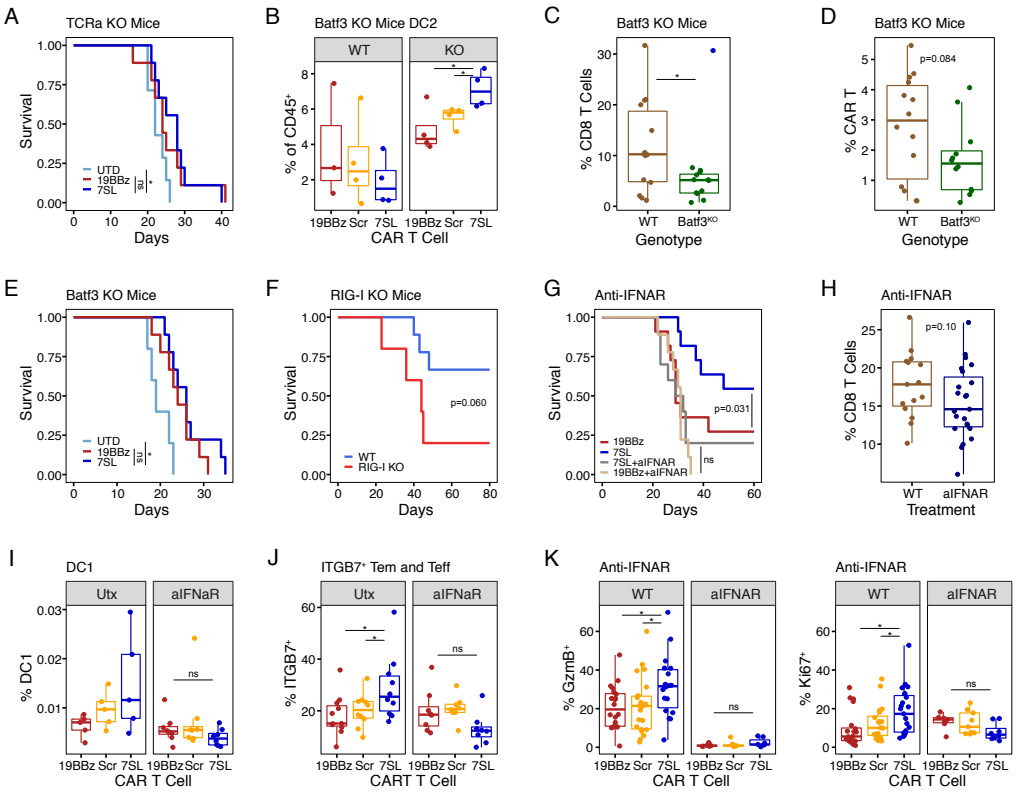

Figure 3.6. Type I IFN production is critical to the activation of 7SL-induced anti-tumor immunity. A) *Trac*$^{-/-}$ mice were implanted with B16-h19 tumors and treated with indicated CAR-T cells at day 5 and 12 along with anti-CTLA4 antibodies. Survival is shown. **B)** B16-h19 tumors were harvested from *Batf3*$^{-/-}$ and WT C57BL/6 mice at day 15 following CAR-T cell treatment. Frequency of cDC2, **C)** CD8^{+} T cells, and **D)** CAR-T cells was assessed by flow cytometry. **E)** *Batf3*$^{-/-}$ mice were were implanted with B16-h19 tumors and treated as in A). **F)** RIG-I KO or WT littermate controls were implanted with B16-h19 tumors and treated with CAR-7SL and anti-CTLA4 as in A). Survival is shown. **G)** Mice were implanted with B16-h19 tumors and treated with indicated CAR-T cells concomitatnly with aIFNAR blocking antibody. Survival is shown. H) Tumors were harvested from mice treated with CAR-T cells + aIFNAR antibody at day 15 to assess CD8^{+} T cell frequency. **I-K)** Mice bearing B16-h19 tumors were treated with the indicated CAR-T cells with and without concomitant aIFNAR antibody treatment. Frequecy of **I)** cDC1, **J)** Itbg7^{+} CD8^{+} T cells and **K)** Granzyme B+ or Ki67+ T cells was assessed by flow cytometry. Itgb7 WT mouse data from 4E utilized for reference comparison.

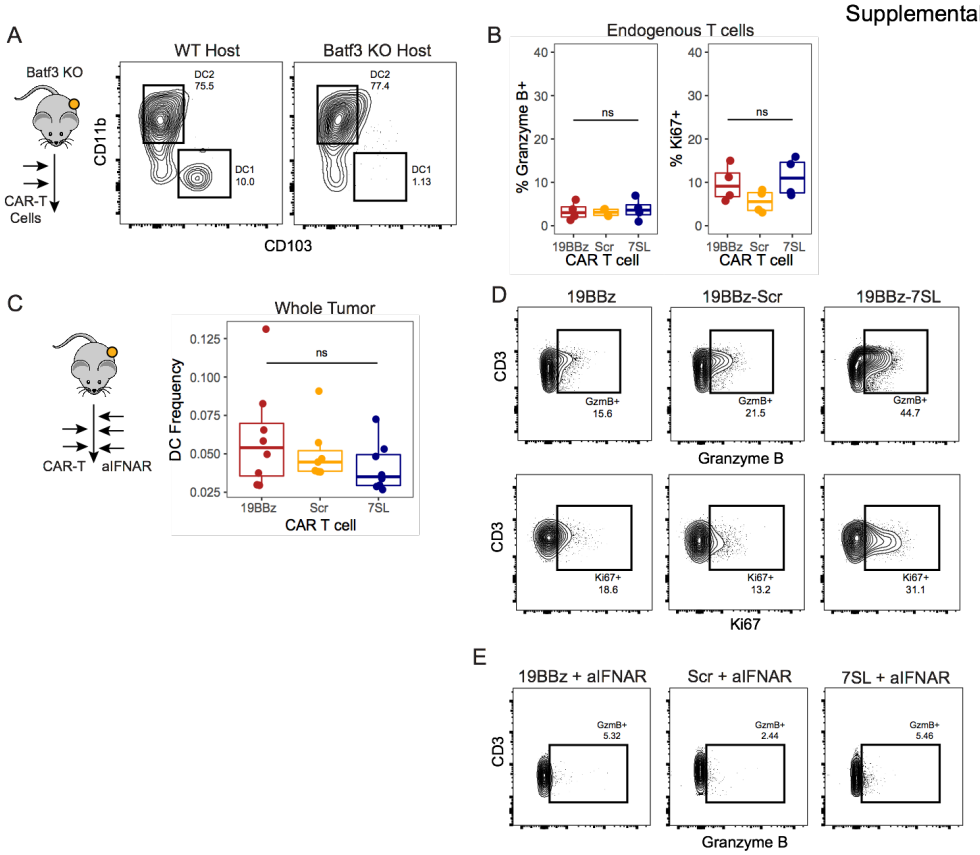

Supplemental Figure 3.6. Batf3+ DCs and Type I IFN contribute to 7SL-induced anti-tumor immunity. A) B16-h19 tumors were harvested from WT or *Batf3*$^{-/-}$ mice and analyzed for the presence of cDC1s. **B)** Endogenous CD8^{+} T cells in tumors from *Batf3*$^{-/-}$ mice treated with indicated CAR-T cells were assessed for expression of activation markers Granzyme B and Ki67. **C)** Frequency of DC infiltration was assessed in mice treated with CAR-T cells concomitantly with aIFNAR antibodies. **D)** Endogenous T cells from tumors in mice treated with indicated CAR-T cells were assessed for Granzyme B and Ki67 expression. **E)** Granzyme B expression in T cells from mice treated as in D) with additional aIFNAR antibody was assessed at ay 15 post-tumor injection.

Section 3.8 – Delivery of 7SL by CAR-T cells orchestrates endogenous immune activation to overcome resistance due to antigen loss

TRP2 is an immunodominant B16-F10 melanoma self-antigen that can mediate tumor rejection (Bloom et al., 1997). To determine if endogenous immune activation by 19BBz-7SL CAR-T cells can enhance the function of TRP2-reactive endogenous $CD8^+$ T cells, we utilized a TRP2 tetramer (Fig S3.7A). As predicted, TRP2-specific $CD8^+$ T cells express higher levels of GzmB and Ki67 in mice treated with 19BBz-7SL CAR-T cells compared to 19BBz or 19BBz-Scr CAR-T cells (Fig. 3.7A). Moreover, this increase was blocked by anti-IFNAR treatment (Fig. S3.7B). Given these findings, we reasoned that 19BBz-7SL CAR-T cells might be less susceptible to CAR-T cell resistance arising from loss of CAR antigen. To simulate this common resistance mechanism, we implanted mice with a 1:1 mix of B16-h19 cells that express human CD19 with control B16 cells that lack human CD19 (Fig. 3.7B). While 19BBz and 19BBz-Scr CAR-T cells are largely ineffective, 19BBz-7SL CAR-T cells eradicate these heterogenous tumors comparably to pure B16-h19 tumors (Fig. 3.7C). Mice treated with 19BBz-7SL CAR-T cells that had a complete response were then rechallenged at day 80 with a pure B16 tumor lacking human CD19. Here, 80% (4 out of 5) mice remain tumor-free at 140+ days, consistent with the generation of endogenous effector-memory T cells against tumor antigens (Fig 3.7D). In total, these data demonstrate that arming CAR-T cells with the ability to deploy 7SL RNA results in the activation of endogenous innate immune cells and tumor-reactive effector-memory T cells. These new functions can make CAR-T cells less susceptible to resistance due to CAR antigen loss (Fig 3.7E).

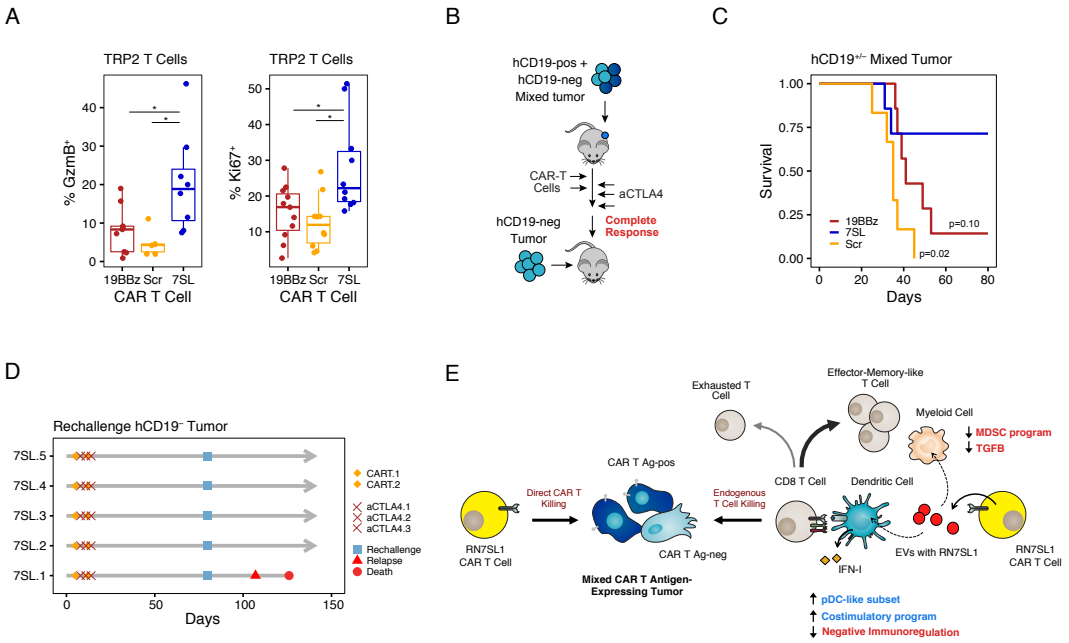

Figure 3.7. 19BBz-7SL CAR-T cells activate tumor-specific CD8⁺ T cells and eliminate heterogenous solid tumors. A) B16-h19 tumors were harvested from mice treated with indicated CAR-T cells at day 15. TRP-2 tetramer+ endogenous CD8⁺ T cells were evaluated for Granzyme B and Ki67 expression by flow cytometry. **B)** Model for heterogenous solid tumor CAR-T cell therapy. **C)** Mice were implanted with a 1:1 mixture of B16-h19 and WT tumor cells and then treated with CAR-T cells and anti-CTLA4. Survival is shown. **D)** 19BBz-7SL CAR-T treated mice from C) were rechallenged with WT B16-F10 tumor cells and survival was monitored. **E)** Proposed model for role of PRR signaling in solid tumors from both endogenous sources and engineered CAR-T cells.

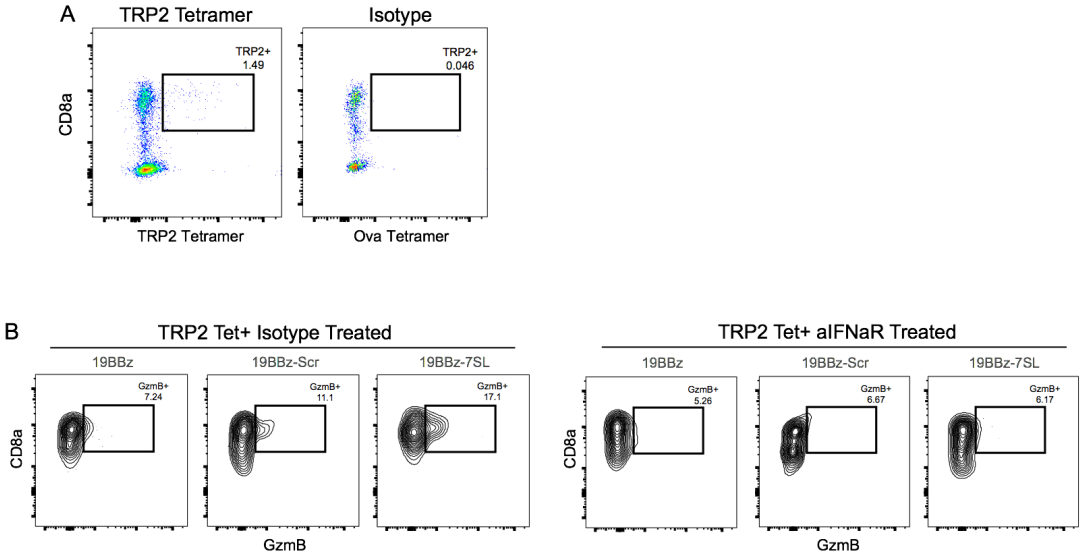

Supplemental Figure 3.7. Tumor-specific CD8$^+$ T cell activation is dependent on Type I IFN. A) B16-h19 tumors were harvested at day 15 and stained with TRP2-specific or Ova control TCR tetramer. **B)** TRP2-tetramer$^+$ CD8$^+$ T cells from B16-h19 tumors were assessed for Granzyme B expression following CAR-T treatment in the presence or absence aIFNAR antibody treatment.

Section 3.9 Discussion

Here we present a novel cell therapy inspired by the discovery of a naturally occurring intratumoral PAMP. Delivery of the immune-stimulatory RNA RN7SL1 enhanced infiltration of both engineered and endogenous immune cells, and appears to bias inflammatory signaling to the intratumoral immune compartment. This improved endogenous T cell proliferation and cytotoxicity, and enhanced survival as a single therapy and or in combination with immune checkpoint inhibitors. This immune response was dependent on BATF3+ DCs and their ability to prime anti-tumor $CD8^+$ T cell responses. These cells are able to take up CAR-T derived RNA and become activated. This may represent a novel priming signal in the TME that facilitates the initiation of anti-tumor immunity, and outlines a novel therapeutic modality for the delivery of immunostimulatory cues.

A key insight of this paper and others is the importance of distinct cellular compartments in determining the outcome of inflammatory signaling with regard to pro-immune or pro-tumor effects. In turn, this is a crucial determinant of survival outcomes in preclinical and clinical studies (Benci et al., 2019). Specifically, we see that in the absence of anti-tumor immunity, 7SL RNA promotes tumor growth by activating ISGs in tumor cells. In contrast, 7SL RNA promotes response to therapy and improved survival when the immune system is primed using ICB. Combining these observations, response is most improved when tumor cells are unable to recognize 7SL through the genetic deletion of RIG-I and the immune system is additionally primed with ICB treatment. This suggests that inflammatory signaling promotes competing processes in distinct cellular compartments, and that targets for enhancing response to immune-based therapies should focus on non-overlapping pathways between immune and cancer cells. For example, our data suggests

targeting a gene crucial to the activation of ISGs in cancer cells, but not in DCs, might bias inflammatory signaling strongly toward the immune compartment. Similarly, activation of pathways exclusive to immune cells such as some TLRs and RLRs (Dajon et al., 2017) may limit cancer cell-associated inflammation while activating anti-tumor immunity.

One way to achieve this preferential signaling may be delivery of immunostimulatory cues by an engineered immune cell. We observe greater uptake of CAR-T RNA by endogenous immune cells than tumor cells in the TME, suggesting immune cells may preferentially interact with one another at sites such as tertiary lymphoid structures (Joshi et al., 2015), which in turn enhances local immune priming events. Intriguingly, CAR-T/DC interactions have been reported in the tumor draining lymph node (Ma et al., 2019), suggesting that these cell types readily interact and may form a crucial signaling axis for CAR-T delivered therapeutics such as those described here. Specifically, we describe a circuit in which CAR-T derived 7SL RNA drives enhanced Type I IFN signaling in myeloid/DC populations, which in turn drives the expansion of an effector-like $CD8^+$ T cell cluster that is able to functionally improve control of solid tumors. This differs from the well-described differentiation into exhausted $CD8^+$ T cells typically observed in solid tumors, which does not control tumor growth. This is somewhat surprising given previous reports suggesting that chronic Type I IFN signaling contributes to T cell exhaustion (Teijaro et al., 2013; Wilson et al., 2013), and again points to the complexity and context-dependent nature of inflammatory pathways in the TME. Our results highlight the acquisition of an effector-like $CD8^+$ T cell program and control of solid tumors; this is consistent with recent reports highlighting the increased efficacy of immunotherapy when T cells are diverted from the exhausted T cell fate (Chen et al., 2019; Lynn et al., 2019; Wei et al., 2019), and suggest a paradigm by which modulating soluble cues has the

potential to influence this process. Interestingly, in a model of acute viral infection IFN-I signaling is crucial for the acquisition of effector phenotype and cytolytic function (Wiesel et al., 2012). This further suggests that 7SL delivery may mimic an acute local viral infection which drives less chronic T cell differentiation and more effector like gene programs. This demonstrates that altering soluble cues involved in T cell priming may drive functionally different T cell fates in the TME, and shows a need for further research into the role for many of these cytokines in anti-tumor T cell responses. Finally, 19BBz-7SL CAR-T cells are able to overcome antigen heterogeneity in a solid tumor model that is not possible with standard-of-care 19BBz CAR-T cells through this activation of endogenous $CD8^+$ T cell responses. This type of epitope spreading represents a major goal for the CAR-T and immunotherapy fields, and provides a significant opportunity to expand these therapeutic modalities into larger patient populations. In total, this work underlines the importance of cellular compartmentalization of signaling in the TME and outlines a novel therapeutic modality to expand the efficacy of CAR-T cells in solid tumors.

CHAPTER 4 – CONCLUSIONS AND FUTURE DIRECTIONS

Section 4.1 – IFNG Signaling in ICB Responses

In Chapter 2 we describe how IFNG signaling between immune cells and cancer cells orchestrates opposing functions to both impact and predict ICB response. In immune cells, IFNG signaling supports anti-tumor responses, while in cancer cells IFNG augments MHC-I expression. Opposing these immune stimulatory effects, IFNG signaling in tumor cells drives feedback inhibition by increasing multiple inhibitory pathways that include PDL1. As a consequence, these inhibitory pathways on cancer cells not only promote T cell exhaustion but also interfere with maturation of NK/ILC1s and protect against their cytotoxic effects. Thus, in tumors that are less reliant on IFN for MHC-I expression and antigen presentation, blocking tumor IFN-driven resistance can improve ICB response. For tumors with adequate neoantigens and high constitutive MHC-I, the improved function of T_{EX} enables CTL-mediated anti-tumor responses. This is associated with immunological memory and can even result in profound spontaneous regression in the absence of ICB. For tumors with depleted neoantigens that are otherwise likely resistant to ICB, ablating tumor IFN signaling also improves T_{EX} function. In this situation, loss of IFN-inducible MHC-I is less consequential for CTL function. Improved ICB response results from enhanced IFNG production by T cells that promotes intratumoral NK/ILC1 accumulation and maturation. This allows a $PD1^{+}$ NK/ILC1-like subset to restore ICB response, an effect that is facilitated by inhibition of Tregs (Benci et al., 2019). Altogether, these results illustrate how IFNG operates between adaptive immune cells, innate immune cells, and cancer cells to coordinate immune stimulatory and inhibitory effects. When the inhibitory effects directed by tumor cells are targeted, this can unleash a feed-forward mechanism

coordinated by adaptive and innate cells with the potential to improve ICB response even in tumors with neoantigen or MHC-I deficiency.

Biomarkers and multivariate models that can accurately predict clinical ICB response are an important step in effectively translating immunotherapies. TMB and IFNG-related genes such as PDL1 are undoubtedly important predictive features. High TMB and expression of IFNG-related genes both can positively associate with ICB response (Ayers et al., 2017; Rizvi et al., 2015), while genomic or copy number alterations within B2M and IFN pathway genes can portend resistance and relapse (Gao et al., 2016; Zaretsky et al., 2016). However, it is also clear that these features are imperfect. For example, patients with high PDL1 or IFNG-related genes frequently fail to respond, while patients with low TMB tumors or mutations in B2M or the IFN pathway may nonetheless benefit from ICB. Reasons for such incongruent observations include the failure of gene signatures to capture the inhibitory functions of IFN signaling, somatic IFN pathway variants that unknowingly interfere with these inhibitory functions, or the possibility that these inhibitory functions impact not only adaptive immunity but innate-immune killing as well. We find that incorporating the ISG.RS or IFN pathway variants into models that include TMB and IFNG-related genes improves the ability to predict clinical ICB response. Indeed, the biology uncovered by our experimental models reflects this improvement and the statistical associations that accompany it. Thus, although using ISGs from experimental models to predict clinical response requires further optimization, and the functional properties of tumor variants in IFN pathway genes requires experimental investigation, our results highlight the importance of biomarkers that capture opposing functions of IFN signaling.

In addition to corroborating known immunostimulatory effects of IFNG, we describe additional properties of IFNG signaling between innate and adaptive immune cells that

can promote ICB response. Our work suggests that even if $CD8^+$ T cells are not able to effectively mediate cytolytic anti-tumor killing due to poor neoantigens or defective antigen presentation, improving the ability of T_{EX} to generate IFNG is important for the accumulation of intratumoral NK/ILC1s that can mediate tumor killing. Such a function of $CD8^+$ T cells and T_{EX} to support NK/ILC1s through IFNG are reminiscent of NKT cells (Godfrey et al., 2018). In fact, our studies suggest that $CD8^+$ T cells required to generate IFNG need not be tumor-specific, as revealed by the ability of cross-primed bystander T cells to sustain NK/ILC1 accumulation and NK/ILC1-dependent tumor killing (Benci et al., 2019). These findings may provide insight into a potential utility of bystander T cells to common viruses and other non-tumor antigens that are abundant in human tumors (Simoni et al., 2018). These stimulatory effects of IFNG on NK/ILC1s may be indirect. IFNG from $CD8^+$ T cells may act on macrophages to drive NK/ILC1 expansion through cytokines such as IL-15 (Spits et al., 2016), enhance NK/ILC1 recruitment through CXCR3 ligands (Pak-Wittel et al., 2013), or promote transdifferentiation of ILCs into ILC1s through cytokines like IL-12 (Nagasawa et al., 2017). Consistent with this notion, macrophages from melanoma patients express the IFNG.GS and positively correlate with the frequency of activated intratumoral NK cells (Benci et al., 2019). In mice, IFNG and the IFNG-regulated CXCR3 ligand CXCL10 influences intratumoral NK/ILC1 accumulation and/or phenotype. Altogether, our findings suggest that IFNG can be harnessed by immunotherapy approaches to link tumor-specific T_{EX}, bystander $CD8^+$ T cells, and various types of innate immune cells against tumors differing in neoantigen status.

In contrast to IFNG signaling in immune cells, IFNG signaling in tumor cells orchestrates resistance to ICB. We previously demonstrated that this tumor-driven feedback inhibition is initiated and maintained by chronic IFN signaling (Benci et al., 2016). This results in high levels of PDL1 and multiple other inhibitory receptor ligands (e.g.,

TNFRSF14, LGAL9, etc.) that promotes the accumulation of T_{EX} with markers of severe exhaustion. Besides the resulting T_{EX} having poor cytolytic function, our data suggest that a consequence of diminished IFNG generated by severe exhaustion is the accumulation of immature CD11b$^{-/low}$ NK/ILC1s, which themselves have decreased production of cytokines such as IFNG, low cytotoxic function, and is associated with human tumors with a poor prognosis (Chiossone et al., 2009; Jin et al., 2013). However, tumor IFNG can also directly interfere with NK/ILC1 function. One mechanism involves the same IFNG-regulated inhibitory receptor ligands that promote T_{EX}. In this study, we focus on PDL1 but do not rule out a role for the other ligands on tumor cells that are controlled by IFNG. A second mechanism involves IFNG decreasing expression of TRAILR2 on tumor cells. For tumors with poor or depleted neo-antigens, our findings suggest the need to first block PD1 on T_{EX} to support NK/ILC1 maturation, and then to block PD1 on a NK/ILC1-llke subset to enable TRAIL-mediated killing. Whether targeting other IFN-regulated pathways or inhibitory receptor ligands on tumor cells or other cell types can further improve NK/ILC1 function will be important to investigate (Benci et al., 2019).

How NK/ILC1 recruitment and maturation specifically relates to the PD1^{+} CD11b^{high} NK/ILC1 subset is currently unclear. Recent reports demonstrate that distinct ILC1-like cells have roles in cancer immunosurveillance (Dadi et al., 2016) or in cancer immunosuppression (Cortez et al., 2017; Gao et al., 2017). For the latter, an ILC1-like population that expresses multiple inhibitory receptors such as PD1, CTLA4, and LAG3, is less able to control tumor growth compared to conventional NK cells. In fact, evidence suggests that TGFB can promote immune suppression by driving the conversion of conventional NK cells into these ILC1-like counterparts. Although comparison between ILC populations between studies is a challenge, these TGFB-regulated ILC1-like cells may share features with the PD1^{+} CD11b^{high} NK/ILC1s in our study. If so, there may be a

precursor-product relationship between maturing CD11b^{int} NK/ILC1s and CD11b^{high} PD1^{+} NK/ILC1s. Alternatively, these two populations might belong to separate lineages that are both dependent on a common cytokine like IL-15, or the ILC1-like cells may arise from the transdifferentiation of ILC2s and ILC3s under the influence of inflammatory cytokines. Regardless, by simultaneously increasing tumor TRAILR2 and decreasing expression of PDL1 and multiple other inhibitory ligands, ablating tumor IFNG signaling may help to reactivate otherwise poorly cytotoxic ILC1-like cells. Our findings also suggest that additionally interfering with Tregs is important to initiate killing by these NK/ILC1s, illustrating the diversity of the immunosuppressive mechanisms that need to be targeted (Benci et al., 2019). Thus, a growing understanding of how NK/ILC1 function can be restored may enable approaches that leverage innate immune killing of neoantigen poor tumors or tumors that have lost MHC-I expression. Observations that tumors with B2M deficiency can nonetheless respond to ICB highlight the potential of such strategies (Rizvi et al., 2018; Rodig et al., 2018).

In this study we focus on how IFNG signaling between tumor cells, T cells, and innate immune cells orchestrates cooperative and opposing effects on anti-tumor immune responses. Besides IFNGR, inhibiting STAT1, IFNAR, or IFNGR and IFNAR in tumor cells also diminishes the expression of resistance-associated ISGs and in some cases result in greater anti-tumor responses than IFNGR knockout alone. Thus, how IFN-I contributes to IFN-driven resistance and differs from IFNG requires additional investigation, as does the roles of individual ISGs in ICB resistance. Such questions are particularly relevant given that mutations in human tumors potentially affecting either or both type I and II IFN pathways are observed.

Interestingly, recent work has identified synthetically designed IFNG molecules that are able to uncouple functions of IFNG signaling in tumor cells (Mendoza et al., 2019).

A directed evolution approach generated IFNG molecules designed to bind IFNGR complexes with differing affinity for IFNGR1 and IFNGR2, in which increased affinity for IFNGR1, but decreased affinity for IFNGR2 resulted in decreased STAT1 signaling, and subsequently a bias towards MHC-I expression over PDL1 (and presumably other inhibitory receptors). This is of particular interest because our CRISPR design strategy utilized in Chapter 2 to create IFNGR$^{-/-}$ cancer cell lines focused exclusively on the IFNGR2 gene body. While previous studies have demonstrated that loss of either IFNGR1 or IFNGR2 abrogates productive signaling through the receptor complex (Bach et al., 1996), a possibility remains that short-lived IFNGR1 homodimers are able to sense IFNG in the absence of IFNGR2, leading to similar immunogenic signaling resulting in MHC-I expression in the absence of PDL1. Future experiments will test this possibility through titrations of IFNG signaling in IFNGR2$^{-/-}$ cell lines and additional deletion of IFNGR1. Regardless, therapeutic strategies such as the directed evolution of novel cytokine molecules represent an opportunity to uncouple pro- and anti- immune effects of IFN signaling in cancer cells. Further, a role for excessive IFNG signaling in T cell fratricide has been reported in the TME (Pai et al., 2019). Our work here does not consider that there may be a threshold at which increased IFNG signaling may become directly detrimental to anti-tumor T cells. It would be of additional interest to observe how altered IFNGR binding by synthetically designed IFNG molecules would affect the balance of fratricide and NK cell activation described in the work here. Finally, IFNGR deletion by CRISPR in adoptive cell therapy (ACT) approaches may also be an attractive strategy to limit this effect.

Beyond IFNG, similar *de novo* design approaches have been taken with additional cytokines that function directly on T cells, such as IL-2 and IL-15 (Silva et al., 2019). These molecules have also been described to have pleiotropic effects in the TME, most notably

expansion of immune-suppressive Tregs (Busse et al., 2010), and systemic host toxicity (Schwartz et al., 2002) that compete with their function to activate $CD8^+$ T cells. By modulating affinity for specific subunits of the common-gamma chain cytokine receptor, Silva et al. were able to specifically focus IL-2 and IL-15 signaling to the $CD8^+$ T cell compartment through computational design of novel cytokines. Our work suggests that therapeutic approaches that target specific cellular compartments in this manner may be particularly efficacious in triggering anti-tumor immunity against a variety of tumor types. For example, identification of novel molecules capable of limiting ISGs specifically associated with ISG.RS might limit tumor ISG-resistance programs while leaving immune activation relatively unaffected. Alternatively, stimulating IFNG.GS genes specifically in immune cells might limit tumor resistance programs driven by the same genes. Additional work is needed to create such molecules in order to validate this hypothesis, but such a view might form the basis for novel targeted approaches to enhancing ICB responses in patients.

Section 4.2 – CAR-T PAMP Delivery Enhances Endogenous Anti-Tumor Immunity

Chapter 3 outlines the design of a novel cell therapy inspired by the discovery of a naturally occurring intratumoral PAMP. Delivery of the immune-stimulatory RNA RN7SL1 enhanced infiltration of engineered cells and activation of endogenous immune cells. This is achieved by localizing inflammatory PRR signaling to the intratumoral immune compartment. This strategy improved endogenous T cell proliferation and cytotoxicity, resulting in improved survival as a monotherapy and also in combination with previously reported ICB therapies. Enhanced response to therapy was dependent on the presence of DC1s and their ability to subsequently prime anti-tumor T cell responses. These cells

were able to uptake CAR-T derived RNA and become subsequently activated. This may represent an important priming signal in the TME that facilitates the initiation of anti-tumor immunity.

Similar to results in Chapter 2, a key insight of this work is the relative contribution of inflammatory signaling in distinct cellular compartments to survival outcomes following ICB. Specifically, we see that in the absence of anti-tumor immunity, 7SL RNA activates ISGs in tumor cells and promotes tumor growth. In contrast, when the immune system is primed through the use of ICB, 7SL RNA promotes response to therapy and improved survival. Finally, response is most improved when tumor cells lack the ability to recognize 7SL through deletion of RIG-I in combination with immune-stimulatory ICB. This suggests that PRR signaling promotes competing processes in different cellular compartments, and that the most promising targets for enhancing response to immune-based therapies should focus on non-overlapping pathways between immune and cancer cells.

One way to achieve preferential PRR signaling in immune cells may be through delivery of a PAMP-like molecule by an engineered immune cell. We observe greater RNA uptake following CAR-T cell administration by endogenous immune cells in the TME as compared to tumor cells, suggesting that immune-based delivery may bias inflammatory signals to the endogenous immune compartment. This may be due to interactions at sites like lymph nodes or tertiary lymphoid structures (Joshi et al., 2015), enhancing local immune priming events. Intriguingly, CAR-T/DC interactions have been reported in the tumor draining lymph node (Ma et al., 2019), suggesting that these cell types readily interact. Our data does not consider lymph node interactions directly, but it is an intriguing possibility that CAR-T delivery of 7SL to DCs in the draining lymph node may drive functionally improved anti-tumor T cells through improved T cell priming. Specifically, we observe that CAR-T-

derived 7SL RNA drives enhanced Type I IFN signaling and preferential expression of costimulatory molecules in intratumoral DCs, particularly DC1. This leads to the expansion of an effector-like $CD8^+$ T cell population that drives enhanced solid tumor control. This differs from control tumors that are populated by more exhausted $CD8^+$ T cells and are unable to control tumor growth.

Interestingly, previous reports suggest that chronic Type I IFN signaling contributes to T cell exhaustion (Teijaro et al., 2013; Wilson et al., 2013). This again highlights the complexity and context-dependent nature of these inflammatory pathways. Our results show the acquisition of an effector-like $CD8^+$ T cell transcriptional program, which is consistent with recent reports highlighting the increased efficacy of immunotherapy when T cells are diverted from the exhausted T cell fate (Chen et al., 2019; Lynn et al., 2019; Wei et al., 2019), and suggest a paradigm by which modulating soluble cues may control this process. Interestingly, during acute viral infection Type I IFN is crucial for the acquisition of effector phenotype and cytolytic function (Wiesel et al., 2012), further suggesting that 7SL delivery via CAR-T cell may be locally mimicking an acute viral infection and driving less chronic T cell differentiation. Thus, altering soluble cues involved in T cell priming may drive functionally different T cell fates in the TME. This highlights the need for further research into the role for many of these cytokines in anti-tumor T cell immunity.

Our analysis has deeply explored the differentiation and activation of $CD8^+$ T cells, but has largely ignored counterpart $CD4^+$ T cells. However, IFN-I is a well-known $CD4^+$ T cell polarization cytokine that drives Th1 differentiation (Havenar-Daughton et al., 2006). Indeed, Th1 $CD4^+$ T cells have been implicated as a positive prognostic marker for response to ICB in murine models of disease as well as patients (Wei et al., 2017; Zhang

et al., 2018). Single cell analysis from 19BBz-7SL CAR-T treated tumors revealed a higher level of costimulatory molecule expression and Hallmark IFN-I signature in cDC2, which have been shown to activate $CD4^+$ T cells (Binnewies et al., 2019). Additionally, $CD4^+$ T cells from these tumors express higher levels of activation markers such as Ki67 (data not shown), suggesting that activation of multiple T cell compartments may be enhanced by 7SL delivery. Further, our single cell dataset shows a modest decrease in Treg frequency following 19BBz-7SL CAR-T treatment, consistent with lower levels of TGFB, and further suggesting that $CD4^+$ T cell differentiation may be influenced by 7SL delivery. In this case, we may be influencing naïve $CD4^+$ T cells away from the Treg fate and toward Th1 polarization through enhanced IFN-I signaling and decreased TGFB signaling (Chen et al., 2003). Future work will focus on the relative contributions of $CD4^+$ and $CD8^+$ T cell differentiation in response to 7SL delivery and TME modulation.

While this work has focused on the inflammatory role of a structured RNA, we believe that these conclusions will extend to other naturally occurring PAMP/PRR combinations in the TME. Similar contradictions in the role of compartment-specific inflammation have been reached in the study of TLR3 (Liu et al., 2016b; Salmon et al., 2016), and IFNGR (Benci et al., 2016; Zaretsky et al., 2016) in recent years. Of particular interest, recent work has characterized active microbial communities within certain tumor types (Geller et al., 2017). The commensal microbiome is a well-known source of PAMP signaling in the gastrointestinal tract (Bach, 2018; Swiatczak and Cohen, 2015), and may well be a rich source for additional PAMP signaling through TLRs and inflammasomes within the TME of solid tumors. In addition, a role for endogenous PRR ligands such as DNA has been defined, but often in the activation of a single PRR (i.e. STING). This ignores any potential role for the simultaneous activation of multiple cooperating PRRs, such as the AIM2

inflammasome in the case of DNA. The effects of combinatorial PRR activation through delivery of single or multiple PAMPs will be a significant focus of this work moving forward.

In addition to combinatorial effects, little research has been carried out on the relative quality of different PRR pathways in activating anti-tumor immunity. To this point, much work has demonstrated that different TLR, RLR, and inflammasome pathways can contribute to the activation of anti-tumor immunity (Segovia et al., 2020; Zitvogel et al., 2015). However, none of this work has yet qualitatively compared the effects of one PRR against others. Similarly, a systematic approach for comparing immune agonists in this context has yet to be described. A major barrier in this case is defining an experimental system that is able to effectively answer this question. CRISPR screens have identified many regulators of tumor cell fitness (Manguso et al., 2017; Patel et al., 2017), but are limited to the identification of cell-intrinsic processes. Appropriate observation of systemic host immune interactions is best suited to *in vivo* models, but such approaches are generally not conducive to CRISPR screening because of scalability. Our work and others suggests that a potential solution to this qualitative question is the *in vitro* screening of DC/T cell interactions in the presence of various reported immunogenic molecules. This might include introduction of various PAMPs to BMDC cultures followed by RNA sequencing to identify IFN-I or IFNG.GS gene signatures that predict enhanced T cell priming and immune response *in vivo*. Alternatively, we might repurpose the BMDC/OT-I system outlined in Section 3.6 and utilize available GzmB-reporter OT-I T cells. In this case PAMPs would be added to BMDC/OT-I cultures and then reporter fluorescence could be assessed in a high-throughput manner to directly assay cytotoxic priming of $CD8^+$ T cells. Chapter 2 suggests that we might then combine these assays with a similar screen on a panel of cancer cell lines in order to identify immunogenic molecules with greater

effects on immune priming than induction of ISG.RS in tumor cells. Many such approaches might be imagined, but answering this question remains a crucial barrier to translating these findings to patient benefit.

In the clinic, PRR agonist therapeutics are currently given as systemic treatments or single local intratumoral injections (Hammerich et al., 2019). These strategies have yielded hints of positive response, but delivery via CAR-T cell as described in Chapter 3 offers several key advantages. First, the CAR construct itself imbues these cells with a synergistic therapeutic capability by their capacity to kill tumor cells. Further, as discussed in Section 3.3, delivery via immune cell seems to bias our inflammatory stimulus toward a beneficial immune-focused PRR activation. This delivery also offers the ability to localize steady production of a therapeutic payload specifically to the TME, instead of systemic treatments that may result in undesirable toxicities (Hu et al., 2019; Sercombe et al., 2015). Additionally, this therapeutic framework could also be built to include safety switches such as inducible expression or suicide genes that have been previously reported (Lim and June, 2017). Finally, engineered T cells have shown an ability to infiltrate previously immune-sparse or “cold” tumors if targeted correctly (Posey et al., 2016). Our work suggests that the addition of immunogenic PAMPs to such therapies has significant potential to jump-start an endogenous anti-tumor immune reaction that would benefit a large portion of currently underserved cancer patients.

Beyond an ability to stimulate endogenous immunity, we believe this cellular engineering architecture is also amenable to emerging technologies such as CRISPR genome editing, as well as more established therapeutic modalities such as RNAi. Currently, the standard method of delivery for these technologies in the clinic is through the use of liposomes. While significant progress has been made in enhancing the specificity and half-life of these

vesicles in the body, a majority are still taken up by off-target tissues (Riley et al., 2019). Approaches like integrin inclusion and membrane charging of synthetic vesicles (Deshpande et al., 2013), as well as direct exosome production (Dai et al., 2008) have improved these targeting capabilities somewhat, but liver and kidney tissue is still a primary sink for these vesicles *in vivo* (Sercombe et al., 2015). Indeed, the only currently approved RNAi therapy targets hATTR amyloidosis, a liver disease (Adams et al., 2018). Thus, strategies that improve the effective delivery of these therapies might greatly improve the reach of RNAi and other biologic therapeutics to a significantly wider range of diseases.

Section 4.3 – Future Directions Understanding TME Inflammation and Broadening Therapeutic Strategies

Our results in Chapter 3 suggest that inflammatory molecules like IFN-I play an important role in shaping the solid tumor TME. Here, we artificially mimic the presence of a naturally occurring PAMP, 7SL (Nabet et al., 2017); however, this is unlikely to be the only RNA of its kind capable of activating PRR signaling. Indeed, activation of IFN-I production may be attributed to many potential sources. Future experiments will focus on the identification of additional RNA PRR ligands and regulators of their expression. Previous studies indicate that de-repression of ERVs through the use of DNMT inhibitors may provoke upregulation of ISGs (Chiappinelli et al., 2015), and unpublished data in the Minn lab suggests that radiation may have a similar effect. Thus, ERVs (which are evolutionarily and structurally related to RN7SL1 (Okada, 1991) may represent an additional source of tumor-intrinsic inflammation. Our results in Section 3.2 suggest that non-therapeutic contexts in which these elements become de-repressed may represent an important cell-intrinsic resistance

mechanism for cancer cells and could represent a powerful prognostic marker. In order to test this hypothesis, we can interrogate a panel of ICB-resistant cell lines generated by the Minn Lab as well publicly available databases for presence of de-repressed ERV elements and correlations to resistance gene signatures like ISG.RS and others.

Additionally, our data suggests that the activation of different PRRs may have important functional consequences. Specifically, 7SL RNA requires recognition by both RIG-I and MDA5 in order to stimulate ISG expression, while Scr control RNA required recognition by only RIG-I. Interestingly, this singular dependence led to significantly worse T cell priming than 7SL RNA in both *in vitro* and *in vivo* assays, albeit still better than non-immunogenic controls in many cases. This dual PRR dependence seems to be a unique property of the 7SL RNA, as most reported RNA PRR ligands display specificity for a single receptor (Brisse and Ly, 2019). We predict that this dual-specificity arises from the specific combination of length, secondary structure, and 5'-triphosphate possessed by 7SL. In order to test this, we might denature our 7SL and Scr RNAs with and without phosphatase treatment specific to the 5'-triphosphate moiety. In this context, we would expect to retain characteristics similar to Scr RNA control when secondary structure is lost but 5'-triphospahte is retained; namely, stimulatory capability dependent on RIG-I only. However, if secondary structure and 5'-triphosphate are lost, we might expect no immunogenic activity from either RNA. Given the size of 7SL RNA as compared to RIG-I or MDA5 binding proteins, we would not expect these proteins to bind 7SL simultaneously. Thus, co-dependence of RIG-I and MDA5 for 7SL recognition might represent a forward-feedback cycle in which both proteins are required in an unexpected way that should be further examined mechanistically. The identification of novel signaling modalities in these

well-characterized networks might uncover fundamental rules for the quality of certain RNA PAMPs as compared to others.

Our work in Chapter 3 demonstrated the ability of CAR-T cells to deliver 7SL to immune cells in the TME via CD19-directed CAR that recognized a CD19-expressing melanoma. This is an artificial system, and demands that future experiments test 7SL delivery in the context of naturally occurring solid tumor antigens. Given that we envision this therapy moving forward in the context of heterogenous solid tumors, appropriate combinations might include mesothelin-targeted (i.e. M5) or Her2-targeted (i.e. 4D5) CARs in the context of lung cancer or breast cancer cell lines, respectively. We will carry out these experiments in both syngeneic models and NSG+ systems. This will be important in order to validate that human immune cells are also capable of RNA export and uptake demonstrated by murine cells in the work published here. Experiments could range from simple co-injection of PBMC with CAR-T cells in order to observe RNA transfer in the TME to more complex models such as BLT or MISTERG humanized mice that would allow measurement of "endogenous" immune infiltration and uptake, and potentially measurement of human cell efficacy if sufficiently reconstituted.

Our results utilizing a heterogenous B16 tumor model also raise the possibility that 7SL delivery might expand the efficacy of previously characterized CAR molecules that have been shelved because of targeting concerns. This is an extension of the "on-target, off-tumor" tradeoff outlined in Section 1.6. CARs designed to recognize and target tumor-specific antigens such as TnMuc1 (Posey et al., 2016), and EGFRvIII (Morgan et al., 2012) are generally effective in preclinical models, but fail to induce durable tumor regression in patients because of incomplete antigen penetrance and target heterogeneity. For this reason, CARs with some off-tumor toxicity (i.e. mesothelin) have been prioritized with

careful dosing (Haas et al., 2019) and the hope of generating strong responses with manageable toxicity. Even so, these therapies are predicted to leave some antigen-negative residual disease. Thus, delivery of an immunogenic RNA such as 7SL might enhance the safety of CAR-T therapy as whole by allowing use of safer CAR molecules that do not target healthy tissue. This would be complimented by the activation of endogenous T cell specificities that are generally not self-reactive. This presents a potentially breakthrough clinical benefit for this therapeutic approach.

Our focus thus far has centered around the delivery of therapeutic RNA molecules. This is an exciting and novel use for engineered cell therapies, but we imagine a much broader therapeutic suite of molecules could be paired with this system. Taking inspiration from previous *de novo* protein design approaches (Hosseinzadeh et al., 2017; Mendoza et al., 2019; Silva et al., 2019; Votteler et al., 2016), we predict that small bioactive peptides might serve as highly selective small molecule inhibitors or agonists in this framework. Future experiments will characterize an approach by which we can identify and optimize these molecules and test their efficacy *in vivo* when paired with CAR-T cell delivery.

For example, DNA PRRs such as STING or TLR9 bind dinucleotide molecules (cGAMP or CpG) that cannot be encoded by DNA/RNA, and are therefore not able to be integrated with traditional cell engineering approaches. The upstream source for these ligands is free-floating DNA, which is also not compatible with viable engineered cells. For this reason, these pathways (and many others) are typically modulated through non-biologic small molecule agonists (Su et al., 2019). In order to target such a pathway, we propose that *de novo* design of a small peptide drug that is DNA-encodable could provide the same functionality and improve efficacy and tolerability through CAR-T cell delivery. To accomplish this, we might take a publicly available structure of STING/TLR9 in an active

conformation and utilize protein folding prediction algorithms to identify candidate peptide molecules that bind STING/TLR9 in this active conformation. Binding specificity might then be improved by applying principles of directed evolution until a small number of optimal candidates was reached. Downstream screening would validate candidates with biological activity, and we could then test delivery via CAR-T cell using the same systems described in Chapter 3. This idea is particularly attractive because it is theoretically applicable to any biological pathway of interest and could affect a variety of chronic disease conditions.

For example, a number of papers in recent years have sought to identify pathways that may antagonize responses to immunotherapy, and would therefore make attractive targets for these *de novo* designed peptides (Benci et al., 2016; Ishizuka et al., 2019; Manguso et al., 2017). Alternatively, pathways that favor tumor cell death have been shown to enhance response to ICB (Vredevoogd et al., 2019; Wang et al., 2019; Zhang et al., 2020). Many of these cell death pathways converge on the SMAC family of proteins that translate extracellular cues into cell death or survival signals through SMAC/IAP interactions. SMAC mimetics that encourage cancer cell death have been designed and are well-tolerated, but lack efficacy (Jensen et al., 2020). Designing an inhibitor to this family of proteins might lower the threshold for immune-mediated cell death and enhance efficacy of CAR-T and/or ICB therapy. Similarly, synthetic-lethal screens have previously identified targeted molecules like PARP-inhibitors that are effective in small subsets of cancers but lack widespread adoption. Disruption of DNA repair pathways might greatly enhance antigenicity and immunogenic cell death, and could contribute strongly to enhanced endogenous immune activation (Harding et al., 2017) in combination with our CAR-T cell approach. We hope to identify several targets such as these in order to design and test the delivery of small peptide therapeutics in combination with CAR-T cell delivery

in the future. We believe this approach will increase local concentration of the relevant therapeutic through constant local production, while minimizing systemic distribution.

At a more basic level, it is important that we understand how and why CAR-T cells seem to interact with immune cells more frequently than other cells in the TME. Potential explanations for this include preferential trafficking to tertiary lymphoid structures (Cabrita et al., 2020; Helmink et al., 2020; Petitprez et al., 2020) and draining lymph node interactions (Ma et al., 2019; Roberts et al., 2016), but detailed studies are needed to confirm this hypothesis. Single-cell spatial transcriptomic assays may provide an opportunity to ask these questions in a comprehensive way. Simultaneous observation of cellular localization in the TME combined with the ability to measure RNA transfer from engineered to endogenous cells would provide powerful evidence for the localization of these interactions. This might also inform outstanding questions about the ways in which cytokine distribution (Oyler-Yaniv et al., 2017) and inhibitory ligand distribution (Binnewies et al., 2018) within the TME affect anti-tumor immune responses. This might elucidate mechanisms by which NK cell maturation and recruitment highlighted in Chapter 2 are achieved by $CD8^+$ T cells. For example, we might predict to find distinct microenvironments within the TME that are enriched for IFNG or TGFB signaling that dictate ILC1/NK cell differentiation. We believe these spatial factors may significantly contribute to the outcome of ICB and we hope to thoroughly address them in the future.

In total, the work presented here outlines a framework for understanding the role of inflammatory signaling in distinct cellular compartments in the TME. This localization of signaling drives divergent outcomes following ICB, and is a crucial regulator of tumor/immune interactions. We find that tumor-intrinsic signaling drives treatment resistance and immune suppression, but localization of the same cues to the immune

compartment drives immune activation and downstream anti-tumor responses. Direct anti-tumor responses include contributions by both T and NK cells depending on the antigenic context of the TME. We are able to leverage this finding through delivery of immunogenic 7SL RNA by CAR-T cell to immune cells within the TME. This results in immune-focused RNA PRR signaling and activation of endogenous anti-tumor immunity. These responses engender clearance of heterogenous tumors: a longstanding goal in the field of immunotherapy. Thus, these findings underpin a novel paradigm for the delivery of immune-focused therapeutics in refractory solid tumors.

CHAPTER 5 – METHODS

Mice

All animal experiments were performed according to protocols approved by the Institutional Animal Care and Use Committee of the University of Pennsylvania. Five to seven week old C57BL/6 (stock# 027) and BALB/c (stock# 28) mice were obtained from Charles River Laboratory. Five to seven week old female C57BL/6 (stock# 000664), Perforin knockout (C57BL/6-Prf1^{tm1Sdz}/J; stock# 002407), IFNG knockout (B6.129SJ-Ifng^{tm1Ts}/J; stock # 002287), RAG1 knockout (B6.129S7-Rag1^{tm1Mom}/J; stock# 002216), OT1 (C57BL/6-Tg(TcraTcrb)1100Mjb/J; stock# 003831), FoxP3-DTR (B6.129(Cg)-Foxp3$^{tm3(DTR/GFP)Ayr}$/J; stock# 016958); Batf3 KO (B6.129S(C)-Batf3^{tm1Kmm}/J; stock#013755), TCRa KO (B6.129S2-Tcra^{tm1Mom}/J; stock#002116), MAVS KO (B6.129-Mavs^{tm1Zjc}/J; stock#008634), RIG-I KO (C57BL/6NJ-DDx58$^{em1(IMPC)J}$/Mmjax; stock#46070-JAX) were ordered from Jackson Laboratory (Bar Harbor, ME). Female mice between the ages of 5-9 weeks were maintained under specific pathogen free conditions in order to be utilized in these experiments.

Cell Lines

B16-F10 melanoma cells (CRL-6457, male), TSA breast cancer cells (CVCL-F736, female), and resistant sublines were derived and cultured as previously described (Twyman-Saint Victor et al., 2015). CT26 colorectal cancer cell lines were purchased from ATCC and similarly cultured (CRL-2638, gender unknown).

CRISPR gene targeting

Gene targeting by CRISPR/Cas9 was accomplished by co-transfection of a Cas9 plasmid (Addgene, 41815), the guide sequence (selected using ZiFit Targeter) cloned into the gBlock plasmid, and a plasmid with the puromycin selection marker. Successful targeting of the gene(s) of interest was determined by treating cells with and without 100 ng/mL of IFNG (PeproTech), 1000 units/mL IFN-beta (PBL Assay Science), or both depending on the target gene, and examining PDL1, B2M, or TRAILR2 surface expression by flow cytometry. Knockout cells were sorted from a bulk knockout population using Fluorescence Activated Cell Sorting (FACS) on the Aria (BD) or FACSJazz (BD) to maintain the diversity of the parent cells. The gene block contains 20 bp target size (N), U6 promoter, gRNA scaffold, and a termination signal. The common gene block sequence is:

TGTACAAAAAAGCAGGCTTTAAAGGAACCAATTCAGTCGACTGGATCCGGTACCAA
GGTCGGGCAGGAAGAGGGCCTATTTCCCATGATTCCTTCATATTTGCATATACGAT
ACAAGGCTGTTAGAGAGATAATTAGAATTAATTTGACTGTAAACACAAAGATATTAGT
ACAAAATACGTGACGTAGAAAGTAATAATTTCTTGGGTAGTTTGCAGTTTTAAAATTA
TGTTTTAAAATGGACTATCATATGCTTACCGTAACTTGAAAGTATTTCGATTTCTTGG
CTTTATATATCTTGTGGAAAGGACGAAACACCG**NNNNNNNNNNNNNNNNNNN**GTTT
TAGAGCTAGAAATAGCAAGTTAAAATAAGGCTAGTCCGTTATCAACTTGAAAAAGTG
GCACCGAGTCGGTGCTTTTTTTCTAGACCCAGCTTTCTTGTACAAAGTTGGCATTA

The guide sequences used are published (Benci et al., 2019; Benci et al., 2016)

In vivo mouse studies

Tumor injection and treatment schedule were done as previously described(Twyman-Saint Victor et al., 2015). In Chapter 2 studies, both flanks were implanted, in Chapter 3 studies a single flank tumor was utilized. Blocking antibodies were given on days 5, 8, and 11 unless otherwise specified. Anti-CD8, anti-NK1.1., and anti-Asialo-GM1 were given on days -2, 0, 4, 8, 12, and 16. Antibodies against CTLA4 (9H10), PDL1 (10F.9G2), or PD1 (RMP1-14) were all administered intraperitoneally at 200 ug/dose. In certain experiments, a single flank tumor was irradiated on day 8 utilizing a targeted SAARP machine. Isotype controls were used to confirm the lack of non-specific effects and a similar response and survival to untreated mice.

Analysis of tumor growth, survival, and group differences

Tumor volumes were determined by caliper measurements. Differences in survival were determined for each group by the Kaplan-Meier method and the overall p-value was calculated by the log-rank test using the *survival* R package. For mouse studies, an event was defined as death or when tumor burden reached a pre-specified size to minimize morbidity. Using the *MASS* R package, a mixed effect generalized linear model with lognormal distribution for tumor volume data was used to determine differences in growth curves. The significance of all two-way comparisons was determined by a two-sample two-tailed t-test, or by a one-tailed t-test when appropriate. For non-parametric data, a Wilcoxon rank-sum test was used.

Single Cell Sequencing Preparation

Tumors were harvested and viable CD45.2^{+} cells were FACS sorted on an Aria II. Single-cell emulsions were obtained using the 10x Genomics Controller and the v2 Library and Gel Bead kit (10X Genomics) for data in Chapter 2, or v3 kit for data in chapter 3. RNA-sequencing libraries were prepared as instructed by the 10x 3' kit protocol. Resulting libraries were sequenced on an Illumina NextSeq using a NextSeq 500/550 v2.5 High Output Kit.

Flow cytometry

Tumors were harvested at day 13-15 post tumor implantation. Single-cell suspensions were prepared and red blood cells were lysed using ACK Lysis Buffer (Life Technologies). For *in vitro* cell lines, untreated or sub-confluent cells treated for 16 hours with 100 ng/mL of IFNG (PeproTech) were harvested and single-cell suspensions prepared. Similarly, 100 ng/mL *in vitro* transcribed RNA formulated with Opti-Mem media and RNAiMax reagent were used to treat cell lines or healthy donor PBMCs and then stain for ISGs in some experiments. Live/dead cell discrimination was performed using Live/Dead Fixable Aqua Dead Cell Stain Kit (Life Technologies). Cell surface staining was done for 30 min at 4 degrees. Intracellular staining was done using a fixation/permeabilization kit (eBioscience). Data acquisition was done using an LSR II (BD) or FACSCalibur (BD) and analysis was performed using FlowJo (TreeStar) or the *flowCore* package in the R language and environment for statistical computing. For high-dimensional flow cytometry, a FACSymphony (BD) was used for data acquisition and data analysis was done using the *cytofkit* R package and a custom analysis pipeline described in Quantification and

Statistical Analysis. Fluorophore-labeled antibodies were purchased from Biolegend, eBioscience, and BD.

Intratumoral cytokine assay

Approximately 200 ug of tumor was harvested, weighed, and placed in complete RPMI media for 4 hours at 37 degrees. The media was then harvested, spun to remove any remaining cells, and analyzed for cytokine expression (Luminex) according to the manufacturer's instructions. Resulting cytokine levels were then divided by the initial tumor weight for each sample.

In vivo cytokine rescue studies

All mice were pre-treated with anti-CD8 Two days before tumor injection. Either 1 ug IFNG or 100 ng CXCL10 was mixed in the PBS/tumor cell suspension prior to injection of the tumor. Mice then continued receiving 500-1000 ng IFNG or 100 ng CXCL10 intra/peritumorally every 3 days post-tumor implantation. For flow cytometry experiments, mice were harvested at day 13 to examine the effects of cytokine addback on immune recruitment in the absence of $CD8^+$ T cells. For survival experiments, intra/peritumoral injections continued every 3 days for the remainder of the experiment.

OT1 mice studies

Transgenic OT1 mice or littermate wild type mice were implanted with tumors using Res 499 cells with IFNGR and B2M knockout. Groups receiving Ova peptide had 50 ng of peptide mixed into the suspension prior to tumor injection and continued to receive intra/peritumoral injections on days 3, 6, 9, and 12. For flow cytometry experiments, mice were harvested on day 13.

Murine chimeric antigen receptor T cells

B16-F10, Res 499, or KP tumor cells were transduced with pCLPs-hCD19 lentivirus to express a truncated human CD19 antigen that is unable to drive intracellular signaling. Cells were double sorted for stable expression. $5x10^4$ tumor cells in log phase growth were implanted into flanks of B6 mice. Murine T cells were stimulated with CD3/CD28 Dynabeads (Invitrogen) for 24 hours and then transduced with pMSGV-h19BBz, pMSGV h19BBz-7SL, or pMSGV h19BBz-Scramble retrovirus. At 48 hours after transduction, CAR-expressing T cells were quantified and $2\text{-}5x10^6$ CAR-expressing T cells were injected i.v. in mice bearing B16-, KP-, or Res499-hCD19 tumors 5 and 12 days after tumor implantation. Controls were either mock PBS-injected or control stimulated CAR-T cells, which gave comparable results. Where indicated, checkpoint blockade was administered on day 8, 11, and 14 when combined with CAR-T administration.

In vivo RNA administration

Mice were implanted with 5×10^4 B16-F10 tumor cells and injected with 200 ng of indicated RNA peritumorally on days 5, 8, and 11. RNA was encapsulated in an emulsion of

RNAiMax reagent and FBS-Free Opti-MEM Media. For flow cytometry experiments, mice were harvested at day 15 to examine the effects of RNA administration on immune recruitment. For immune-deficient survival experiments, mice were depleted of $CD4^+$ (GK1.5) and $CD8^+$ (2.43) T cells 2 days before tumor injection, and were continually administered depleting antibodies every 4 days following. When combined with ICB, ICB antibodies (9H10, RMP1-14) were administered at day 8, 11, and 14.

Extracellular Vesicle Purification

T cells were expanded in culture as described above and harvested by centrifugation at 2,000 rpm on day 4. Cell-free media was then spun again at 4,000 rpm for 10 minutes and subsequently filtered through a .2 uM filter. Vesicles were then obtained by centrifugation at 100,000 x g for 2.5 hours. RNA was purified from vesicles using Qiagen RNAEasy kit, and used for qPCR of transcripts of interest or BMDC stimulation.

CAR-T RNA Labeling Experiments

T cells were expanded as above and transduced with retroviral constructs as specified. Immediately prior to injection, cells were incubated with 500 nM solution of SytoRNA Select dye in PBS at 37 C for 30 min. Cells were washed three times to remove unbound dye, and then resuspended in 50 uL PBS for intratumoral injection. Tumors were harvested 24 hours later, and flow cytometry was performed to observe RNA fluorescence in various populations. In indicated experiments, cells were treated with 20 ug/mL of NSMi GW4869 or DMSO 24 hours prior to T cell harvest and injection. For qPCR experiments,

45.2+ endogenous immune cells that were labeled with SytoRNA dye derived from CAR-T cells were sorted on an Aria II cell sorter followed by RNA isolation using Qiagen RNAEasy kit.

BMDC/OT-I Co-Culture

BMDC of indicated genotypes were prepared by flushing bone marrow from mouse hindlimbs and plating 10^5 cells/mL in RPMI media + 10% FBS and 30 ng/mL of GM-CSF. Media was changed at day 4 of culture while retaining non-adherent cells. BMDC were stimulated with 100 ng/mL of IVT RNA or 50 ng/mL of EV-RNA at day 4. RNA was prepared using serum-free OptiMEM media and RNAiMax reagent. On day 6, BMDC were harvested and loaded with 1 ug/mL SIINFEKL Ova peptide in serum-free PBS at 37 C for 2 hours. BMDC were then washed three times to remove excess peptide and residual RNA and were resuspended in RPMI + 10% FBS. OT-I T cells were harvested from spleens of OT-I mice by $CD8^+$ T cell enrichment and then cultured with peptide-loaded BMDC at a 1:1 ratio in 12 well plates. In indicated experiments, aIFNAR blocking antibody MAR1-5A3 was added to cultures at the time of T cell co-culture to block Signal 3 priming.

qRT-PCR Gene Expression

Relative gene expression levels after qRT-PCR were defined using either ΔCt or the ΔΔCt method and normalizing to GAPDH (cellular RNA) or 18s (EV RNA). Human-specific 7SL primers were designed to target a 3 bp difference in the mouse and human 7s1 and 7SL genes at the 3' primer terminus.

Human 7SL
F: GCTACTCGGGAGGCTGAGGCT
R: TATTCACAGGCGCGATCC

Scramble 7SL
F: CTTCGCGGGAACATTCTCA
R: GACCGAGCTGGCATCATATC

GAPDH
F: AGGTCGGTGTGAACGGATTTG
R: TGTAGACCATGTAGTTGAGGTCA

18S
F: CCCCATGAACGAGGGAATT
R: GGGACTTAATCAACGCAAGCTT

IFNB
F: GGAGATGACGGAGAAGATGC
R: CCCAGTGCTGGAGAAATTG

IFNA7
F: CATCTGCTGCTTGGGATGGAT
R: TTCCTGGGTCAGAGGAGGTTC

IFNA12
F: CAGCAGGTGGGGGTGCAGGAG
R: TTTCTTCTCTCTCAGGTACAC

IFNA primers identified by (Li and Sherry, 2010)

In Vivo aIFNAR Blocking Experiments

C57BL/6 mice were implanted with $5x10^4$ B16-hCD19 tumor cells. 24 hours prior to CAR-T treatment, mice were injected with 200 ug of aIFNAR blocking antibody MAR1-5A3 or PBS control intraperitoneally. Additional injections were administered every 4 days until mice reached experimental endpoints. For flow cytometry experiments, mice were sacrificed at day 15. Tumor growth and survival experiments were monitored by caliper as described above.

B16 Memory Rechallenge

C57BL/6 mice were implanted with $5x10^4$ tumor cells mixed at a 1:1 ratio of B16-h19 and B16-F10 WT cells. Mice were then treated with CAR-T + ICB regimen as described above. On day 80, mice that had achieved complete responses via treatment with 19BBz-7SL CAR-T cells were challenged with $5x10^4$ B16-F10 WT tumor cells and tumor relapse was monitored. Mice were sacrificed at endpoints described above.

Analysis of genomic features from clinical melanoma samples

Processed bulk RNA-seq data from two different cohorts of melanoma patients treated with anti-PD1 (Hugo et al., 2017; Riaz et al., 2017) were downloaded from the GEO. CIBERSORT (Newman et al., 2015) was used to infer relative frequencies of immune cells in the tumor. For immune cell types with values for both resting and activated states, the values for the resting state were subtracted from values for the activated state. To calculate metagenes, gene expression data were centered and scaled using the sample mean and standard deviation, respectively. Then, the average expression of the genes in each gene set was calculated for each sample to give the metagene value. For tumor mutational burden, the provided values were log10 transformed.

Single-cell RNA-sequencing analysis

For single-cell immune cell data from mouse tumors using the 10X Genomics platform, data were first processed using the *Cell Ranger* pipeline (10X Genomics). This included demultiplexing BCL files into FASTQ, performing alignment with STAR, UMI counting, and aggregating replicates of the same condition. Cells that had fewer than 500 genes detected, over 10% mitochondrial content, or over 3.5 times the median UMI count were removed. Genes expressed in less than 1% of cells were also removed. After these QC steps, UMI counts were imputed with *SAVER* (Huang et al., 2018). *Seurat* was then used to normalize data to sequencing depth using a LogNormalize implementation, and mitochondrial contamination and cell cycle effects were regressed out. Clustering was performed using *Seurat's* graph-based clustering approach and visualized with tSNE or UMAP. Clusters were classified using a collection of manually curated immune marker genes (Chapter 2), or previously published genesets corresponding to known immune populations (Alshetaiwi et al., 2020; Beltra et al., 2020; Zilionis et al., 2019) (Chapter 3). Pseudotime analysis was performed using the *Monocle* package in R. Unsupervised analysis specified a seed population of cells and subsequent cell "states" along the pseudotime trajectory based on differentially expressed genes derived from comparisons between Seurat-identified clusters. States were then matched to known immune populations by reference genesets in the same manner as Seurat-identified clusters. Metagene values for IFNG.GS and Hallmark IFN-I geneset were determined similarly to the clinical analysis. The average scaled values for *Mki67* and *Top2a*, and the average scaled values for *Cxcl9* and *Cxcl10* were used to calculate the proliferation and Cxcl9/10 metagene, respectively. For visualization purposes, metagene values less than or greater than 2.5 times the interquartile range were removed. Comparison of expression values between groups was done using a Wilcoxon rank-sum test. GSEA was performed using the *fgsea* R package. Statistical significance was determined by FDR when comparing

between conditions and against enrichment of random gene sets when comparing across clusters. Gene sets for LCMV terminal exhausted T cells, progenitor exhausted T cells, and intratumoral ILC1 populations in Chapter 2 were curated from previously published reports (Gao et al., 2017; Miller et al., 2019).

Multivariable classification, regression, and survival analysis

Random forest (RF) for classification, regression, and survival analysis is a multivariable non-parametric ensemble partitioning tree method that can be used to model the effect of all interactions between genes on a response variable (Ishwaran, 2015). We used the *randomForestSRC* package version 2.5.1.14 and the following parameters: 5000 trees, node size of 2, and default values for mtry. The default splitting rule was used for classification and the log-rank slitting rule was used for survival analysis. The default value for nsplit was used except for models containing both two-level factor variables and continuous variables. In this case, the nsplit parameter was set to 2 in order to prevent bias against the factor-level variables. Importance scores were calculated using the random ensemble method. For classification problems where the two classes were imbalanced, a random forest quantile-classifier approach was employed. Response was defined as complete or partial response. All predicted values, error rates, and importance scores were based on cross-validation using out-of-bag samples. For variable selection and assessing variable robustness, we considered the set of immune cell frequencies (inferred by CIBERSORT), TMB, IFNG.GS, ISG.RS, and/or the difference between IFNG.GS and ISG.RS (dISG) in a model for immune checkpoint blockade response. Prior treatment status and cohort were included to ensure the lack of confounding from these

variables. Balanced undersampling of the majority class was performed and variable selection was determined using minimal depth (Ishwaran and Kogalur, 2010). The frequency that each variable was selected and its associated importance score were averaged over 100 iterations.

To complement the RF approach for modeling probability of clinical response to immune checkpoint blockade, we also performed multivariable logistic regression. From this, odds ratios and 95% confidence intervals were determined for each log10 increase in TMB or 0.5 unit increase in metagene expression values. To complement RF variable selection using minimal depth, we performed lasso regression using the *glmnet* R package. Both RF and linear regression methods yielded comparable results.

High-dimensional flow cytometry analysis

Fluorescence intensity data were analyzed using the *flowCore* R package and transformed using the logicle method. After excluding debris, dead cells, doublets and $CD45^-$ cells, $CD8^+$ T cells and NK/ILC1 cells were gated and separately analyzed. $CD8^+$ T cells were identified as $TCRB^+$ and CD8, while NK/ILC1 cells were identified as $TCRB^-$ and $NK1.1^+$. For each population, an aggregate data matrix from random sampling of 1000 events from each sample was used for dimensionality reduction and for clustering analysis. Clusters were identified using Phenograph (Levine et al., 2015) as implemented in the *cytofkit* R package and visualized by tSNE. Using cluster membership as class definitions, a RF classifier was developed using the same aggregate data matrix. After confirming a low misclassification error rate for each class, this RF classifier was used to assign all cells in all samples to one of the clusters. Using the two-dimensional tSNE

coordinates, a RF classifier was also developed and used to assign all cells to the tSNE map, allowing the distribution and frequencies of immune cells across clusters to be estimated for each sample. To analyze which immune clusters are strongly associated with wild type or IFNGR knockout tumors, the frequencies of immune cells within each cluster were used as features in a RF model, and the resulting importance scores were examined.

Variant analysis of clinical lung cancer tumors

We used previously published processed data for somatic non-synonymous variants from non-small cell lung cancer patients treated with anti-PD1 and anti-CTLA4 (CheckMate-012 study) or from TCGA (Hellmann et al., 2018). Variants in one of 11 genes involved in type I or II IFN pathway signaling (IFNGR1, IFNGR2, IFNAR1, IFNAR2, JAK1, JAK2, TYK2, STAT1, STAT2, IRF9, and B2M) were examined. To exclude likely normal or benign variants, missense variants were annotated with *ANNOVAR*. Any missense variant found in all individuals in the ExAC database at a relative frequency greater than 0.0001 was removed. In order to predict benign from pathogenic missense or nonsense variants, two algorithms for scoring deleterious variants were used that included DANN, a deep learning algorithm, and CADD, a machine learning algorithm. For each method, an optimal cut point was selected by training on ClinVar data. Here, ClinVar variants classified as likely benign were considered benign and those classified as likely pathogenic were classified as pathogenic. The optimal cut points based on ROC accuracy were then applied to test accuracy in predicting these labels. Any variant below the ROC cut points for both DANN and CADD was categorized as benign. This yielded an overall accuracy of

0.80, sensitivity of 0.95, and specificity of 0.54. This criterion was then applied to the TCGA lung cancer data and the lung cancer tumors from CheckMate-012. For indels, SIFT was used for evaluation and non-frameshift indels and indels predicted to be neutral were excluded. Examining the IFN pathway variants, any patient with at least one predicted pathogenic missense variant, pathogenic nonsense mutation, or deleterious indel resulting in a frameshift was classified as IFN pathway variant positive.

The progression-free survival (PFS) of patients stratified by IFN pathway variant status was determined by Kaplan-Meier survival. The likelihood of response was determined by a multivariable logistic regression using variant status, log10 transformed values for TMB, and a previously used %PDL1 staining cut off of greater than or equal to 1%. The p-value for odds ratios was calculated by bootstrapping. In addition, a non-parametric model for response employing multivariable random forest was also used and without the need to transform any of the variables. The out-of-bag error rate and importance scores from this random forest model was then determined. To evaluate the significance of the observed association between IFN pathway variant status with PFS and decreased %PDL1 staining, the variant status of random sets of 11 genes were evaluated and used to stratify patients. Then, the hazard ratio for PFS and the associated p-value, and the %PDL1 staining for variant-positive and negative patients were recorded for 10,000 iterations and compared to the observed values.

BIBLIOGRAPHY

(2018). JCAR015 in ALL: A Root-Cause Investigation. Cancer Discov *8*, 4-5.
Abels, E.R., and Breakefield, X.O. (2016). Introduction to Extracellular Vesicles: Biogenesis, RNA Cargo Selection, Content, Release, and Uptake. Cell Mol Neurobiol *36*, 301-312.
Ablasser, A., Schmid-Burgk, J.L., Hemmerling, I., Horvath, G.L., Schmidt, T., Latz, E., and Hornung, V. (2013). Cell intrinsic immunity spreads to bystander cells via the intercellular transfer of cGAMP. Nature *503*, 530-534.
Adams, D., Gonzalez-Duarte, A., O'Riordan, W.D., Yang, C.C., Ueda, M., Kristen, A.V., Tournev, I., Schmidt, H.H., Coelho, T., Berk, J.L*., et al.* (2018). Patisiran, an RNAi Therapeutic, for Hereditary Transthyretin Amyloidosis. N Engl J Med *379*, 11-21.
Ager, C.R., Reilley, M.J., Nicholas, C., Bartkowiak, T., Jaiswal, A.R., and Curran, M.A. (2017). Intratumoral STING Activation with T-cell Checkpoint Modulation Generates Systemic Antitumor Immunity. Cancer Immunol Res *5*, 676-684.
Ahmed, N., Ratnayake, M., Savoldo, B., Perlaky, L., Dotti, G., Wels, W.S., Bhattacharjee, M.B., Gilbertson, R.J., Shine, H.D., Weiss, H.L*., et al.* (2007). Regression of experimental medulloblastoma following transfer of HER2-specific T cells. Cancer Res *67*, 5957-5964.
Alexandrov, L.B., Nik-Zainal, S., Wedge, D.C., Aparicio, S.A., Behjati, S., Biankin, A.V., Bignell, G.R., Bolli, N., Borg, A., Borresen-Dale, A.L*., et al.* (2013). Signatures of mutational processes in human cancer. Nature *500*, 415-421.
Alfei, F., Kanev, K., Hofmann, M., Wu, M., Ghoneim, H.E., Roelli, P., Utzschneider, D.T., von Hoesslin, M., Cullen, J.G., Fan, Y*., et al.* (2019). TOX reinforces the phenotype and longevity of exhausted T cells in chronic viral infection. Nature *571*, 265-269.
Alizadeh, D., Wong, R.A., Yang, X., Wang, D., Pecoraro, J.R., Kuo, C.F., Aguilar, B., Qi, Y., Ann, D.K., Starr, R*., et al.* (2019). IL15 Enhances CAR-T Cell Antitumor Activity by Reducing mTORC1 Activity and Preserving Their Stem Cell Memory Phenotype. Cancer Immunol Res *7*, 759-772.
Alshetaiwi, H., Pervolarakis, N., McIntyre, L.L., Ma, D., Nguyen, Q., Rath, J.A., Nee, K., Hernandez, G., Evans, K., Torosian, L*., et al.* (2020). Defining the emergence of myeloid-derived suppressor cells in breast cancer using single-cell transcriptomics. Sci Immunol *5*.
Anani, W., and Shurin, M.R. (2017). Targeting Myeloid-Derived Suppressor Cells in Cancer. Adv Exp Med Biol *1036*, 105-128.
Arasanz, H., Gato-Canas, M., Zuazo, M., Ibanez-Vea, M., Breckpot, K., Kochan, G., and Escors, D. (2017). PD1 signal transduction pathways in T cells. Oncotarget *8*, 51936-51945.
Asjo, B., Kiessling, R., Klein, G., and Povey, S. (1977). Genetic variation in antibody response and natural killer cell activity against a Moloney virus-induced lymphoma (YAC). Eur J Immunol *7*, 554-558.
Ayers, M., Lunceford, J., Nebozhyn, M., Murphy, E., Loboda, A., Kaufman, D.R., Albright, A., Cheng, J.D., Kang, S.P., Shankaran, V*., et al.* (2017). IFN-gamma-related mRNA profile predicts clinical response to PD-1 blockade. J Clin Invest *127*, 2930-2940.
Bach, E.A., Tanner, J.W., Marsters, S., Ashkenazi, A., Aguet, M., Shaw, A.S., and Schreiber, R.D. (1996). Ligand-induced assembly and activation of the gamma interferon receptor in intact cells. Mol Cell Biol *16*, 3214-3221.
Bach, J.F. (2018). The hygiene hypothesis in autoimmunity: the role of pathogens and commensals. Nat Rev Immunol *18*, 105-120.

Barber, D.L., Wherry, E.J., Masopust, D., Zhu, B., Allison, J.P., Sharpe, A.H., Freeman, G.J., and Ahmed, R. (2006). Restoring function in exhausted CD8+ T cells during chronic viral infection. Nature *439*, 682-687.
Barber, G.N. (2015). STING: infection, inflammation and cancer. Nat Rev Immunol *15*, 760-770.
Batlle, E., and Massague, J. (2019). Transforming Growth Factor-beta Signaling in Immunity and Cancer. Immunity *50*, 924-940.
Beatty, G.L., Chiorean, E.G., Fishman, M.P., Saboury, B., Teitelbaum, U.R., Sun, W., Huhn, R.D., Song, W., Li, D., Sharp, L.L*., et al.* (2011). CD40 agonists alter tumor stroma and show efficacy against pancreatic carcinoma in mice and humans. Science *331*, 1612-1616.
Bebelman, M.P., Smit, M.J., Pegtel, D.M., and Baglio, S.R. (2018). Biogenesis and function of extracellular vesicles in cancer. Pharmacol Ther *188*, 1-11.
Becker, A., Thakur, B.K., Weiss, J.M., Kim, H.S., Peinado, H., and Lyden, D. (2016). Extracellular Vesicles in Cancer: Cell-to-Cell Mediators of Metastasis. Cancer Cell *30*, 836-848.
Beltra, J.C., Manne, S., Abdel-Hakeem, M.S., Kurachi, M., Giles, J.R., Chen, Z., Casella, V., Ngiow, S.F., Khan, O., Huang, Y.J*., et al.* (2020). Developmental Relationships of Four Exhausted CD8(+) T Cell Subsets Reveals Underlying Transcriptional and Epigenetic Landscape Control Mechanisms. Immunity.
Benci, J.L., Johnson, L.R., Choa, R., Xu, Y., Qiu, J., Zhou, Z., Xu, B., Ye, D., Nathanson, K.L., June, C.H*., et al.* (2019). Opposing Functions of Interferon Coordinate Adaptive and Innate Immune Responses to Cancer Immune Checkpoint Blockade. Cell *178*, 933-948 e914.
Benci, J.L., Xu, B., Qiu, Y., Wu, T.J., Dada, H., Twyman-Saint Victor, C., Cucolo, L., Lee, D.S.M., Pauken, K.E., Huang, A.C*., et al.* (2016). Tumor Interferon Signaling Regulates a Multigenic Resistance Program to Immune Checkpoint Blockade. Cell *167*, 1540-1554 e1512.
Bengsch, B., Johnson, A.L., Kurachi, M., Odorizzi, P.M., Pauken, K.E., Attanasio, J., Stelekati, E., McLane, L.M., Paley, M.A., Delgoffe, G.M*., et al.* (2016). Bioenergetic Insufficiencies Due to Metabolic Alterations Regulated by the Inhibitory Receptor PD-1 Are an Early Driver of CD8(+) T Cell Exhaustion. Immunity *45*, 358-373.
Binnewies, M., Mujal, A.M., Pollack, J.L., Combes, A.J., Hardison, E.A., Barry, K.C., Tsui, J., Ruhland, M.K., Kersten, K., Abushawish, M.A*., et al.* (2019). Unleashing Type-2 Dendritic Cells to Drive Protective Antitumor CD4(+) T Cell Immunity. Cell *177*, 556-571 e516.
Binnewies, M., Roberts, E.W., Kersten, K., Chan, V., Fearon, D.F., Merad, M., Coussens, L.M., Gabrilovich, D.I., Ostrand-Rosenberg, S., Hedrick, C.C*., et al.* (2018). Understanding the tumor immune microenvironment (TIME) for effective therapy. Nat Med *24*, 541-550.
Bloom, M.B., Perry-Lalley, D., Robbins, P.F., Li, Y., el-Gamil, M., Rosenberg, S.A., and Yang, J.C. (1997). Identification of tyrosinase-related protein 2 as a tumor rejection antigen for the B16 melanoma. J Exp Med *185*, 453-459.
Boelens, M.C., Wu, T.J., Nabet, B.Y., Xu, B., Qiu, Y., Yoon, T., Azzam, D.J., Twyman-Saint Victor, C., Wiemann, B.Z., Ishwaran, H*., et al.* (2014). Exosome transfer from stromal to breast cancer cells regulates therapy resistance pathways. Cell *159*, 499-513.
Boise, L.H., Gonzalez-Garcia, M., Postema, C.E., Ding, L., Lindsten, T., Turka, L.A., Mao, X., Nunez, G., and Thompson, C.B. (1993). bcl-x, a bcl-2-related gene that functions as a dominant regulator of apoptotic cell death. Cell *74*, 597-608.
Borden, E.C. (2019). Interferons alpha and beta in cancer: therapeutic opportunities from new insights. Nat Rev Drug Discov *18*, 219-234.
Boudreau, J.E., Giglio, F., Gooley, T.A., Stevenson, P.A., Le Luduec, J.B., Shaffer, B.C., Rajalingam, R., Hou, L., Hurley, C.K., Noreen, H*., et al.* (2017). KIR3DL1/HLA-B Subtypes Govern Acute

Myelogenous Leukemia Relapse After Hematopoietic Cell Transplantation. J Clin Oncol *35*, 2268-2278.
Bridgeman, A., Maelfait, J., Davenne, T., Partridge, T., Peng, Y., Mayer, A., Dong, T., Kaever, V., Borrow, P., and Rehwinkel, J. (2015). Viruses transfer the antiviral second messenger cGAMP between cells. Science *349*, 1228-1232.
Brisse, M., and Ly, H. (2019). Comparative Structure and Function Analysis of the RIG-I-Like Receptors: RIG-I and MDA5. Front Immunol *10*, 1586.
Broz, M.L., Binnewies, M., Boldajipour, B., Nelson, A.E., Pollack, J.L., Erle, D.J., Barczak, A., Rosenblum, M.D., Daud, A., Barber, D.L.*, et al.* (2014). Dissecting the Tumor Myeloid Compartment Reveals Rare Activating Antigen-Presenting Cells Critical for T Cell Immunity. Cancer Cell *26*, 938.
Buck, M.D., O'Sullivan, D., Klein Geltink, R.I., Curtis, J.D., Chang, C.H., Sanin, D.E., Qiu, J., Kretz, O., Braas, D., van der Windt, G.J.*, et al.* (2016). Mitochondrial Dynamics Controls T Cell Fate through Metabolic Programming. Cell *166*, 63-76.
Busse, D., de la Rosa, M., Hobiger, K., Thurley, K., Flossdorf, M., Scheffold, A., and Hofer, T. (2010). Competing feedback loops shape IL-2 signaling between helper and regulatory T lymphocytes in cellular microenvironments. Proc Natl Acad Sci U S A *107*, 3058-3063.
Cabrita, R., Lauss, M., Sanna, A., Donia, M., Skaarup Larsen, M., Mitra, S., Johansson, I., Phung, B., Harbst, K., Vallon-Christersson, J.*, et al.* (2020). Tertiary lymphoid structures improve immunotherapy and survival in melanoma. Nature *577*, 561-565.
Campbell, K.J., and White, R.J. (2014). MYC regulation of cell growth through control of transcription by RNA polymerases I and III. Cold Spring Harb Perspect Med *4*.
Carpenito, C., Milone, M.C., Hassan, R., Simonet, J.C., Lakhal, M., Suhoski, M.M., Varela-Rohena, A., Haines, K.M., Heitjan, D.F., Albelda, S.M.*, et al.* (2009). Control of large, established tumor xenografts with genetically retargeted human T cells containing CD28 and CD137 domains. Proc Natl Acad Sci U S A *106*, 3360-3365.
Carreno, B.M., Becker-Hapak, M., Huang, A., Chan, M., Alyasiry, A., Lie, W.R., Aft, R.L., Cornelius, L.A., Trinkaus, K.M., and Linette, G.P. (2013). IL-12p70-producing patient DC vaccine elicits Tc1-polarized immunity. J Clin Invest *123*, 3383-3394.
Carreno, B.M., Magrini, V., Becker-Hapak, M., Kaabinejadian, S., Hundal, J., Petti, A.A., Ly, A., Lie, W.R., Hildebrand, W.H., Mardis, E.R.*, et al.* (2015). Cancer immunotherapy. A dendritic cell vaccine increases the breadth and diversity of melanoma neoantigen-specific T cells. Science *348*, 803-808.
Castro, F., Cardoso, A.P., Goncalves, R.M., Serre, K., and Oliveira, M.J. (2018). Interferon-Gamma at the Crossroads of Tumor Immune Surveillance or Evasion. Front Immunol *9*, 847.
Cerwenka, A., Baron, J.L., and Lanier, L.L. (2001). Ectopic expression of retinoic acid early inducible-1 gene (RAE-1) permits natural killer cell-mediated rejection of a MHC class I-bearing tumor in vivo. Proc Natl Acad Sci U S A *98*, 11521-11526.
Chen, G., Huang, A.C., Zhang, W., Zhang, G., Wu, M., Xu, W., Yu, Z., Yang, J., Wang, B., Sun, H.*, et al.* (2018). Exosomal PD-L1 contributes to immunosuppression and is associated with anti-PD-1 response. Nature *560*, 382-386.
Chen, J., Lopez-Moyado, I.F., Seo, H., Lio, C.J., Hempleman, L.J., Sekiya, T., Yoshimura, A., Scott-Browne, J.P., and Rao, A. (2019). NR4A transcription factors limit CAR T cell function in solid tumours. Nature *567*, 530-534.
Chen, L., and Flies, D.B. (2013). Molecular mechanisms of T cell co-stimulation and co-inhibition. Nat Rev Immunol *13*, 227-242.

Chen, Q., Sun, L., and Chen, Z.J. (2016). Regulation and function of the cGAS-STING pathway of cytosolic DNA sensing. Nat Immunol *17*, 1142-1149.
Chen, W., Jin, W., Hardegen, N., Lei, K.J., Li, L., Marinos, N., McGrady, G., and Wahl, S.M. (2003). Conversion of peripheral CD4+CD25- naive T cells to CD4+CD25+ regulatory T cells by TGF-beta induction of transcription factor Foxp3. J Exp Med *198*, 1875-1886.
Cheng, L., Ma, J., Li, J., Li, D., Li, G., Li, F., Zhang, Q., Yu, H., Yasui, F., Ye, C.*, et al.* (2017). Blocking type I interferon signaling enhances T cell recovery and reduces HIV-1 reservoirs. J Clin Invest *127*, 269-279.
Chiappinelli, K.B., Strissel, P.L., Desrichard, A., Li, H., Henke, C., Akman, B., Hein, A., Rote, N.S., Cope, L.M., Snyder, A.*, et al.* (2015). Inhibiting DNA Methylation Causes an Interferon Response in Cancer via dsRNA Including Endogenous Retroviruses. Cell *162*, 974-986.
Chiossone, L., Chaix, J., Fuseri, N., Roth, C., Vivier, E., and Walzer, T. (2009). Maturation of mouse NK cells is a 4-stage developmental program. Blood *113*, 5488-5496.
Chiossone, L., Dumas, P.Y., Vienne, M., and Vivier, E. (2018). Natural killer cells and other innate lymphoid cells in cancer. Nat Rev Immunol *18*, 671-688.
Cho, J.H., Collins, J.J., and Wong, W.W. (2018). Universal Chimeric Antigen Receptors for Multiplexed and Logical Control of T Cell Responses. Cell *173*, 1426-1438 e1411.
Coley, W.B. (1991). The treatment of malignant tumors by repeated inoculations of erysipelas. With a report of ten original cases. 1893. Clin Orthop Relat Res, 3-11.
Corrales, L., Glickman, L.H., McWhirter, S.M., Kanne, D.B., Sivick, K.E., Katibah, G.E., Woo, S.R., Lemmens, E., Banda, T., Leong, J.J.*, et al.* (2015). Direct Activation of STING in the Tumor Microenvironment Leads to Potent and Systemic Tumor Regression and Immunity. Cell Rep *11*, 1018-1030.
Cortez, V.S., Ulland, T.K., Cervantes-Barragan, L., Bando, J.K., Robinette, M.L., Wang, Q., White, A.J., Gilfillan, S., Cella, M., and Colonna, M. (2017). SMAD4 impedes the conversion of NK cells into ILC1-like cells by curtailing non-canonical TGF-beta signaling. Nat Immunol *18*, 995-1003.
Cristescu, R., Mogg, R., Ayers, M., Albright, A., Murphy, E., Yearley, J., Sher, X., Liu, X.Q., Lu, H., Nebozhyn, M.*, et al.* (2018). Pan-tumor genomic biomarkers for PD-1 checkpoint blockade-based immunotherapy. Science *362*.
Crouse, J., Kalinke, U., and Oxenius, A. (2015). Regulation of antiviral T cell responses by type I interferons. Nat Rev Immunol *15*, 231-242.
Cruz, F.M., Colbert, J.D., Merino, E., Kriegsman, B.A., and Rock, K.L. (2017). The Biology and Underlying Mechanisms of Cross-Presentation of Exogenous Antigens on MHC-I Molecules. Annu Rev Immunol *35*, 149-176.
Cui, G., Staron, M.M., Gray, S.M., Ho, P.C., Amezquita, R.A., Wu, J., and Kaech, S.M. (2015). IL-7-Induced Glycerol Transport and TAG Synthesis Promotes Memory CD8+ T Cell Longevity. Cell *161*, 750-761.
Curtale, G., Citarella, F., Carissimi, C., Goldoni, M., Carucci, N., Fulci, V., Franceschini, D., Meloni, F., Barnaba, V., and Macino, G. (2010). An emerging player in the adaptive immune response: microRNA-146a is a modulator of IL-2 expression and activation-induced cell death in T lymphocytes. Blood *115*, 265-273.
Curtsinger, J.M., and Mescher, M.F. (2010). Inflammatory cytokines as a third signal for T cell activation. Curr Opin Immunol *22*, 333-340.
D'Angelo, S.P., Melchiori, L., Merchant, M.S., Bernstein, D., Glod, J., Kaplan, R., Grupp, S., Tap, W.D., Chagin, K., Binder, G.K.*, et al.* (2018). Antitumor Activity Associated with Prolonged

Persistence of Adoptively Transferred NY-ESO-1 (c259)T Cells in Synovial Sarcoma. Cancer Discov *8*, 944-957.
Dadi, S., Chhangawala, S., Whitlock, B.M., Franklin, R.A., Luo, C.T., Oh, S.A., Toure, A., Pritykin, Y., Huse, M., Leslie, C.S.*, et al.* (2016). Cancer Immunosurveillance by Tissue-Resident Innate Lymphoid Cells and Innate-like T Cells. Cell *164*, 365-377.
Dai, S., Wei, D., Wu, Z., Zhou, X., Wei, X., Huang, H., and Li, G. (2008). Phase I clinical trial of autologous ascites-derived exosomes combined with GM-CSF for colorectal cancer. Mol Ther *16*, 782-790.
Dajon, M., Iribarren, K., and Cremer, I. (2017). Toll-like receptor stimulation in cancer: A pro- and anti-tumor double-edged sword. Immunobiology *222*, 89-100.
Dammeijer, F., Lievense, L.A., Kaijen-Lambers, M.E., van Nimwegen, M., Bezemer, K., Hegmans, J.P., van Hall, T., Hendriks, R.W., and Aerts, J.G. (2017). Depletion of Tumor-Associated Macrophages with a CSF-1R Kinase Inhibitor Enhances Antitumor Immunity and Survival Induced by DC Immunotherapy. Cancer Immunol Res *5*, 535-546.
Dangi, A., Zhang, L., Zhang, X., and Luo, X. (2018). Murine CMV induces type 1 IFN that impairs differentiation of MDSCs critical for transplantation tolerance. Blood Adv *2*, 669-680.
Davila, M.L., Riviere, I., Wang, X., Bartido, S., Park, J., Curran, K., Chung, S.S., Stefanski, J., Borquez-Ojeda, O., Olszewska, M.*, et al.* (2014). Efficacy and toxicity management of 19-28z CAR T cell therapy in B cell acute lymphoblastic leukemia. Sci Transl Med *6*, 224ra225.
De Palma, M., Biziato, D., and Petrova, T.V. (2017). Microenvironmental regulation of tumour angiogenesis. Nat Rev Cancer *17*, 457-474.
Deng, L., Liang, H., Xu, M., Yang, X., Burnette, B., Arina, A., Li, X.D., Mauceri, H., Beckett, M., Darga, T.*, et al.* (2014). STING-Dependent Cytosolic DNA Sensing Promotes Radiation-Induced Type I Interferon-Dependent Antitumor Immunity in Immunogenic Tumors. Immunity *41*, 843-852.
Deng, W., Gowen, B.G., Zhang, L., Wang, L., Lau, S., Iannello, A., Xu, J., Rovis, T.L., Xiong, N., and Raulet, D.H. (2015). Antitumor immunity. A shed NKG2D ligand that promotes natural killer cell activation and tumor rejection. Science *348*, 136-139.
Denks, K., Vogt, A., Sachelaru, I., Petriman, N.A., Kudva, R., and Koch, H.G. (2014). The Sec translocon mediated protein transport in prokaryotes and eukaryotes. Mol Membr Biol *31*, 58-84.
Deshpande, P.P., Biswas, S., and Torchilin, V.P. (2013). Current trends in the use of liposomes for tumor targeting. Nanomedicine (Lond) *8*, 1509-1528.
Diamond, M.S., Kinder, M., Matsushita, H., Mashayekhi, M., Dunn, G.P., Archambault, J.M., Lee, H., Arthur, C.D., White, J.M., Kalinke, U.*, et al.* (2011). Type I interferon is selectively required by dendritic cells for immune rejection of tumors. J Exp Med *208*, 1989-2003.
Dighe, A.S., Richards, E., Old, L.J., and Schreiber, R.D. (1994). Enhanced in vivo growth and resistance to rejection of tumor cells expressing dominant negative IFN gamma receptors. Immunity *1*, 447-456.
Dou, Z., Ghosh, K., Vizioli, M.G., Zhu, J., Sen, P., Wangensteen, K.J., Simithy, J., Lan, Y., Lin, Y., Zhou, Z.*, et al.* (2017). Cytoplasmic chromatin triggers inflammation in senescence and cancer. Nature *550*, 402-406.
Durgeau, A., Virk, Y., Corgnac, S., and Mami-Chouaib, F. (2018). Recent Advances in Targeting CD8+ T-Cell Immunity for More Effective Cancer Immunotherapy. Front Immunol *9*, 14.
Dyck, L., and Mills, K.H.G. (2017). Immune checkpoints and their inhibition in cancer and infectious diseases. Eur J Immunol *47*, 765-779.
Esensten, J.H., Helou, Y.A., Chopra, G., Weiss, A., and Bluestone, J.A. (2016). CD28 Costimulation: From Mechanism to Therapy. Immunity *44*, 973-988.

Frasca, L., Nasso, M., Spensieri, F., Fedele, G., Palazzo, R., Malavasi, F., and Ausiello, C.M. (2008). IFN-gamma arms human dendritic cells to perform multiple effector functions. J Immunol *180*, 1471-1481.
Fu, C., and Jiang, A. (2018). Dendritic Cells and CD8+ T Cell Immunity in Tumor Microenvironment. Front Immunol *9*, 3059.
Fuertes, M.B., Kacha, A.K., Kline, J., Woo, S.R., Kranz, D.M., Murphy, K.M., and Gajewski, T.F. (2011). Host type I IFN signals are required for antitumor CD8+ T cell responses through CD8{alpha}+ dendritic cells. J Exp Med *208*, 2005-2016.
Gabrilovich, D.I. (2017). Myeloid-Derived Suppressor Cells. Cancer Immunol Res *5*, 3-8.
Gandhi, L., Rodriguez-Abreu, D., Gadgeel, S., Esteban, E., Felip, E., De Angelis, F., Domine, M., Clingan, P., Hochmair, M.J., Powell, S.F.*, et al.* (2018). Pembrolizumab plus Chemotherapy in Metastatic Non-Small-Cell Lung Cancer. N Engl J Med *378*, 2078-2092.
Gao, J., Shi, L.Z., Zhao, H., Chen, J., Xiong, L., He, Q., Chen, T., Roszik, J., Bernatchez, C., Woodman, S.E.*, et al.* (2016). Loss of IFN-gamma Pathway Genes in Tumor Cells as a Mechanism of Resistance to Anti-CTLA-4 Therapy. Cell *167*, 397-404 e399.
Gao, Y., Souza-Fonseca-Guimaraes, F., Bald, T., Ng, S.S., Young, A., Ngiow, S.F., Rautela, J., Straube, J., Waddell, N., Blake, S.J.*, et al.* (2017). Tumor immunoevasion by the conversion of effector NK cells into type 1 innate lymphoid cells. Nat Immunol *18*, 1004-1015.
Gardner, A., and Ruffell, B. (2016). Dendritic Cells and Cancer Immunity. Trends Immunol *37*, 855-865.
Gardner, R., Wu, D., Cherian, S., Fang, M., Hanafi, L.A., Finney, O., Smithers, H., Jensen, M.C., Riddell, S.R., Maloney, D.G.*, et al.* (2016). Acquisition of a CD19-negative myeloid phenotype allows immune escape of MLL-rearranged B-ALL from CD19 CAR-T-cell therapy. Blood *127*, 2406-2410.
Gejman, R.S., Chang, A.Y., Jones, H.F., DiKun, K., Hakimi, A.A., Schietinger, A., and Scheinberg, D.A. (2018). Rejection of immunogenic tumor clones is limited by clonal fraction. Elife *7*.
Geller, L.T., Barzily-Rokni, M., Danino, T., Jonas, O.H., Shental, N., Nejman, D., Gavert, N., Zwang, Y., Cooper, Z.A., Shee, K.*, et al.* (2017). Potential role of intratumor bacteria in mediating tumor resistance to the chemotherapeutic drug gemcitabine. Science *357*, 1156-1160.
Gentili, M., Kowal, J., Tkach, M., Satoh, T., Lahaye, X., Conrad, C., Boyron, M., Lombard, B., Durand, S., Kroemer, G.*, et al.* (2015). Transmission of innate immune signaling by packaging of cGAMP in viral particles. Science *349*, 1232-1236.
Godfrey, D.I., Le Nours, J., Andrews, D.M., Uldrich, A.P., and Rossjohn, J. (2018). Unconventional T Cell Targets for Cancer Immunotherapy. Immunity *48*, 453-473.
Guedan, S., Posey, A.D., Jr., Shaw, C., Wing, A., Da, T., Patel, P.R., McGettigan, S.E., Casado-Medrano, V., Kawalekar, O.U., Uribe-Herranz, M.*, et al.* (2018). Enhancing CAR T cell persistence through ICOS and 4-1BB costimulation. JCI Insight *3*.
Haas, A.R., Tanyi, J.L., O'Hara, M.H., Gladney, W.L., Lacey, S.F., Torigian, D.A., Soulen, M.C., Tian, L., McGarvey, M., Nelson, A.M.*, et al.* (2019). Phase I Study of Lentiviral-Transduced Chimeric Antigen Receptor-Modified T Cells Recognizing Mesothelin in Advanced Solid Cancers. Mol Ther *27*, 1919-1929.
Halic, M., and Beckmann, R. (2005). The signal recognition particle and its interactions during protein targeting. Curr Opin Struct Biol *15*, 116-125.
Halle, S., Halle, O., and Forster, R. (2017). Mechanisms and Dynamics of T Cell-Mediated Cytotoxicity In Vivo. Trends Immunol *38*, 432-443.

Hammerich, L., Marron, T.U., Upadhyay, R., Svensson-Arvelund, J., Dhainaut, M., Hussein, S., Zhan, Y., Ostrowski, D., Yellin, M., Marsh, H.*, et al.* (2019). Systemic clinical tumor regressions and potentiation of PD1 blockade with in situ vaccination. Nat Med *25*, 814-824.
Harding, S.M., Benci, J.L., Irianto, J., Discher, D.E., Minn, A.J., and Greenberg, R.A. (2017). Mitotic progression following DNA damage enables pattern recognition within micronuclei. Nature *548*, 466-470.
Harlin, H., Meng, Y., Peterson, A.C., Zha, Y., Tretiakova, M., Slingluff, C., McKee, M., and Gajewski, T.F. (2009). Chemokine expression in melanoma metastases associated with CD8+ T-cell recruitment. Cancer Res *69*, 3077-3085.
Havenar-Daughton, C., Kolumam, G.A., and Murali-Krishna, K. (2006). Cutting Edge: The direct action of type I IFN on CD4 T cells is critical for sustaining clonal expansion in response to a viral but not a bacterial infection. J Immunol *176*, 3315-3319.
He, X., Feng, Z., Ma, J., Ling, S., Cao, Y., Gurung, B., Wu, Y., Katona, B.W., O'Dwyer, K.P., Siegel, D.L.*, et al.* (2020). Bispecific and split CAR T cells targeting CD13 and TIM3 eradicate acute myeloid leukemia. Blood *135*, 713-723.
Heath, W.R., Hurd, M.E., Carbone, F.R., and Sherman, L.A. (1989). Peptide-dependent recognition of H-2Kb by alloreactive cytotoxic T lymphocytes. Nature *341*, 749-752.
Hellmann, M.D., Nathanson, T., Rizvi, H., Creelan, B.C., Sanchez-Vega, F., Ahuja, A., Ni, A., Novik, J.B., Mangarin, L.M.B., Abu-Akeel, M.*, et al.* (2018). Genomic Features of Response to Combination Immunotherapy in Patients with Advanced Non-Small-Cell Lung Cancer. Cancer Cell *33*, 843-852 e844.
Helmink, B.A., Reddy, S.M., Gao, J., Zhang, S., Basar, R., Thakur, R., Yizhak, K., Sade-Feldman, M., Blando, J., Han, G.*, et al.* (2020). B cells and tertiary lymphoid structures promote immunotherapy response. Nature *577*, 549-555.
Henriksson, J., Chen, X., Gomes, T., Ullah, U., Meyer, K.B., Miragaia, R., Duddy, G., Pramanik, J., Yusa, K., Lahesmaa, R.*, et al.* (2019). Genome-wide CRISPR Screens in T Helper Cells Reveal Pervasive Crosstalk between Activation and Differentiation. Cell *176*, 882-896 e818.
Hoshino, A., Costa-Silva, B., Shen, T.L., Rodrigues, G., Hashimoto, A., Tesic Mark, M., Molina, H., Kohsaka, S., Di Giannatale, A., Ceder, S.*, et al.* (2015). Tumour exosome integrins determine organotropic metastasis. Nature *527*, 329-335.
Hosseinzadeh, P., Bhardwaj, G., Mulligan, V.K., Shortridge, M.D., Craven, T.W., Pardo-Avila, F., Rettie, S.A., Kim, D.E., Silva, D.A., Ibrahim, Y.M.*, et al.* (2017). Comprehensive computational design of ordered peptide macrocycles. Science *358*, 1461-1466.
Hoves, S., Ooi, C.H., Wolter, C., Sade, H., Bissinger, S., Schmittnaegel, M., Ast, O., Giusti, A.M., Wartha, K., Runza, V.*, et al.* (2018). Rapid activation of tumor-associated macrophages boosts preexisting tumor immunity. J Exp Med *215*, 859-876.
Hu, Q., Ren, H., Li, G., Wang, D., Zhou, Q., Wu, J., Zheng, J., Huang, J., Slade, D.A., Wu, X.*, et al.* (2019). STING-mediated intestinal barrier dysfunction contributes to lethal sepsis. EBioMedicine *41*, 497-508.
Huang, A.C., Postow, M.A., Orlowski, R.J., Mick, R., Bengsch, B., Manne, S., Xu, W., Harmon, S., Giles, J.R., Wenz, B.*, et al.* (2017). T-cell invigoration to tumour burden ratio associated with anti-PD-1 response. Nature *545*, 60-65.
Huang, M., Wang, J., Torre, E., Dueck, H., Shaffer, S., Bonasio, R., Murray, J.I., Raj, A., Li, M., and Zhang, N.R. (2018). SAVER: gene expression recovery for single-cell RNA sequencing. Nat Methods *15*, 539-542.

Hugo, W., Zaretsky, J.M., Sun, L., Song, C., Moreno, B.H., Hu-Lieskovan, S., Berent-Maoz, B., Pang, J., Chmielowski, B., Cherry, G.*, et al.* (2017). Genomic and Transcriptomic Features of Response to Anti-PD-1 Therapy in Metastatic Melanoma. Cell *168*, 542.
Ishizuka, J.J., Manguso, R.T., Cheruiyot, C.K., Bi, K., Panda, A., Iracheta-Vellve, A., Miller, B.C., Du, P.P., Yates, K.B., Dubrot, J.*, et al.* (2019). Loss of ADAR1 in tumours overcomes resistance to immune checkpoint blockade. Nature *565*, 43-48.
Ishwaran, H. (2015). The Effect of Splitting on Random Forests. Mach Learn *99*, 75-118.
Ishwaran, H., and Kogalur, U.B. (2010). Consistency of Random Survival Forests. Stat Probab Lett *80*, 1056-1064.
Ivashkiv, L.B. (2018). IFNgamma: signalling, epigenetics and roles in immunity, metabolism, disease and cancer immunotherapy. Nat Rev Immunol *18*, 545-558.
Jackson, H.J., Rafiq, S., and Brentjens, R.J. (2016). Driving CAR T-cells forward. Nat Rev Clin Oncol *13*, 370-383.
Jensen, S., Seidelin, J.B., LaCasse, E.C., and Nielsen, O.H. (2020). SMAC mimetics and RIPK inhibitors as therapeutics for chronic inflammatory diseases. Sci Signal *13*.
Jiang, P., Gu, S., Pan, D., Fu, J., Sahu, A., Hu, X., Li, Z., Traugh, N., Bu, X., Li, B.*, et al.* (2018). Signatures of T cell dysfunction and exclusion predict cancer immunotherapy response. Nat Med *24*, 1550-1558.
Jin, J., Fu, B., Mei, X., Yue, T., Sun, R., Tian, Z., and Wei, H. (2013). CD11b(-)CD27(-) NK cells are associated with the progression of lung carcinoma. PLoS One *8*, e61024.
Joffre, O., Nolte, M.A., Sporri, R., and Reis e Sousa, C. (2009). Inflammatory signals in dendritic cell activation and the induction of adaptive immunity. Immunol Rev *227*, 234-247.
Jordan, M.S., and Koretzky, G.A. (2010). Coordination of receptor signaling in multiple hematopoietic cell lineages by the adaptor protein SLP-76. Cold Spring Harb Perspect Biol *2*, a002501.
Josefowicz, S.Z., Lu, L.F., and Rudensky, A.Y. (2012). Regulatory T cells: mechanisms of differentiation and function. Annu Rev Immunol *30*, 531-564.
Joshi, N.S., Akama-Garren, E.H., Lu, Y., Lee, D.Y., Chang, G.P., Li, A., DuPage, M., Tammela, T., Kerper, N.R., Farago, A.F.*, et al.* (2015). Regulatory T Cells in Tumor-Associated Tertiary Lymphoid Structures Suppress Anti-tumor T Cell Responses. Immunity *43*, 579-590.
June, C.H., O'Connor, R.S., Kawalekar, O.U., Ghassemi, S., and Milone, M.C. (2018). CAR T cell immunotherapy for human cancer. Science *359*, 1361-1365.
Kaech, S.M., and Cui, W. (2012). Transcriptional control of effector and memory CD8+ T cell differentiation. Nat Rev Immunol *12*, 749-761.
Kaech, S.M., Wherry, E.J., and Ahmed, R. (2002). Effector and memory T-cell differentiation: implications for vaccine development. Nat Rev Immunol *2*, 251-262.
Kandasamy, M., Suryawanshi, A., Tundup, S., Perez, J.T., Schmolke, M., Manicassamy, S., and Manicassamy, B. (2016). RIG-I Signaling Is Critical for Efficient Polyfunctional T Cell Responses during Influenza Virus Infection. PLoS Pathog *12*, e1005754.
Kaneda, M.M., Messer, K.S., Ralainirina, N., Li, H., Leem, C.J., Gorjestani, S., Woo, G., Nguyen, A.V., Figueiredo, C.C., Foubert, P.*, et al.* (2016). PI3Kgamma is a molecular switch that controls immune suppression. Nature *539*, 437-442.
Karin, N., and Wildbaum, G. (2015). The Role of Chemokines in Shaping the Balance Between CD4(+) T Cell Subsets and Its Therapeutic Implications in Autoimmune and Cancer Diseases. Front Immunol *6*, 609.

Karre, K., Ljunggren, H.G., Piontek, G., and Kiessling, R. (1986). Selective rejection of H-2-deficient lymphoma variants suggests alternative immune defence strategy. Nature *319*, 675-678.
Kawalekar, O.U., O'Connor, R.S., Fraietta, J.A., Guo, L., McGettigan, S.E., Posey, A.D., Jr., Patel, P.R., Guedan, S., Scholler, J., Keith, B.*, et al.* (2016). Distinct Signaling of Coreceptors Regulates Specific Metabolism Pathways and Impacts Memory Development in CAR T Cells. Immunity *44*, 380-390.
Kawasaki, T., and Kawai, T. (2014). Toll-like receptor signaling pathways. Front Immunol *5*, 461.
Keskin, D.B., Anandappa, A.J., Sun, J., Tirosh, I., Mathewson, N.D., Li, S., Oliveira, G., Giobbie-Hurder, A., Felt, K., Gjini, E.*, et al.* (2019). Neoantigen vaccine generates intratumoral T cell responses in phase Ib glioblastoma trial. Nature *565*, 234-239.
Khan, O., Giles, J.R., McDonald, S., Manne, S., Ngiow, S.F., Patel, K.P., Werner, M.T., Huang, A.C., Alexander, K.A., Wu, J.E.*, et al.* (2019). TOX transcriptionally and epigenetically programs CD8(+) T cell exhaustion. Nature *571*, 211-218.
Kloss, C.C., Lee, J., Zhang, A., Chen, F., Melenhorst, J.J., Lacey, S.F., Maus, M.V., Fraietta, J.A., Zhao, Y., and June, C.H. (2018). Dominant-Negative TGF-beta Receptor Enhances PSMA-Targeted Human CAR T Cell Proliferation And Augments Prostate Cancer Eradication. Mol Ther *26*, 1855-1866.
Kolumam, G.A., Thomas, S., Thompson, L.J., Sprent, J., and Murali-Krishna, K. (2005). Type I interferons act directly on CD8+ T cells to allow clonal expansion and memory formation in response to viral infection. J Exp Med *202*, 637-650.
Kumar, R., Mandal, M., Lipton, A., Harvey, H., and Thompson, C.B. (1996). Overexpression of HER2 modulates bcl-2, bcl-XL, and tamoxifen-induced apoptosis in human MCF-7 breast cancer cells. Clin Cancer Res *2*, 1215-1219.
Lanier, L.L. (2005). NK cell recognition. Annu Rev Immunol *23*, 225-274.
Laviron, M., and Boissonnas, A. (2019). Ontogeny of Tumor-Associated Macrophages. Front Immunol *10*, 1799.
Laydon, D.J., Bangham, C.R., and Asquith, B. (2015). Estimating T-cell repertoire diversity: limitations of classical estimators and a new approach. Philos Trans R Soc Lond B Biol Sci *370*.
Leach, D.R., Krummel, M.F., and Allison, J.P. (1996). Enhancement of antitumor immunity by CTLA-4 blockade. Science *271*, 1734-1736.
Lee, A.J., and Ashkar, A.A. (2018). The Dual Nature of Type I and Type II Interferons. Front Immunol *9*, 2061.
Lee, A.K., Pan, D., Bao, X., Hu, M., Li, F., and Li, C.Y. (2020). Endogenous Retrovirus Activation as a Key Mechanism of Anti-Tumor Immune Response in Radiotherapy. Radiat Res *193*, 305-317.
Levine, J.H., Simonds, E.F., Bendall, S.C., Davis, K.L., Amir el, A.D., Tadmor, M.D., Litvin, O., Fienberg, H.G., Jager, A., Zunder, E.R.*, et al.* (2015). Data-Driven Phenotypic Dissection of AML Reveals Progenitor-like Cells that Correlate with Prognosis. Cell *162*, 184-197.
Li, L., and Sherry, B. (2010). IFN-alpha expression and antiviral effects are subtype and cell type specific in the cardiac response to viral infection. Virology *396*, 59-68.
Li, T., and Chen, Z.J. (2018). The cGAS-cGAMP-STING pathway connects DNA damage to inflammation, senescence, and cancer. J Exp Med *215*, 1287-1299.
Lim, W.A., and June, C.H. (2017). The Principles of Engineering Immune Cells to Treat Cancer. Cell *168*, 724-740.
Liu, X., Ranganathan, R., Jiang, S., Fang, C., Sun, J., Kim, S., Newick, K., Lo, A., June, C.H., Zhao, Y.*, et al.* (2016a). A Chimeric Switch-Receptor Targeting PD1 Augments the Efficacy of Second-Generation CAR T Cells in Advanced Solid Tumors. Cancer Res *76*, 1578-1590.

Liu, Y., Gu, Y., Han, Y., Zhang, Q., Jiang, Z., Zhang, X., Huang, B., Xu, X., Zheng, J., and Cao, X. (2016b). Tumor Exosomal RNAs Promote Lung Pre-metastatic Niche Formation by Activating Alveolar Epithelial TLR3 to Recruit Neutrophils. Cancer Cell *30*, 243-256.
Lohmueller, J.J., Ham, J.D., Kvorjak, M., and Finn, O.J. (2017). mSA2 affinity-enhanced biotin-binding CAR T cells for universal tumor targeting. Oncoimmunology *7*, e1368604.
Long, A.H., Haso, W.M., Shern, J.F., Wanhainen, K.M., Murgai, M., Ingaramo, M., Smith, J.P., Walker, A.J., Kohler, M.E., Venkateshwara, V.R.*, et al.* (2015). 4-1BB costimulation ameliorates T cell exhaustion induced by tonic signaling of chimeric antigen receptors. Nat Med *21*, 581-590.
Longhi, M.P., Trumpfheller, C., Idoyaga, J., Caskey, M., Matos, I., Kluger, C., Salazar, A.M., Colonna, M., and Steinman, R.M. (2009). Dendritic cells require a systemic type I interferon response to mature and induce CD4+ Th1 immunity with poly IC as adjuvant. J Exp Med *206*, 1589-1602.
Lynn, R.C., Weber, E.W., Sotillo, E., Gennert, D., Xu, P., Good, Z., Anbunathan, H., Lattin, J., Jones, R., Tieu, V.*, et al.* (2019). c-Jun overexpression in CAR T cells induces exhaustion resistance. Nature *576*, 293-300.
Ma, L., Dichwalkar, T., Chang, J.Y.H., Cossette, B., Garafola, D., Zhang, A.Q., Fichter, M., Wang, C., Liang, S., Silva, M.*, et al.* (2019). Enhanced CAR-T cell activity against solid tumors by vaccine boosting through the chimeric receptor. Science *365*, 162-168.
MacKay, M., Afshinnekoo, E., Rub, J., Hassan, C., Khunte, M., Baskaran, N., Owens, B., Liu, L., Roboz, G.J., Guzman, M.L.*, et al.* (2020). The therapeutic landscape for cells engineered with chimeric antigen receptors. Nat Biotechnol *38*, 233-244.
Mahoney, K.M., Rennert, P.D., and Freeman, G.J. (2015). Combination cancer immunotherapy and new immunomodulatory targets. Nat Rev Drug Discov *14*, 561-584.
Manguso, R.T., Pope, H.W., Zimmer, M.D., Brown, F.D., Yates, K.B., Miller, B.C., Collins, N.B., Bi, K., LaFleur, M.W., Juneja, V.R.*, et al.* (2017). In vivo CRISPR screening identifies Ptpn2 as a cancer immunotherapy target. Nature *547*, 413-418.
Mariathasan, S., Turley, S.J., Nickles, D., Castiglioni, A., Yuen, K., Wang, Y., Kadel, E.E., III, Koeppen, H., Astarita, J.L., Cubas, R.*, et al.* (2018). TGFbeta attenuates tumour response to PD-L1 blockade by contributing to exclusion of T cells. Nature *554*, 544-548.
Marrack, P., Kappler, J., and Mitchell, T. (1999). Type I interferons keep activated T cells alive. J Exp Med *189*, 521-530.
Martinez, M., and Moon, E.K. (2019). CAR T Cells for Solid Tumors: New Strategies for Finding, Infiltrating, and Surviving in the Tumor Microenvironment. Front Immunol *10*, 128.
Mata, M., Gerken, C., Nguyen, P., Krenciute, G., Spencer, D.M., and Gottschalk, S. (2017). Inducible Activation of MyD88 and CD40 in CAR T Cells Results in Controllable and Potent Antitumor Activity in Preclinical Solid Tumor Models. Cancer Discov *7*, 1306-1319.
Matsuo, M., Nagata, Y., Sato, E., Atanackovic, D., Valmori, D., Chen, Y.T., Ritter, G., Mellman, I., Old, L.J., and Gnjatic, S. (2004). IFN-gamma enables cross-presentation of exogenous protein antigen in human Langerhans cells by potentiating maturation. Proc Natl Acad Sci U S A *101*, 14467-14472.
Maude, S.L., Laetsch, T.W., Buechner, J., Rives, S., Boyer, M., Bittencourt, H., Bader, P., Verneris, M.R., Stefanski, H.E., Myers, G.D.*, et al.* (2018). Tisagenlecleucel in Children and Young Adults with B-Cell Lymphoblastic Leukemia. N Engl J Med *378*, 439-448.
Mavers, M., and Bertaina, A. (2018). High-Risk Leukemia: Past, Present, and Future Role of NK Cells. J Immunol Res *2018*, 1586905.

McGranahan, N., Furness, A.J., Rosenthal, R., Ramskov, S., Lyngaa, R., Saini, S.K., Jamal-Hanjani, M., Wilson, G.A., Birkbak, N.J., Hiley, C.T.*, et al.* (2016). Clonal neoantigens elicit T cell immunoreactivity and sensitivity to immune checkpoint blockade. Science *351*, 1463-1469.
Mendoza, J.L., Escalante, N.K., Jude, K.M., Sotolongo Bellon, J., Su, L., Horton, T.M., Tsutsumi, N., Berardinelli, S.J., Haltiwanger, R.S., Piehler, J.*, et al.* (2019). Structure of the IFNgamma receptor complex guides design of biased agonists. Nature *567*, 56-60.
Mezzadra, R., Sun, C., Jae, L.T., Gomez-Eerland, R., de Vries, E., Wu, W., Logtenberg, M.E.W., Slagter, M., Rozeman, E.A., Hofland, I.*, et al.* (2017). Identification of CMTM6 and CMTM4 as PD-L1 protein regulators. Nature *549*, 106-110.
Miller, B.C., Sen, D.R., Al Abosy, R., Bi, K., Virkud, Y.V., LaFleur, M.W., Yates, K.B., Lako, A., Felt, K., Naik, G.S.*, et al.* (2019). Subsets of exhausted CD8(+) T cells differentially mediate tumor control and respond to checkpoint blockade. Nat Immunol *20*, 326-336.
Morgan, R.A., Johnson, L.A., Davis, J.L., Zheng, Z., Woolard, K.D., Reap, E.A., Feldman, S.A., Chinnasamy, N., Kuan, C.T., Song, H.*, et al.* (2012). Recognition of glioma stem cells by genetically modified T cells targeting EGFRvIII and development of adoptive cell therapy for glioma. Hum Gene Ther *23*, 1043-1053.
Morgan, R.A., Yang, J.C., Kitano, M., Dudley, M.E., Laurencot, C.M., and Rosenberg, S.A. (2010). Case report of a serious adverse event following the administration of T cells transduced with a chimeric antigen receptor recognizing ERBB2. Mol Ther *18*, 843-851.
Muliaditan, T., Caron, J., Okesola, M., Opzoomer, J.W., Kosti, P., Georgouli, M., Gordon, P., Lall, S., Kuzeva, D.M., Pedro, L.*, et al.* (2018). Macrophages are exploited from an innate wound healing response to facilitate cancer metastasis. Nat Commun *9*, 2951.
Murphy, K.M. (2013). Transcriptional control of dendritic cell development. Adv Immunol *120*, 239-267.
Musumeci, A., Lutz, K., Winheim, E., and Krug, A.B. (2019). What Makes a pDC: Recent Advances in Understanding Plasmacytoid DC Development and Heterogeneity. Front Immunol *10*, 1222.
Nabet, B.Y., Qiu, Y., Shabason, J.E., Wu, T.J., Yoon, T., Kim, B.C., Benci, J.L., DeMichele, A.M., Tchou, J., Marcotrigiano, J.*, et al.* (2017). Exosome RNA Unshielding Couples Stromal Activation to Pattern Recognition Receptor Signaling in Cancer. Cell *170*, 352-366 e313.
Nagasawa, M., Germar, K., Blom, B., and Spits, H. (2017). Human CD5(+) Innate Lymphoid Cells Are Functionally Immature and Their Development from CD34(+) Progenitor Cells Is Regulated by Id2. Front Immunol *8*, 1047.
Newman, A.M., Liu, C.L., Green, M.R., Gentles, A.J., Feng, W., Xu, Y., Hoang, C.D., Diehn, M., and Alizadeh, A.A. (2015). Robust enumeration of cell subsets from tissue expression profiles. Nat Methods *12*, 453-457.
Okada, N. (1991). SINEs. Curr Opin Genet Dev *1*, 498-504.
Oyler-Yaniv, A., Oyler-Yaniv, J., Whitlock, B.M., Liu, Z., Germain, R.N., Huse, M., Altan-Bonnet, G., and Krichevsky, O. (2017). A Tunable Diffusion-Consumption Mechanism of Cytokine Propagation Enables Plasticity in Cell-to-Cell Communication in the Immune System. Immunity *46*, 609-620.
Paczulla, A.M., Rothfelder, K., Raffel, S., Konantz, M., Steinbacher, J., Wang, H., Tandler, C., Mbarga, M., Schaefer, T., Falcone, M.*, et al.* (2019). Absence of NKG2D ligands defines leukaemia stem cells and mediates their immune evasion. Nature *572*, 254-259.
Pai, C.S., Huang, J.T., Lu, X., Simons, D.M., Park, C., Chang, A., Tamaki, W., Liu, E., Roybal, K.T., Seagal, J.*, et al.* (2019). Clonal Deletion of Tumor-Specific T Cells by Interferon-gamma Confers Therapeutic Resistance to Combination Immune Checkpoint Blockade. Immunity *50*, 477-492 e478.

Pak-Wittel, M.A., Yang, L., Sojka, D.K., Rivenbark, J.G., and Yokoyama, W.M. (2013). Interferon-gamma mediates chemokine-dependent recruitment of natural killer cells during viral infection. Proc Natl Acad Sci U S A *110*, E50-59.
Paley, M.A., Kroy, D.C., Odorizzi, P.M., Johnnidis, J.B., Dolfi, D.V., Barnett, B.E., Bikoff, E.K., Robertson, E.J., Lauer, G.M., Reiner, S.L*., et al.* (2012). Progenitor and terminal subsets of CD8+ T cells cooperate to contain chronic viral infection. Science *338*, 1220-1225.
Park, S.H., Kang, K., Giannopoulou, E., Qiao, Y., Kang, K., Kim, G., Park-Min, K.H., and Ivashkiv, L.B. (2017). Type I interferons and the cytokine TNF cooperatively reprogram the macrophage epigenome to promote inflammatory activation. Nat Immunol *18*, 1104-1116.
Patel, S.A., and Minn, A.J. (2018). Combination Cancer Therapy with Immune Checkpoint Blockade: Mechanisms and Strategies. Immunity *48*, 417-433.
Patel, S.J., Sanjana, N.E., Kishton, R.J., Eidizadeh, A., Vodnala, S.K., Cam, M., Gartner, J.J., Jia, L., Steinberg, S.M., Yamamoto, T.N*., et al.* (2017). Identification of essential genes for cancer immunotherapy. Nature *548*, 537-542.
Pauken, K.E., Sammons, M.A., Odorizzi, P.M., Manne, S., Godec, J., Khan, O., Drake, A.M., Chen, Z., Sen, D.R., Kurachi, M*., et al.* (2016). Epigenetic stability of exhausted T cells limits durability of reinvigoration by PD-1 blockade. Science *354*, 1160-1165.
Pearce, E.L., Walsh, M.C., Cejas, P.J., Harms, G.M., Shen, H., Wang, L.S., Jones, R.G., and Choi, Y. (2009). Enhancing CD8+ T-cell memory by modulating fatty acid metabolism. Nature *460*, 103-107.
Pesce, S., Greppi, M., Grossi, F., Del Zotto, G., Moretta, L., Sivori, S., Genova, C., and Marcenaro, E. (2019). PD/1-PD-Ls Checkpoint: Insight on the Potential Role of NK Cells. Front Immunol *10*, 1242.
Petitprez, F., de Reynies, A., Keung, E.Z., Chen, T.W., Sun, C.M., Calderaro, J., Jeng, Y.M., Hsiao, L.P., Lacroix, L., Bougouin, A*., et al.* (2020). B cells are associated with survival and immunotherapy response in sarcoma. Nature *577*, 556-560.
Phatnani, H.P., and Greenleaf, A.L. (2006). Phosphorylation and functions of the RNA polymerase II CTD. Genes Dev *20*, 2922-2936.
Posey, A.D., Jr., Schwab, R.D., Boesteanu, A.C., Steentoft, C., Mandel, U., Engels, B., Stone, J.D., Madsen, T.D., Schreiber, K., Haines, K.M*., et al.* (2016). Engineered CAR T Cells Targeting the Cancer-Associated Tn-Glycoform of the Membrane Mucin MUC1 Control Adenocarcinoma. Immunity *44*, 1444-1454.
Pucci, F., Garris, C., Lai, C.P., Newton, A., Pfirschke, C., Engblom, C., Alvarez, D., Sprachman, M., Evavold, C., Magnuson, A*., et al.* (2016). SCS macrophages suppress melanoma by restricting tumor-derived vesicle-B cell interactions. Science *352*, 242-246.
Pule, M.A., Savoldo, B., Myers, G.D., Rossig, C., Russell, H.V., Dotti, G., Huls, M.H., Liu, E., Gee, A.P., Mei, Z*., et al.* (2008). Virus-specific T cells engineered to coexpress tumor-specific receptors: persistence and antitumor activity in individuals with neuroblastoma. Nat Med *14*, 1264-1270.
Pyonteck, S.M., Akkari, L., Schuhmacher, A.J., Bowman, R.L., Sevenich, L., Quail, D.F., Olson, O.C., Quick, M.L., Huse, J.T., Teijeiro, V*., et al.* (2013). CSF-1R inhibition alters macrophage polarization and blocks glioma progression. Nat Med *19*, 1264-1272.
Quail, D.F., and Joyce, J.A. (2013). Microenvironmental regulation of tumor progression and metastasis. Nat Med *19*, 1423-1437.
Ramakrishna, S., Highfill, S.L., Walsh, Z., Nguyen, S.M., Lei, H., Shern, J.F., Qin, H., Kraft, I.L., Stetler-Stevenson, M., Yuan, C.M*., et al.* (2019). Modulation of Target Antigen Density Improves CAR T-cell Functionality and Persistence. Clin Cancer Res *25*, 5329-5341.

Ramanjulu, J.M., Pesiridis, G.S., Yang, J., Concha, N., Singhaus, R., Zhang, S.Y., Tran, J.L., Moore, P., Lehmann, S., Eberl, H.C.*, et al.* (2018). Design of amidobenzimidazole STING receptor agonists with systemic activity. Nature *564*, 439-443.
Raposo, G., and Stoorvogel, W. (2013). Extracellular vesicles: exosomes, microvesicles, and friends. J Cell Biol *200*, 373-383.
Reck, M., Rodriguez-Abreu, D., Robinson, A.G., Hui, R., Csoszi, T., Fulop, A., Gottfried, M., Peled, N., Tafreshi, A., Cuffe, S.*, et al.* (2016). Pembrolizumab versus Chemotherapy for PD-L1-Positive Non-Small-Cell Lung Cancer. N Engl J Med *375*, 1823-1833.
Reikine, S., Nguyen, J.B., and Modis, Y. (2014). Pattern Recognition and Signaling Mechanisms of RIG-I and MDA5. Front Immunol *5*, 342.
Riaz, N., Havel, J.J., Makarov, V., Desrichard, A., Urba, W.J., Sims, J.S., Hodi, F.S., Martin-Algarra, S., Mandal, R., Sharfman, W.H.*, et al.* (2017). Tumor and Microenvironment Evolution during Immunotherapy with Nivolumab. Cell *171*, 934-949 e916.
Ribas, A., and Wolchok, J.D. (2018). Cancer immunotherapy using checkpoint blockade. Science *359*, 1350-1355.
Richman, L.P., Vonderheide, R.H., and Rech, A.J. (2019). Neoantigen Dissimilarity to the Self-Proteome Predicts Immunogenicity and Response to Immune Checkpoint Blockade. Cell Syst *9*, 375-382 e374.
Richman, S.A., Nunez-Cruz, S., Moghimi, B., Li, L.Z., Gershenson, Z.T., Mourelatos, Z., Barrett, D.M., Grupp, S.A., and Milone, M.C. (2018). High-Affinity GD2-Specific CAR T Cells Induce Fatal Encephalitis in a Preclinical Neuroblastoma Model. Cancer Immunol Res *6*, 36-46.
Riley, R.S., June, C.H., Langer, R., and Mitchell, M.J. (2019). Delivery technologies for cancer immunotherapy. Nat Rev Drug Discov *18*, 175-196.
Rizvi, H., Sanchez-Vega, F., La, K., Chatila, W., Jonsson, P., Halpenny, D., Plodkowski, A., Long, N., Sauter, J.L., Rekhtman, N.*, et al.* (2018). Molecular Determinants of Response to Anti-Programmed Cell Death (PD)-1 and Anti-Programmed Death-Ligand 1 (PD-L1) Blockade in Patients With Non-Small-Cell Lung Cancer Profiled With Targeted Next-Generation Sequencing. J Clin Oncol *36*, 633-641.
Rizvi, N.A., Hellmann, M.D., Snyder, A., Kvistborg, P., Makarov, V., Havel, J.J., Lee, W., Yuan, J., Wong, P., Ho, T.S.*, et al.* (2015). Cancer immunology. Mutational landscape determines sensitivity to PD-1 blockade in non-small cell lung cancer. Science *348*, 124-128.
Roberts, E.W., Broz, M.L., Binnewies, M., Headley, M.B., Nelson, A.E., Wolf, D.M., Kaisho, T., Bogunovic, D., Bhardwaj, N., and Krummel, M.F. (2016). Critical Role for CD103(+)/CD141(+) Dendritic Cells Bearing CCR7 for Tumor Antigen Trafficking and Priming of T Cell Immunity in Melanoma. Cancer Cell *30*, 324-336.
Rodgers, D.T., Mazagova, M., Hampton, E.N., Cao, Y., Ramadoss, N.S., Hardy, I.R., Schulman, A., Du, J., Wang, F., Singer, O.*, et al.* (2016). Switch-mediated activation and retargeting of CAR-T cells for B-cell malignancies. Proc Natl Acad Sci U S A *113*, E459-468.
Rodig, S.J., Gusenleitner, D., Jackson, D.G., Gjini, E., Giobbie-Hurder, A., Jin, C., Chang, H., Lovitch, S.B., Horak, C., Weber, J.S.*, et al.* (2018). MHC proteins confer differential sensitivity to CTLA-4 and PD-1 blockade in untreated metastatic melanoma. Sci Transl Med *10*.
Rooney, M.S., Shukla, S.A., Wu, C.J., Getz, G., and Hacohen, N. (2015). Molecular and genetic properties of tumors associated with local immune cytolytic activity. Cell *160*, 48-61.
Rosato, P.C., Wijeyesinghe, S., Stolley, J.M., Nelson, C.E., Davis, R.L., Manlove, L.S., Pennell, C.A., Blazar, B.R., Chen, C.C., Geller, M.A.*, et al.* (2019). Virus-specific memory T cells populate tumors and can be repurposed for tumor immunotherapy. Nat Commun *10*, 567.

Roth, T.L., Li, P.J., Blaeschke, F., Nies, J.F., Apathy, R., Mowery, C., Yu, R., Nguyen, M.L.T., Lee, Y., Truong, A.*, et al.* (2020). Pooled Knockin Targeting for Genome Engineering of Cellular Immunotherapies. Cell *181*, 728-744 e721.
Roudko, V., Greenbaum, B., and Bhardwaj, N. (2020). Computational Prediction and Validation of Tumor-Associated Neoantigens. Front Immunol *11*, 27.
Roybal, K.T., Williams, J.Z., Morsut, L., Rupp, L.J., Kolinko, I., Choe, J.H., Walker, W.J., McNally, K.A., and Lim, W.A. (2016). Engineering T Cells with Customized Therapeutic Response Programs Using Synthetic Notch Receptors. Cell *167*, 419-432 e416.
Sade-Feldman, M., Jiao, Y.J., Chen, J.H., Rooney, M.S., Barzily-Rokni, M., Eliane, J.P., Bjorgaard, S.L., Hammond, M.R., Vitzthum, H., Blackmon, S.M.*, et al.* (2017). Resistance to checkpoint blockade therapy through inactivation of antigen presentation. Nat Commun *8*, 1136.
Salmon, H., Idoyaga, J., Rahman, A., Leboeuf, M., Remark, R., Jordan, S., Casanova-Acebes, M., Khudoynazarova, M., Agudo, J., Tung, N.*, et al.* (2016). Expansion and Activation of CD103(+) Dendritic Cell Progenitors at the Tumor Site Enhances Tumor Responses to Therapeutic PD-L1 and BRAF Inhibition. Immunity *44*, 924-938.
Santini, S.M., Lapenta, C., Logozzi, M., Parlato, S., Spada, M., Di Pucchio, T., and Belardelli, F. (2000). Type I interferon as a powerful adjuvant for monocyte-derived dendritic cell development and activity in vitro and in Hu-PBL-SCID mice. J Exp Med *191*, 1777-1788.
Schadt, L., Sparano, C., Schweiger, N.A., Silina, K., Cecconi, V., Lucchiari, G., Yagita, H., Guggisberg, E., Saba, S., Nascakova, Z.*, et al.* (2019). Cancer-Cell-Intrinsic cGAS Expression Mediates Tumor Immunogenicity. Cell Rep *29*, 1236-1248 e1237.
Schick, B., and Berke, G. (1977). Activity of tumor-associated lymphoid cells at short intervals after administration of irradiated syngeneic and allogeneic tumor cells. J Immunol *118*, 986-991.
Schlee, M., and Hartmann, G. (2016). Discriminating self from non-self in nucleic acid sensing. Nat Rev Immunol *16*, 566-580.
Schumacher, T.N., and Schreiber, R.D. (2015). Neoantigens in cancer immunotherapy. Science *348*, 69-74.
Schwartz, R.N., Stover, L., and Dutcher, J.P. (2002). Managing toxicities of high-dose interleukin-2. Oncology (Williston Park) *16*, 11-20.
Scott, A.C., Dundar, F., Zumbo, P., Chandran, S.S., Klebanoff, C.A., Shakiba, M., Trivedi, P., Menocal, L., Appleby, H., Camara, S.*, et al.* (2019). TOX is a critical regulator of tumour-specific T cell differentiation. Nature *571*, 270-274.
Segovia, M., Russo, S., Girotti, M.R., Rabinovich, G.A., and Hill, M. (2020). Role of inflammasome activation in tumor immunity triggered by immune checkpoint blockers. Clin Exp Immunol *200*, 155-162.
Seo, H., Chen, J., Gonzalez-Avalos, E., Samaniego-Castruita, D., Das, A., Wang, Y.H., Lopez-Moyado, I.F., Georges, R.O., Zhang, W., Onodera, A.*, et al.* (2019). TOX and TOX2 transcription factors cooperate with NR4A transcription factors to impose CD8(+) T cell exhaustion. Proc Natl Acad Sci U S A *116*, 12410-12415.
Sercombe, L., Veerati, T., Moheimani, F., Wu, S.Y., Sood, A.K., and Hua, S. (2015). Advances and Challenges of Liposome Assisted Drug Delivery. Front Pharmacol *6*, 286.
Sharpe, A.H., and Pauken, K.E. (2018). The diverse functions of the PD1 inhibitory pathway. Nat Rev Immunol *18*, 153-167.
Shelke, G.V., Yin, Y., Jang, S.C., Lasser, C., Wennmalm, S., Hoffmann, H.J., Li, L., Gho, Y.S., Nilsson, J.A., and Lotvall, J. (2019). Endosomal signalling via exosome surface TGFbeta-1. J Extracell Vesicles *8*, 1650458.

Sheng, W., LaFleur, M.W., Nguyen, T.H., Chen, S., Chakravarthy, A., Conway, J.R., Li, Y., Chen, H., Yang, H., Hsu, P.H.*, et al.* (2018). LSD1 Ablation Stimulates Anti-tumor Immunity and Enables Checkpoint Blockade. Cell *174*, 549-563 e519.
Shin, D.S., Zaretsky, J.M., Escuin-Ordinas, H., Garcia-Diaz, A., Hu-Lieskovan, S., Kalbasi, A., Grasso, C.S., Hugo, W., Sandoval, S., Torrejon, D.Y.*, et al.* (2017). Primary Resistance to PD-1 Blockade Mediated by JAK1/2 Mutations. Cancer Discov *7*, 188-201.
Shum, T., Omer, B., Tashiro, H., Kruse, R.L., Wagner, D.L., Parikh, K., Yi, Z., Sauer, T., Liu, D., Parihar, R.*, et al.* (2017). Constitutive Signaling from an Engineered IL7 Receptor Promotes Durable Tumor Elimination by Tumor-Redirected T Cells. Cancer Discov *7*, 1238-1247.
Silva, D.A., Yu, S., Ulge, U.Y., Spangler, J.B., Jude, K.M., Labao-Almeida, C., Ali, L.R., Quijano-Rubio, A., Ruterbusch, M., Leung, I.*, et al.* (2019). De novo design of potent and selective mimics of IL-2 and IL-15. Nature *565*, 186-191.
Simoni, Y., Becht, E., Fehlings, M., Loh, C.Y., Koo, S.L., Teng, K.W.W., Yeong, J.P.S., Nahar, R., Zhang, T., Kared, H.*, et al.* (2018). Bystander CD8(+) T cells are abundant and phenotypically distinct in human tumour infiltrates. Nature *557*, 575-579.
Smith-Garvin, J.E., Koretzky, G.A., and Jordan, M.S. (2009). T cell activation. Annu Rev Immunol *27*, 591-619.
Snell, L.M., McGaha, T.L., and Brooks, D.G. (2017). Type I Interferon in Chronic Virus Infection and Cancer. Trends Immunol *38*, 542-557.
Snyder, A., Makarov, V., Merghoub, T., Yuan, J., Zaretsky, J.M., Desrichard, A., Walsh, L.A., Postow, M.A., Wong, P., Ho, T.S.*, et al.* (2014). Genetic basis for clinical response to CTLA-4 blockade in melanoma. N Engl J Med *371*, 2189-2199.
Sotillo, E., Barrett, D.M., Black, K.L., Bagashev, A., Oldridge, D., Wu, G., Sussman, R., Lanauze, C., Ruella, M., Gazzara, M.R.*, et al.* (2015). Convergence of Acquired Mutations and Alternative Splicing of CD19 Enables Resistance to CART-19 Immunotherapy. Cancer Discov *5*, 1282-1295.
Spits, H., Bernink, J.H., and Lanier, L. (2016). NK cells and type 1 innate lymphoid cells: partners in host defense. Nat Immunol *17*, 758-764.
Spranger, S., Bao, R., and Gajewski, T.F. (2015). Melanoma-intrinsic beta-catenin signalling prevents anti-tumour immunity. Nature *523*, 231-235.
Spranger, S., Dai, D., Horton, B., and Gajewski, T.F. (2017). Tumor-Residing Batf3 Dendritic Cells Are Required for Effector T Cell Trafficking and Adoptive T Cell Therapy. Cancer Cell *31*, 711-723 e714.
Sprokholt, J.K., Kaptein, T.M., van Hamme, J.L., Overmars, R.J., Gringhuis, S.I., and Geijtenbeek, T.B.H. (2017a). RIG-I-like receptor activation by dengue virus drives follicular T helper cell formation and antibody production. PLoS Pathog *13*, e1006738.
Sprokholt, J.K., Kaptein, T.M., van Hamme, J.L., Overmars, R.J., Gringhuis, S.I., and Geijtenbeek, T.B.H. (2017b). RIG-I-like Receptor Triggering by Dengue Virus Drives Dendritic Cell Immune Activation and TH1 Differentiation. J Immunol *198*, 4764-4771.
Stadtmauer, E.A., Fraietta, J.A., Davis, M.M., Cohen, A.D., Weber, K.L., Lancaster, E., Mangan, P.A., Kulikovskaya, I., Gupta, M., Chen, F.*, et al.* (2020). CRISPR-engineered T cells in patients with refractory cancer. Science *367*.
Su, T., Zhang, Y., Valerie, K., Wang, X.Y., Lin, S., and Zhu, G. (2019). STING activation in cancer immunotherapy. Theranostics *9*, 7759-7771.
Sun, C., Mezzadra, R., and Schumacher, T.N. (2018). Regulation and Function of the PD-L1 Checkpoint. Immunity *48*, 434-452.

Swiatczak, B., and Cohen, I.R. (2015). Gut feelings of safety: tolerance to the microbiota mediated by innate immune receptors. Microbiol Immunol *59*, 573-585.
Tanaka, A., and Sakaguchi, S. (2017). Regulatory T cells in cancer immunotherapy. Cell Res *27*, 109-118.
Tang, N., Cheng, C., Zhang, X., Qiao, M., Li, N., Mu, W., Wei, X.F., Han, W., and Wang, H. (2020). TGF-beta inhibition via CRISPR promotes the long-term efficacy of CAR T cells against solid tumors. JCI Insight *5*.
Taube, J.M., Anders, R.A., Young, G.D., Xu, H., Sharma, R., McMiller, T.L., Chen, S., Klein, A.P., Pardoll, D.M., Topalian, S.L.*, et al.* (2012). Colocalization of inflammatory response with B7-h1 expression in human melanocytic lesions supports an adaptive resistance mechanism of immune escape. Sci Transl Med *4*, 127ra137.
Teijaro, J.R., Ng, C., Lee, A.M., Sullivan, B.M., Sheehan, K.C., Welch, M., Schreiber, R.D., de la Torre, J.C., and Oldstone, M.B. (2013). Persistent LCMV infection is controlled by blockade of type I interferon signaling. Science *340*, 207-211.
Teng, M.W., Ngiow, S.F., Ribas, A., and Smyth, M.J. (2015). Classifying Cancers Based on T-cell Infiltration and PD-L1. Cancer Res *75*, 2139-2145.
Thommen, D.S., and Schumacher, T.N. (2018). T Cell Dysfunction in Cancer. Cancer Cell *33*, 547-562.
Tirosh, I., Izar, B., Prakadan, S.M., Wadsworth, M.H., 2nd, Treacy, D., Trombetta, J.J., Rotem, A., Rodman, C., Lian, C., Murphy, G.*, et al.* (2016). Dissecting the multicellular ecosystem of metastatic melanoma by single-cell RNA-seq. Science *352*, 189-196.
Trajkovic, K., Hsu, C., Chiantia, S., Rajendran, L., Wenzel, D., Wieland, F., Schwille, P., Brugger, B., and Simons, M. (2008). Ceramide triggers budding of exosome vesicles into multivesicular endosomes. Science *319*, 1244-1247.
Tumeh, P.C., Harview, C.L., Yearley, J.H., Shintaku, I.P., Taylor, E.J., Robert, L., Chmielowski, B., Spasic, M., Henry, G., Ciobanu, V.*, et al.* (2014). PD-1 blockade induces responses by inhibiting adaptive immune resistance. Nature *515*, 568-571.
Twyman-Saint Victor, C., Rech, A.J., Maity, A., Rengan, R., Pauken, K.E., Stelekati, E., Benci, J.L., Xu, B., Dada, H., Odorizzi, P.M.*, et al.* (2015). Radiation and dual checkpoint blockade activate non-redundant immune mechanisms in cancer. Nature *520*, 373-377.
van de Weijer, M.L., Luteijn, R.D., and Wiertz, E.J. (2015). Viral immune evasion: Lessons in MHC class I antigen presentation. Semin Immunol *27*, 125-137.
van den Broek, M.F., Kagi, D., Zinkernagel, R.M., and Hengartner, H. (1995). Perforin dependence of natural killer cell-mediated tumor control in vivo. Eur J Immunol *25*, 3514-3516.
Vasan, N., Baselga, J., and Hyman, D.M. (2019). A view on drug resistance in cancer. Nature *575*, 299-309.
Vignuzzi, M., and Lopez, C.B. (2019). Defective viral genomes are key drivers of the virus-host interaction. Nat Microbiol *4*, 1075-1087.
Votteler, J., Ogohara, C., Yi, S., Hsia, Y., Nattermann, U., Belnap, D.M., King, N.P., and Sundquist, W.I. (2016). Designed proteins induce the formation of nanocage-containing extracellular vesicles. Nature *540*, 292-295.
Vredevoogd, D.W., Kuilman, T., Ligtenberg, M.A., Boshuizen, J., Stecker, K.E., de Bruijn, B., Krijgsman, O., Huang, X., Kenski, J.C.N., Lacroix, R.*, et al.* (2019). Augmenting Immunotherapy Impact by Lowering Tumor TNF Cytotoxicity Threshold. Cell *178*, 585-599 e515.

Wang, W., Green, M., Choi, J.E., Gijon, M., Kennedy, P.D., Johnson, J.K., Liao, P., Lang, X., Kryczek, I., Sell, A.*, et al.* (2019). CD8(+) T cells regulate tumour ferroptosis during cancer immunotherapy. Nature *569*, 270-274.
Warburg, O. (1956). On the origin of cancer cells. Science *123*, 309-314.
Webster, B., Assil, S., and Dreux, M. (2016). Cell-Cell Sensing of Viral Infection by Plasmacytoid Dendritic Cells. J Virol *90*, 10050-10053.
Wei, J., Long, L., Zheng, W., Dhungana, Y., Lim, S.A., Guy, C., Wang, Y., Wang, Y.D., Qian, C., Xu, B.*, et al.* (2019). Targeting REGNASE-1 programs long-lived effector T cells for cancer therapy. Nature *576*, 471-476.
Wei, S.C., Levine, J.H., Cogdill, A.P., Zhao, Y., Anang, N.A.S., Andrews, M.C., Sharma, P., Wang, J., Wargo, J.A., Pe'er, D.*, et al.* (2017). Distinct Cellular Mechanisms Underlie Anti-CTLA-4 and Anti-PD-1 Checkpoint Blockade. Cell *170*, 1120-1133 e1117.
Weichselbaum, R.R., Ishwaran, H., Yoon, T., Nuyten, D.S., Baker, S.W., Khodarev, N., Su, A.W., Shaikh, A.Y., Roach, P., Kreike, B.*, et al.* (2008). An interferon-related gene signature for DNA damage resistance is a predictive marker for chemotherapy and radiation for breast cancer. Proc Natl Acad Sci U S A *105*, 18490-18495.
Wherry, E.J., and Kurachi, M. (2015). Molecular and cellular insights into T cell exhaustion. Nat Rev Immunol *15*, 486-499.
Whiteside, T.L. (2016). Exosomes and tumor-mediated immune suppression. J Clin Invest *126*, 1216-1223.
Whiteside, T.L. (2018). Exosome and mesenchymal stem cell cross-talk in the tumor microenvironment. Semin Immunol *35*, 69-79.
Wiesel, M., Crouse, J., Bedenikovic, G., Sutherland, A., Joller, N., and Oxenius, A. (2012). Type-I IFN drives the differentiation of short-lived effector CD8+ T cells in vivo. Eur J Immunol *42*, 320-329.
Wilson, E.B., Yamada, D.H., Elsaesser, H., Herskovitz, J., Deng, J., Cheng, G., Aronow, B.J., Karp, C.L., and Brooks, D.G. (2013). Blockade of chronic type I interferon signaling to control persistent LCMV infection. Science *340*, 202-207.
Wolchok, J.D., Kluger, H., Callahan, M.K., Postow, M.A., Rizvi, N.A., Lesokhin, A.M., Segal, N.H., Ariyan, C.E., Gordon, R.A., Reed, K.*, et al.* (2013). Nivolumab plus ipilimumab in advanced melanoma. N Engl J Med *369*, 122-133.
Wu, C.Y., Roybal, K.T., Puchner, E.M., Onuffer, J., and Lim, W.A. (2015). Remote control of therapeutic T cells through a small molecule-gated chimeric receptor. Science *350*, aab4077.
Wu, T.D., Madireddi, S., de Almeida, P.E., Banchereau, R., Chen, Y.J., Chitre, A.S., Chiang, E.Y., Iftikhar, H., O'Gorman, W.E., Au-Yeung, A.*, et al.* (2020). Peripheral T cell expansion predicts tumour infiltration and clinical response. Nature *579*, 274-278.
Xie, Y.J., Dougan, M., Jailkhani, N., Ingram, J., Fang, T., Kummer, L., Momin, N., Pishesha, N., Rickelt, S., Hynes, R.O.*, et al.* (2019). Nanobody-based CAR T cells that target the tumor microenvironment inhibit the growth of solid tumors in immunocompetent mice. Proc Natl Acad Sci U S A *116*, 7624-7631.
Yang, F., Ning, Z., Ma, L., Liu, W., Shao, C., Shu, Y., and Shen, H. (2017). Exosomal miRNAs and miRNA dysregulation in cancer-associated fibroblasts. Mol Cancer *16*, 148.
Yao, C., Sun, H.W., Lacey, N.E., Ji, Y., Moseman, E.A., Shih, H.Y., Heuston, E.F., Kirby, M., Anderson, S., Cheng, J.*, et al.* (2019). Single-cell RNA-seq reveals TOX as a key regulator of CD8(+) T cell persistence in chronic infection. Nat Immunol *20*, 890-901.

Yu, S., Liu, C., Su, K., Wang, J., Liu, Y., Zhang, L., Li, C., Cong, Y., Kimberly, R., Grizzle, W.E*., et al.* (2007). Tumor exosomes inhibit differentiation of bone marrow dendritic cells. J Immunol *178*, 6867-6875.
Zaretsky, J.M., Garcia-Diaz, A., Shin, D.S., Escuin-Ordinas, H., Hugo, W., Hu-Lieskovan, S., Torrejon, D.Y., Abril-Rodriguez, G., Sandoval, S., Barthly, L*., et al.* (2016). Mutations Associated with Acquired Resistance to PD-1 Blockade in Melanoma. N Engl J Med *375*, 819-829.
Zhang, L., Yu, X., Zheng, L., Zhang, Y., Li, Y., Fang, Q., Gao, R., Kang, B., Zhang, Q., Huang, J.Y*., et al.* (2018). Lineage tracking reveals dynamic relationships of T cells in colorectal cancer. Nature *564*, 268-272.
Zhang, Z., Zhang, Y., Xia, S., Kong, Q., Li, S., Liu, X., Junqueira, C., Meza-Sosa, K.F., Mok, T.M.Y., Ansara, J*., et al.* (2020). Gasdermin E suppresses tumour growth by activating anti-tumour immunity. Nature *579*, 415-420.
Zhao, Z., Condomines, M., van der Stegen, S.J.C., Perna, F., Kloss, C.C., Gunset, G., Plotkin, J., and Sadelain, M. (2015). Structural Design of Engineered Costimulation Determines Tumor Rejection Kinetics and Persistence of CAR T Cells. Cancer Cell *28*, 415-428.
Zhong, X.S., Matsushita, M., Plotkin, J., Riviere, I., and Sadelain, M. (2010). Chimeric antigen receptors combining 4-1BB and CD28 signaling domains augment PI3kinase/AKT/Bcl-XL activation and CD8+ T cell-mediated tumor eradication. Mol Ther *18*, 413-420.
Zilionis, R., Engblom, C., Pfirschke, C., Savova, V., Zemmour, D., Saatcioglu, H.D., Krishnan, I., Maroni, G., Meyerovitz, C.V., Kerwin, C.M*., et al.* (2019). Single-Cell Transcriptomics of Human and Mouse Lung Cancers Reveals Conserved Myeloid Populations across Individuals and Species. Immunity *50*, 1317-1334 e1310.
Zitvogel, L., Galluzzi, L., Kepp, O., Smyth, M.J., and Kroemer, G. (2015). Type I interferons in anticancer immunity. Nat Rev Immunol *15*, 405-414.